AD-A101 090 EG AND G WASHINGTON ANALYTICAL SERVICES CENTER INC R--ETC F/G 8/10
AIR DEPLOYED OCEANOGRAPHIC MOORING (ADOM).(U)
APR 81 N00014-79-C-0227
UNCLASSIFIED EG/G-TR-D370-0003 NL

1 OF 2
AD
A101090

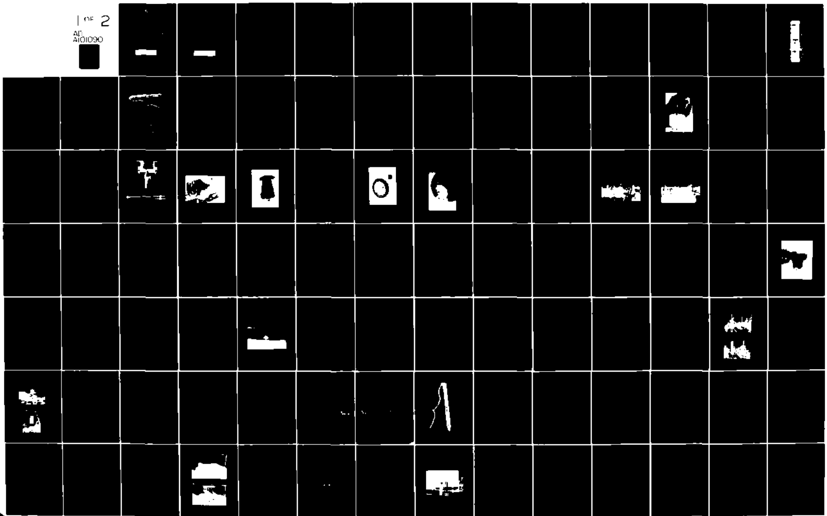

LEVEL 2

APRIL 1981

AIR DEPLOYED OCEANOGRAPHIC MOORING (ADOM)

PROGRESS REPORT FOR 1980

N00014-79-C-0227

[redacted]

OCEAN TECHNOLOGY PROGRAM (CODE 485)
OCEAN SCIENCE AND TECHNOLOGY DIVISION
OFFICE OF NAVAL RESEARCH-DETACHMENT
NSTL STATION, MISSISSIPPI 39529

APRIL 1981

AIR DEPLOYED OCEANOGRAPHIC MOORING (ADOM)

PROGRESS REPORT FOR 1980

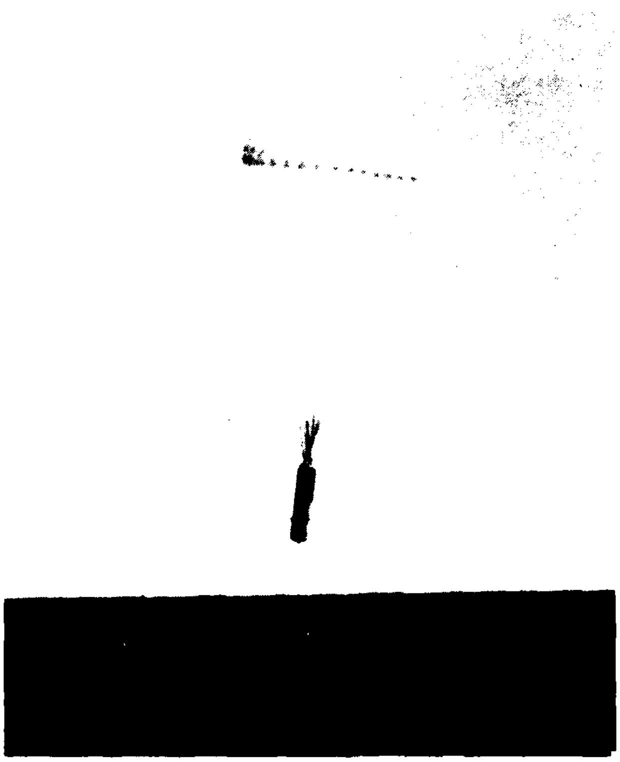

OCEAN TECHNOLOGY PROGRAM (CODE 485)
OCEAN SCIENCE AND TECHNOLOGY DIVISION
OFFICE OF NAVAL RESEARCH-DETACHMENT
NSTL STATION, MISSISSIPPI 39529

UNCLASSIFIED
SECURITY CLASSIFICATION OF THIS PAGE (When Data Entered)

REPORT DOCUMENTATION PAGE

READ INSTRUCTIONS BEFORE COMPLETING FORM

1. REPORT NUMBER: TR-D370-0003
2. GOVT ACCESSION NO.: AD-A101
3. RECIPIENT'S CATALOG NUMBER: 090
4. TITLE (and Subtitle): AIR DEPLOYED OCEANOGRAPHIC MOORING (ADOM). Progess Report for 1980
5. TYPE OF REPORT & PERIOD COVERED: Technical
6. PERFORMING ORG. REPORT NUMBER
7. AUTHOR(s)
8. CONTRACT OR GRANT NUMBER(s): N00014-79-C-0227
9. PERFORMING ORGANIZATION NAME AND ADDRESS: EG&G Washington Analytical Services Center, Inc. 2150 Fields Road Rockville, Maryland 20850
10. PROGRAM ELEMENT, PROJECT, TASK AREA & WORK UNIT NUMBERS
11. CONTROLLING OFFICE NAME AND ADDRESS: Ocean Science and Technology Division (Code 485) Office of Navy Research - Detachment NSTL Station, Mississippi 39529
12. REPORT DATE: April 1981
13. NUMBER OF PAGES: 104
14. MONITORING AGENCY NAME & ADDRESS (if different from Controlling Office)
15. SECURITY CLASS. (of this report): UNCLASSIFIED
15a. DECLASSIFICATION/DOWNGRADING SCHEDULE
16. DISTRIBUTION STATEMENT (of this Report)

Distribution of this document is unlimited.

17. DISTRIBUTION STATEMENT (of the abstract entered in Block 20, if different from Report)
18. SUPPLEMENTARY NOTES
19. KEY WORDS (Continue on reverse side if necessary and identify by block number)

Oceanographic Mooring, Air Deployed
Buoys, ocean
Ice drilling, remote control
Microcomputer

20. ABSTRACT (Continue on reverse side if necessary and identify by block number)

This document describes accomplishments in the Air Deployed Oceanographic Mooring (ADOM) program during 1980. A wide variety of scientific investigations can be pursued with air deployed oceanographic moorings which are configured to specific scientific requirements. Also, a number of important oceanographic studies could be accomplished by deploying oceanographic moorings through the polar sea ice from long-range aircraft.

(Continued on next page)

DD FORM 1 JAN 73 1473 EDITION OF 1 NOV 65 IS OBSOLETE
S/N 0102-014-6601

UNCLASSIFIED
SECURITY CLASSIFICATION OF THIS PAGE (When Data Entered)

3 1 1 1 1

(Block 20 continued)

Two systems are being developed:

a. Open ocean moored system
b. Ice covered ocean suspended system.

Both systems are configured to measure temperature, conductivity, and pressure; however, the system design maintains flexibility to allow the addition of other types of sensors.

TABLE OF CONTENTS

TABLE OF CONTENTS (Cont'd)

LIST OF ILLUSTRATIONS

LIST OF ILLUSTRATIONS (Cont'd)

LIST OF ILLUSTRATIONS (Cont'd)

LIST OF TABLES

EXECUTIVE SUMMARY

This document describes accomplishments in the Air Deployed Oceanographic Mooring (ADOM) program during 1980. A wide variety of scientific investigations can be pursued with air deployed oceanographic moorings which are configured to specific scientific requirements. Also, a number of important oceanographic studies could be accomplished by deploying oceanographic moorings through the polar sea ice from long-range aircraft.

Two systems are being developed:

a. Open ocean moored system
b. Ice covered ocean suspended system

Both systems are configured to measure temperature, conductivity, and pressure; however, the system design maintains flexibilty to allow the addition of other types of sensors.

The open ocean moored system, Figure 1a, is essentially an automatically moored two stage instrumented mooring. The electronics and power supply are located in the subsurface buoy. The sensor array forms the upper portion of the mooring line. Data retrieval is from the transmitter in the surface buoy, through the LES-9 satellite to a shore station.

The ice covered ocean suspended system, when deployed, consists of an ice-penetration drill, a lander structure, and a suspended sensor array, as shown in Figure 1b. The electronic system housed in the lander is similar to that in the open ocean moored ADOM.

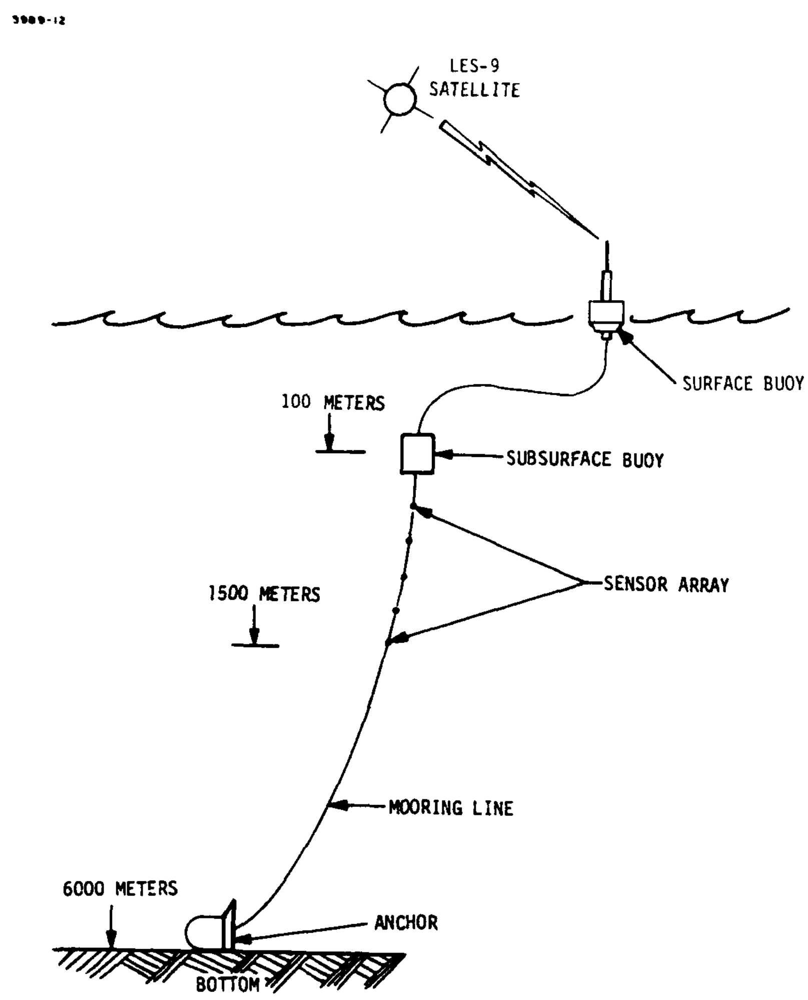

Figure 1a. Open Ocean ADOM System

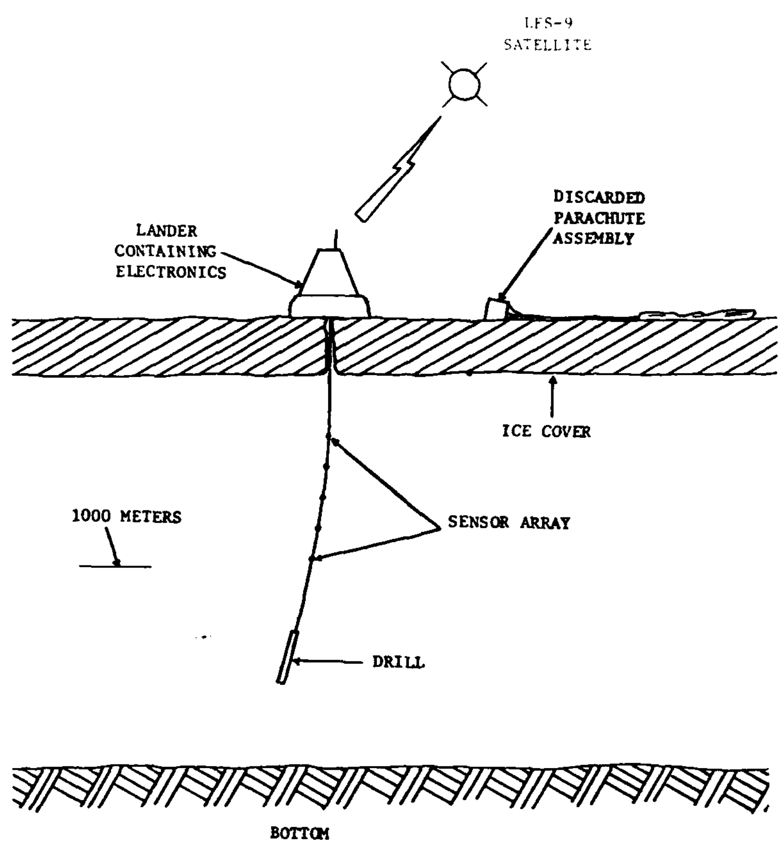

Figure 1b. Arctic ADOM Configuration

The open ocean moored subsystem is composed of the buoys, anchor assembly, and decelerator assembly. The assembled unit is 3.3m long, 71 cm diameter, and weighs 1100 kg. The buoy system (Figure 2) has been packaged for deployment from a C-130 aircraft with a multi-stage decelerator, and an automatic mooring sequence. A 1500m double-armored steel, single conductor sensor cable, 4.3 mm in diameter, and 4500m of Kevlar® lower cable 0.5 cm diameter, are packaged in the anchor assembly. The surface float is connected to the subsurface float by a compliant cable assembly to keep the tension in the tether nearly constant as waves buffet the float.

The components that are included in the electronic and sensor system are shown in Figure 3. The ADOM processor with its data memory and power pack form the central electronic assembly. The segmented cable has terminations to allow the insertion of individually calibrated sensors. Above the processor is a cable to the transmitter in the surface float. The electronic assembly of processor, data memory and power pack is housed in a pressure housing in the ADOM subsurface buoy.

For the Open Ocean ADOM, progress in 1980 was marked by fabrication and testing of subassemblies of the ADOM system, as well as several component tests. The anchor assembly was tested at sea to evaluate design refinements. The complete ADOM buoy was deployed in a drifting mode to validate component separation and array and tether payout. Based on the results of these tests, the ADOM buoy appears to have a reliable automatic mooring system.

To date, more than 4000 hours of processor operations and 2000 hours of memory operation have been achieved. The processor and array have been successfully sea tested. During the year, a real time clock with update provision and memory extension was added to the system to facilitate transmission to the LES-9 satellite. Two sensor arrays have been constructed and one deployed during the drift test.

® Trademark of E.I. Dupont de Nemours, Inc.

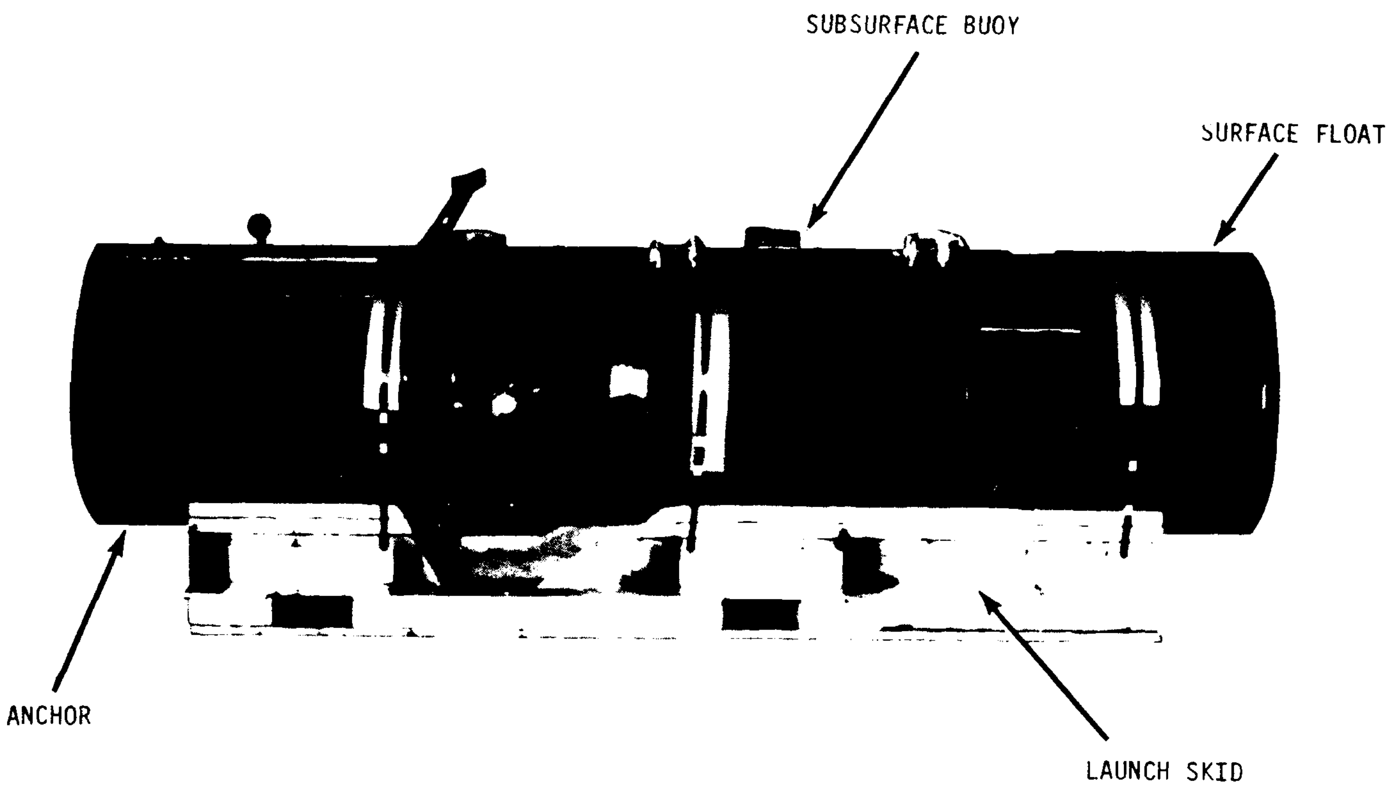

Figure 2. ADOM on Air Deployment Skid (Less Parachute)

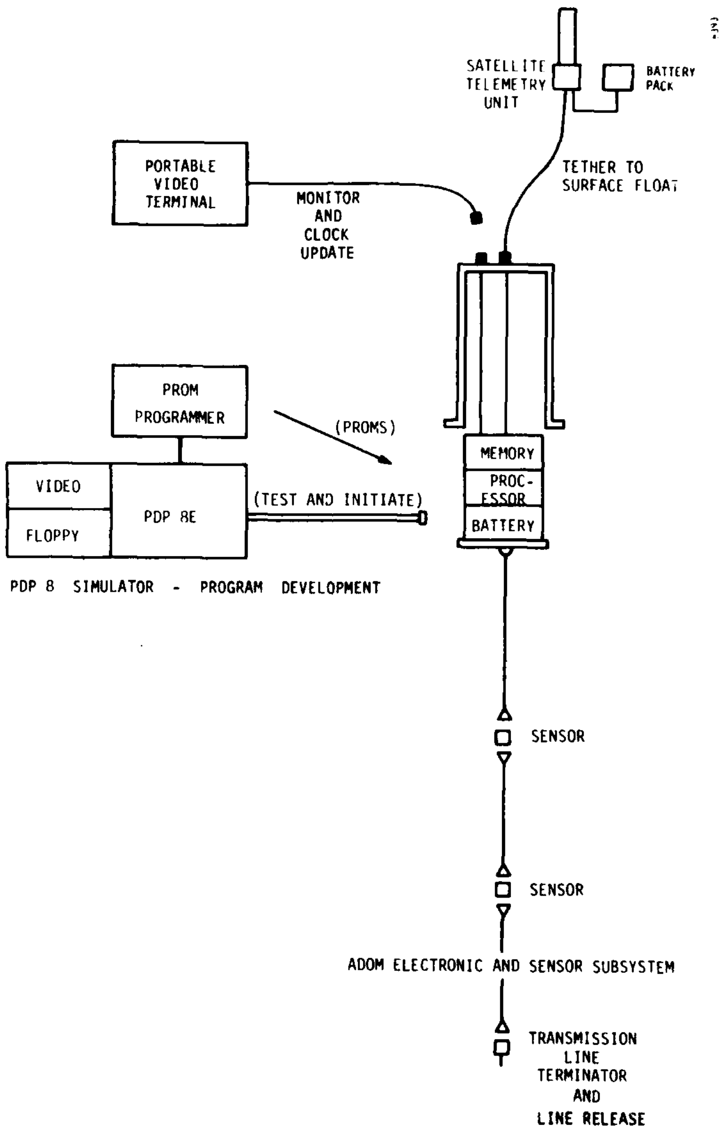

Figure 3. The ADOM Electronic and Sensor System

The design of the transmitter was completed and the prototype device manufactured during calendar year 1980. Concurrent with the above, a shore station was assembled to receive telemetry from the LES-9 satellite. Experimental signals received from the satellite so far have been weaker than expected. The best reception has been about 5 dB lower than expected and bit error rates of 0.01 percent are being experienced. However, small equipment modifications should significantly reduce error rates.

Based upon the Open Ocean ADOM progress to date, two tests are planned for 1981 as follows:

a. Ship-launch one complete ADOM buoy in June 1981, including the complete electronics and sensor array. Transmit data through the LES-9 satellite to the ADOM shore station in Key Biscayne, Florida. Recover buoy after one day and inspect it.

b. Air-launch two ADOM buoys in October 1981. Recover and inspect one buoy after two days' deployment. Recover and inspect the second buoy after 2 to 3 months. Throughout the deployed period, transmit data to Key Biscayne for processing and evaluation.

The major components of the Arctic ADOM lander - the parachute assembly, impact absorbing torus, flotation material, as well as the recirculating jet drill, power cable, batteries, sensor string, and electronics housings - are shown in Figure 4. The torus absorbs impacts from any direction with deceleration rates less than 100 g's. All electronics are sealed in a watertight pressure housing for open water landings, and the lander will float. The sensor string and parachute assembly are similar to those of the Open Ocean ADOM.

The Concept Validation Model (CVM) recirculating water jet drill fabricated and tested during 1980 is shown in Figure 5. During the jet drilling phase, water heated within the drill body is pumped out at high velocity

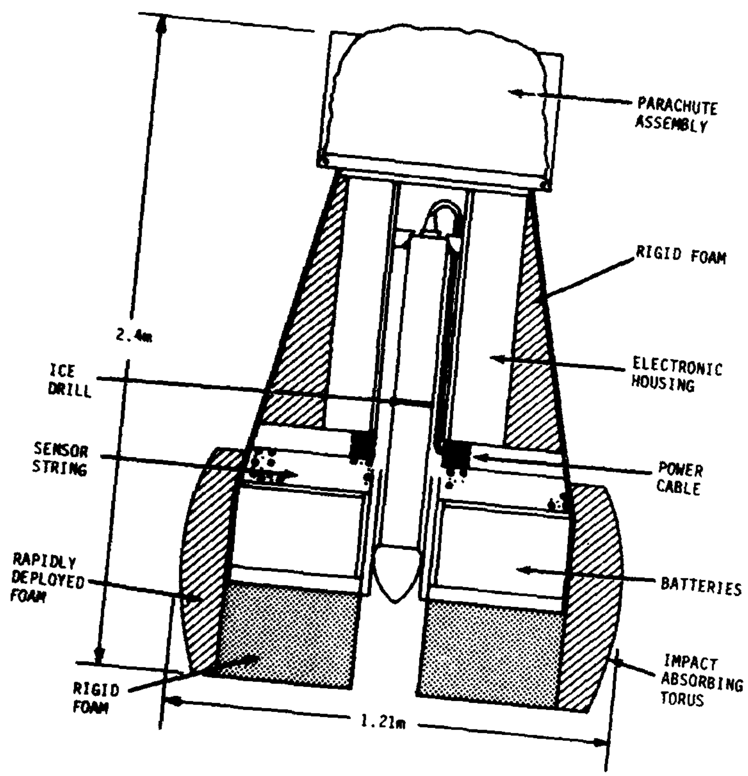

Figure 4. Arctic ADOM Lander

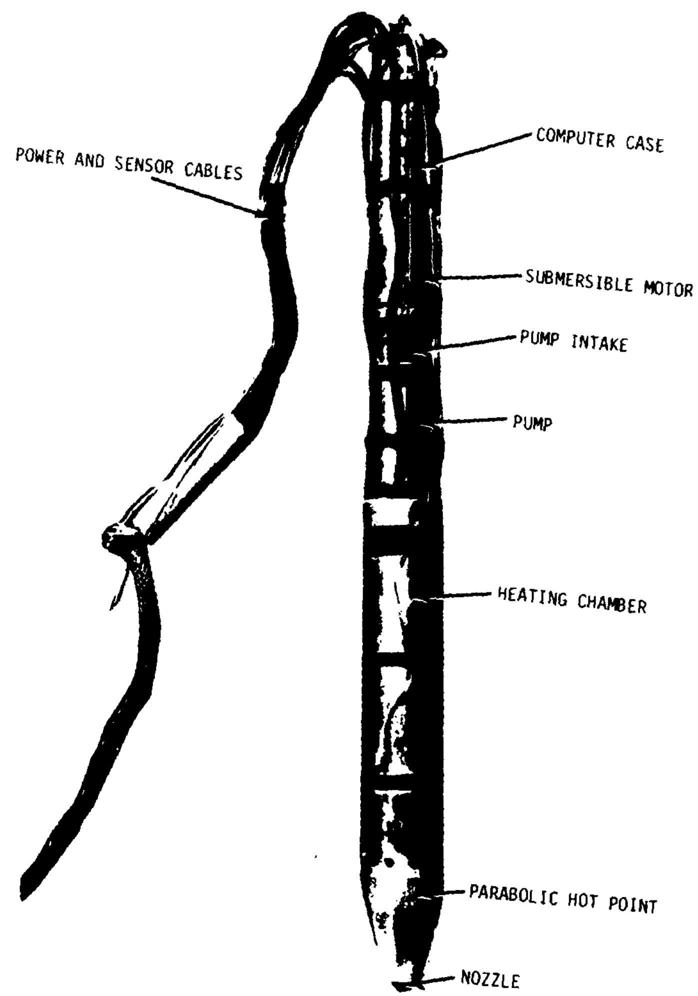

Figure 5. Arctic ADOM Ice Drill
(Concept Validation Model)

through a nozzle in the drill tip. The melt water is recirculated into the drill and pumped out as a warmed jet stream. The jet stream transfers heat from the drill to the ice much faster than natural conduction and convection. Test data confirmed the computer model of the drill, and established that the jet drill is a practical tool for boring a 15 cm hole through 10m of ice and would require 26 kWh of electrical energy.

The components of the Arctic ADOM control system are shown in Figure 6. The processor, memory, power switches, and supporting circuitry are sealed in a canister at the top of the drill body. Control sensors are located at several key points in the drill body. The descending drill drags sensor and power cables from the lander body, where the batteries are stored. When the probe breaks through the ice, it pulls a connector free in the lander, turning the drill off.

During 1980, prototype programs were written for the control computer in the ice drill. Control by a microcomputer adapts the drill to abnormal conditions and provides optimum drilling efficiency. Since large amounts of power are used in the drilling operation, it is very important that this energy be used efficiently. It is equally important that the heaters be shut down to avoid burn out when the drill encounters a void in the ice layer where no melt water is present.

The microcomputer monitors the operation of the drill components. Failed parts are isolated while drilling continues with the remaining portions of the system. Two separate mechanisms are included to shut off a heater whose temperature rises unacceptably. If the microcomputer fails, the system makes a final drilling attempt with the hot point heater.

A simulation computer was developed in 1980 to define and perform initial testing of the candidate control strategies. The simulation computer uses a series of potentiometers to simulate the analog signals from the temperature sensors in the ADOM thermal drill. The computer analyzes the simulated data and generates a control response. The control response is displayed visually as lights on a control panel marked to indicate which heater banks should be

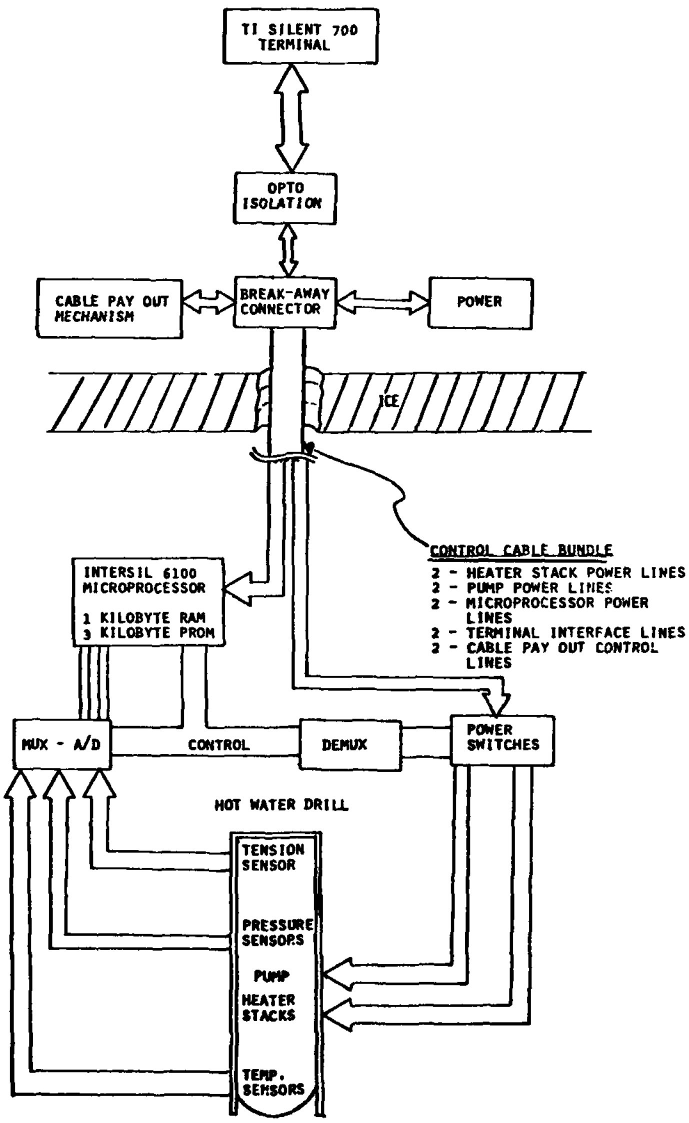

Figure 6. Arctic ADOM Control System

turned on, whether the pump should be running, etc. The control signal is also available at an output port that can be connected to the actual thermal drill control lines. Further, the actual drill temperature sensors can be connected to the computer in place of the potentiometers so that the ADOM simulator is actually the ADOM thermal drill control computer.

The planned actions for the Arctic ADOM during 1981 are as follows:

a. Complete the Advanced Deployment Model (ADM) control system software and computer development.

b. Complete ADM drill development, culminating in testing at Cold Regions Research and Engineering Laboratory (CRREL).

c. Continue landing system design and component testing.

SECTION I
INTRODUCTION

1.1 PURPOSE

This document describes accomplishments in the Air Deployed Oceanographic Mooring (ADOM) program during 1980.

1.2 BACKGROUND

Technology is being developed for deploying oceanographic sensors from an aircraft in two regions of the world's oceans - the open ocean and the polar seas. Two corresponding systems are being developed - an Open Ocean ADOM (OO-ADOM), and an Arctic ADOM (A-ADOM). Both types are configured to measure temperature, conductivity, and pressure. However, the systems have sufficient flexibility to allow the addition of other types of sensors.

1.3 PROJECT ORGANIZATION

The ADOM program is being conducted under the direction of Dr. E. A. Silva, Ocean Technology Program (Code 485), Ocean Science and Technology Division, Office of Naval Research-Detachment. Mr. Ronald K. McGregor, ONR Code 461, shares responsibility for the Arctic ADOM work. The project is divided into technological areas as follows:

a. Open Ocean Moored System:

(1) Mooring Mechanics - Mr. R. Walden, Woods Hole Oceanographic Institution

(2) Hydrodynamics - Mr. L. W. Bonde, EG&G Washington Analytical Services Center, Inc.

(3) Aero Mechanics - Mr. E. Reed, Naval Air Development Center

(4) Electronics - Dr. E. Softley, Ocean Electronic Applications, Inc.

b. Arctic Ocean System:

(1) Arctic Engineering - Dr. R. Corell, University of New Hampshire

(2) Mooring Mechanics - Mr. R. Walden, Woods Hole Oceanographic Institution

(3) Hydrodynamics - Mr. L. W. Bonde, EG&G Washington Analytical Services Center, Inc.

(4) Aero Mechanics - Mr. E. Reed, Naval Air Development Center

(5) Electronics - Dr. E. Softley, Ocean Electronic Applications, Inc.

SECTION II
FINDINGS - OPEN OCEAN ADOM

2.1 GENERAL

Progress on Open Ocean ADOM was marked by fabricating and testing subassemblies of the ADOM system, as well as several component tests. The anchor assembly was tested at sea, and the complete ADOM buoy was deployed in a drifting mode. Data transmission tests were made both from the laboratory and at sea to the LES-9 satellite.

2.2 OPEN OCEAN ADOM ACCOMPLISHMENTS

The Open Ocean ADOM configuration is shown in Figure 2-1. Each of the subassemblies and components will be discussed below. This will include the surface float, tether, subsurface buoy, anchor assembly, electronic and sensor subsystem, and decelerator assembly. Also, the Drift Test conducted in 1980 will be discussed.

2.3 SURFACE FLOAT

The surface float supports the antenna, transmitter, and batteries. The float uses an aluminum tube for basic structure, surrounded by buoyant syntactic foam,and covered with a fiberglass skin. Figure 2-1 shows the OO-ADOM configuration including the surface float and its connection with the decelerator and subsurface buoy.

Figure 2-2 shows the full scale surface float fabricated during 1980. The antenna is shown extended for transmission. The float, as built, has characteristics as follows:

Weight in Air	115 Kg (225 lb)*
Freeboard	20 cm (8 in.)

* Including 13 Kg (25 lb) of ballast.

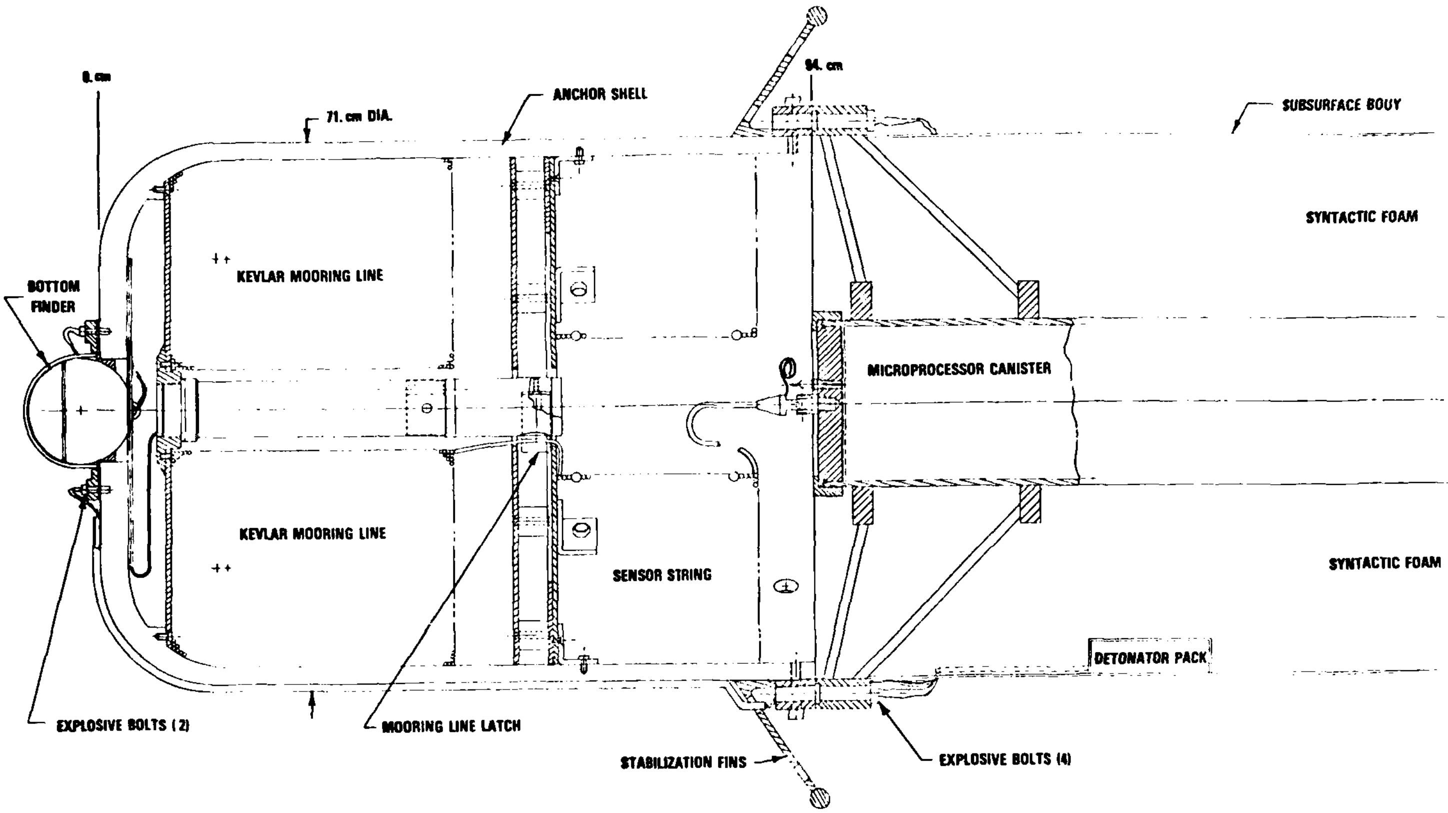

0. cm
71. cm DIA.
ANCHOR SHELL
94. cm
SUBSURFACE BOUY
SYNTACTIC FOAM
BOTTOM FINDER
KEVLAR MOORING LINE
MICROPROCESSOR CANISTER
KEVLAR MOORING LINE
SENSOR STRING
SYNTACTIC FOAM
DETONATOR PACK
EXPLOSIVE BOLTS (2)
MOORING LINE LATCH
STABILIZATION FINS
EXPLOSIVE BOLTS (4)

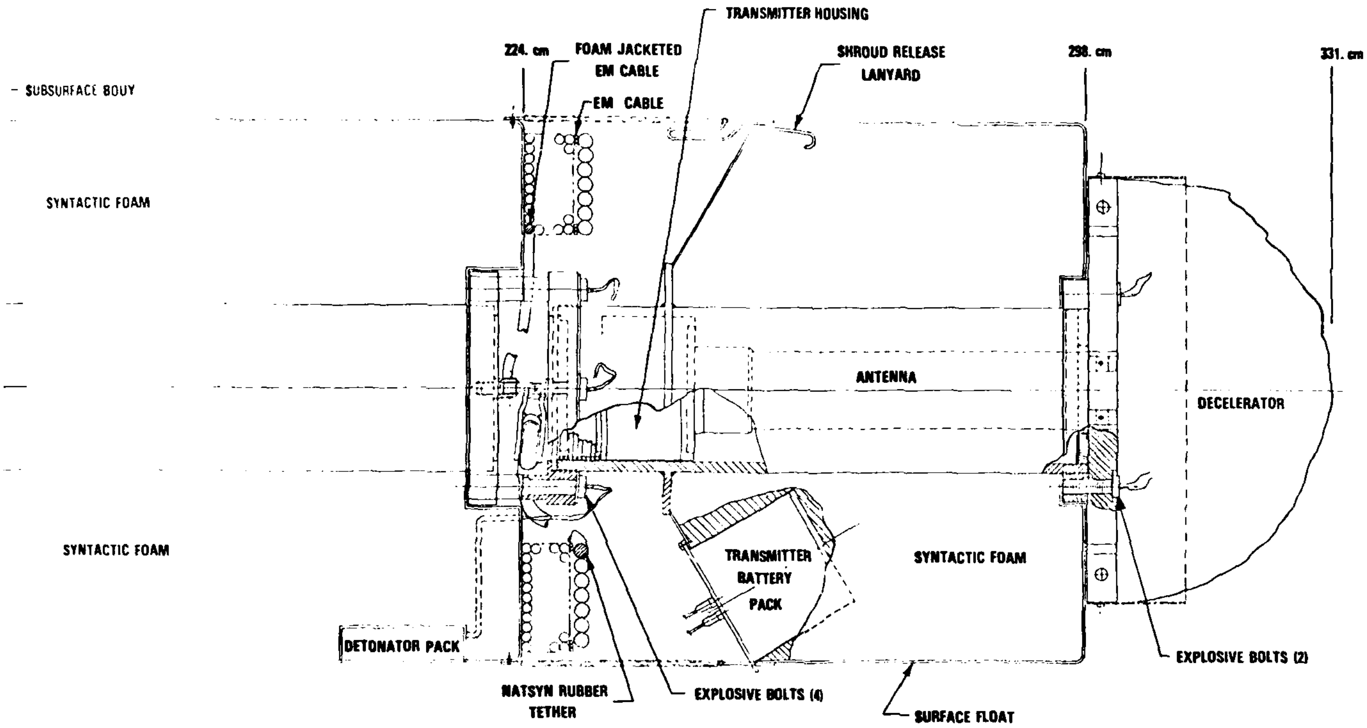

Figure 2-1. Open Ocean ADOM Configuration

2

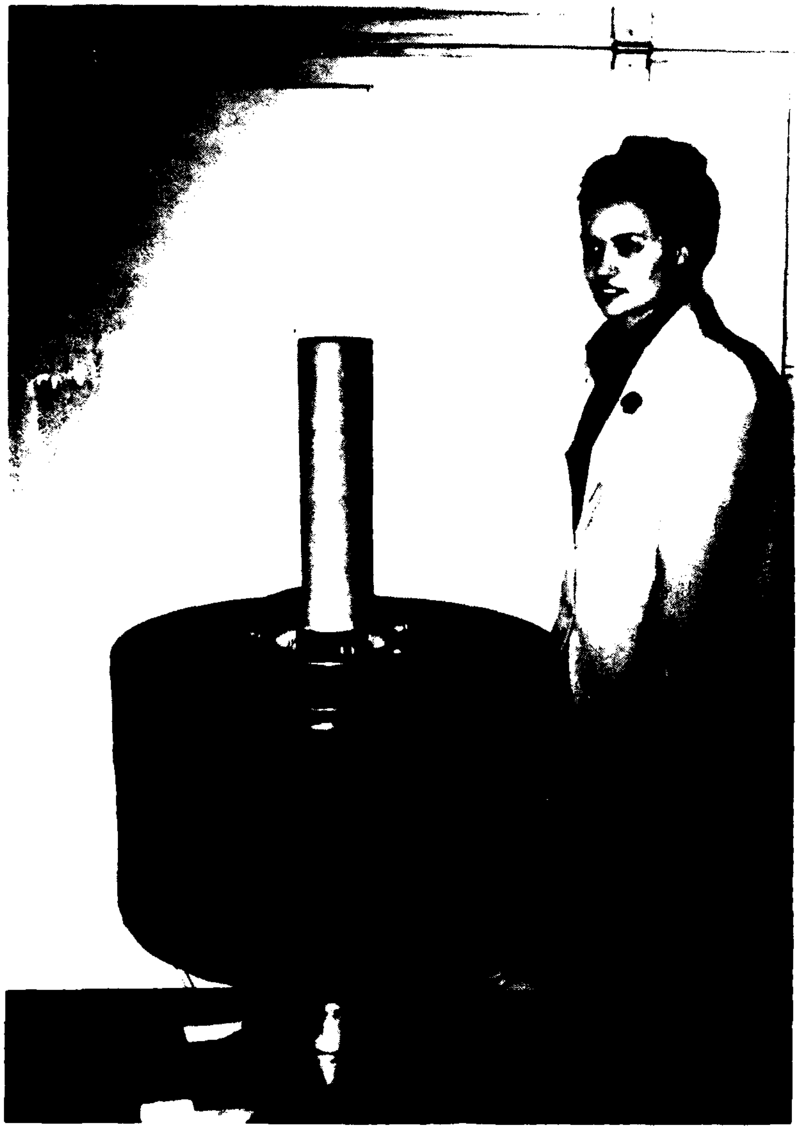

Figure 2-2. Surface Float With Antenna Extended

Reserve Buoyancy	78 Kg (170 lb)
Natural Heave Period	1-1.3 seconds
Natural Roll Period	3 seconds
Depth Capability	600m (1900 ft)

The syntactic foam for both the surface float and subsurface buoy was manufactured from 7.5 cm (3 in.) diameter epoxy balls, 0.1 to 0.15 cm (1/4 to 3/8 in.) diameter epoxy peas, and epoxy resin binder extended with glass "micro-balloons." This composition achieved a 0.32 g/cm^3 (20 lb/ft^3) density. The balls alone will sustain 2069 kPa (300 psi) continuously, and 4827 kPa (700 psi) for short durations. The resin and micro-balloon binder and fiberglass skin are expected to double the pressure capacity of the balls.

2.4 TETHER.

The design for the surface float tether was reported in the ADOM Progress Report for 1978. Figures 2-3 and 2-4 illustrate the concept. The 15.2m length of Natsyn rubber keeps the tension in the tether nearly constant by virtue of its compliance as waves buffet the float. The parallel EM cable is 3.5 times as long as the unstretched length of the rubber section. It carries the data signal to the transmitter in the float and provides a redundant member if the rubber fails. The elastic tension of the rubber will immerse the float before the EM cable becomes taut. The 122m segment of bare EM cable and the similar segment of foamed cable form an "s" shaped arc that prevents subsurface buoy fouling in low-current conditions. The lengths have been chosen so that the apex of the buoyant segment remains submerged even in still water with the anchor cable (Kevlar) 50m too long.

During 1980, a packaging scheme for the tether was developed. The foamed and jacketed sections of the tether were wound in a tray, using a "one over/one under" technique. The tether loops are secured to the tray with a high melting point wax. The Natsyn section was wound similarly. The clamps joining the Natsyn and EM cable were secured to the tray using fine wire (44N (10 lb) breaking strength). The lower end of the Natsyn was coupled to a Preform Grip epoxied to the EM cable. This packaging scheme and the Preform Grip were successfully tested in the lab and utilized in the drift test discussed in Section 2.9

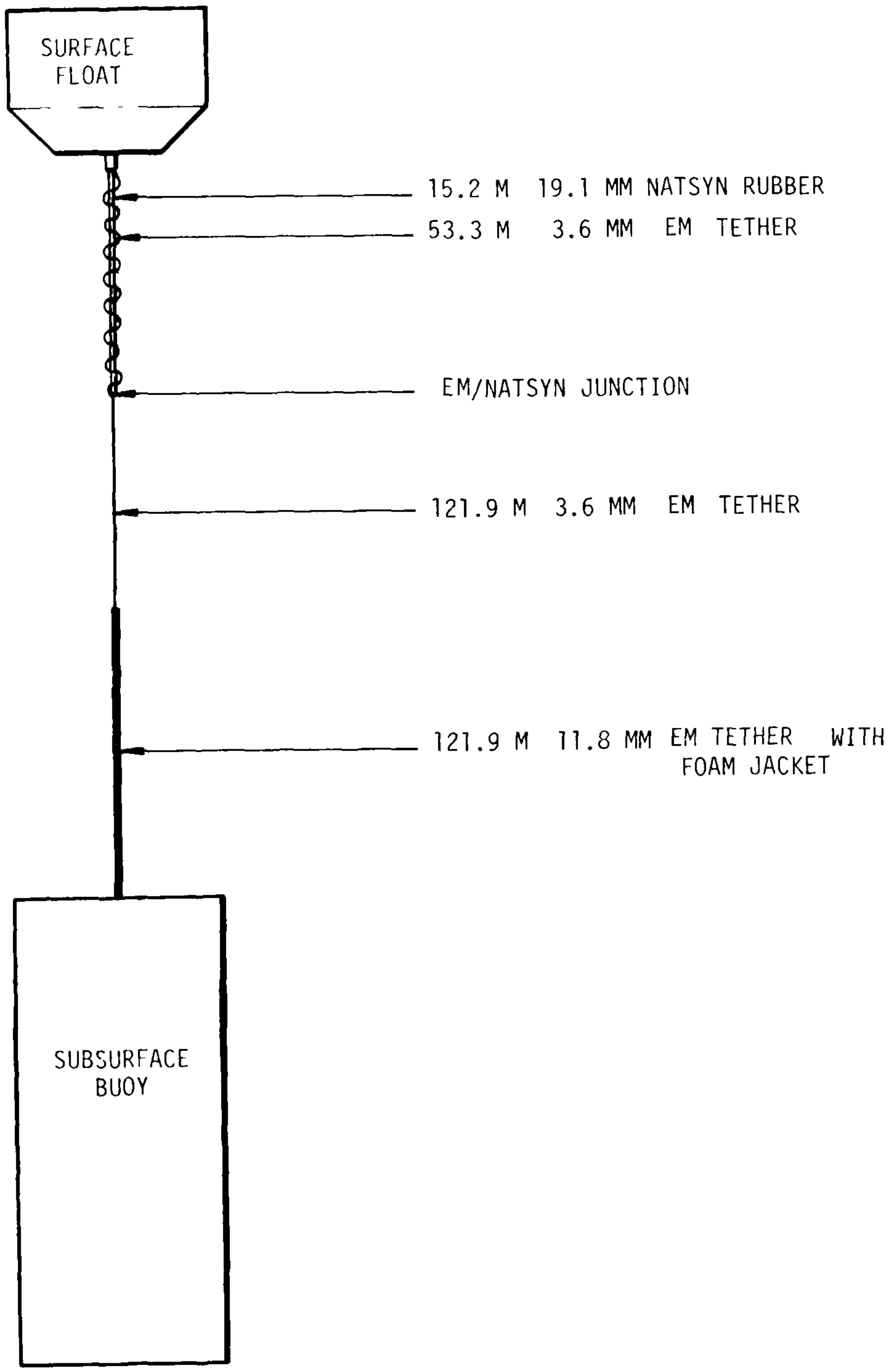

Figure 2-3. The Surface Tether

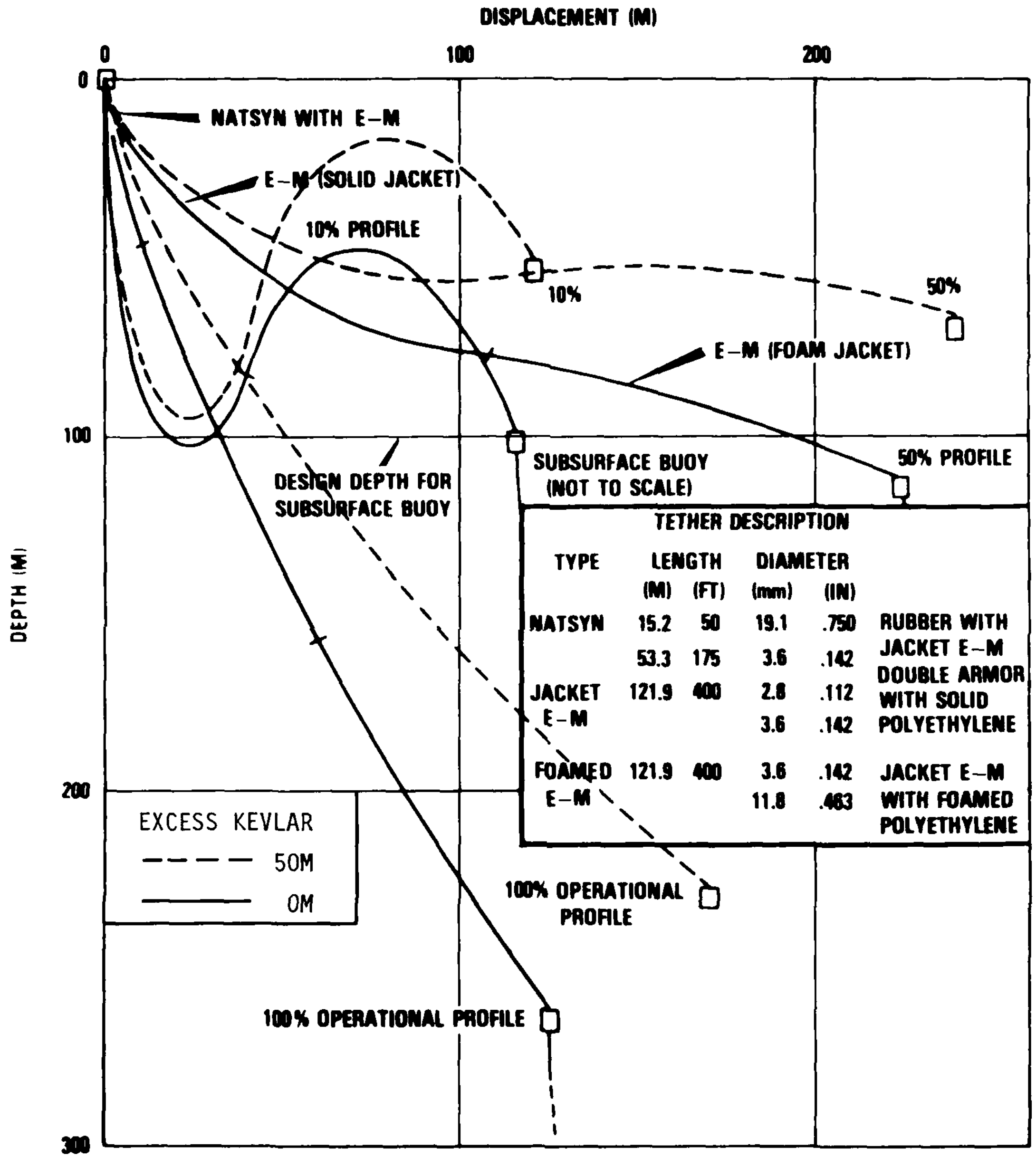

Figure 2-4. ADOM Buoyant Tether Concept

Figure 2-5 shows the fittings used to connect both the Natsyn rubber and EM cable to the surface float. The universal joints that connect the EM cable epoxy termination to the surface float and subsurface buoy, and the thimble in the Natsyn rubber, are shown in Figure 2-5. Clamps to bind the EM tether to the Natsyn in slack bights are shown in Figure 2-6.

2.5 SUBSURFACE BUOY

The ADOM subsurface buoy's design shown in Figure 2-1 is similar to the surface float. A central aluminum tube provides the structural support and houses the microprocessor. Syntactic foam provides concentric buoyancy, and a fiberglass skin protects the buoy from damage in handling. The buoy is joined to the surface float and anchor during storage, delivery, and air deployment, by four explosive bolts at these junctions.

A full-scale subsurface buoy was fabricated during 1980. It is shown on its launching pallet in Figure 2-7. The subsurface buoy weighs 240 Kg (525 lb) and has a displacement of 525 Kg (1150 lb) of water, yielding a net buoyancy of 285 Kg (625 lb). The subsurface buoy is capable of withstanding hydrostatic pressures of 600 m (1900 ft).

2.6 ANCHOR ASSEMBLY

The ADOM anchor is a heavy-wall cast ductile steel housing (Figure 2-8) which contains four subassemblies shown in Figure 2-9. The sensors and 1500 meters of electromechanical cable are stored in the top of the shell, nearest the subsurface buoy. Kevlar mooring line is contained in a spool below the sensor cable and separated from it by guide plates. A heavy post mounted in the center of the mooring line spool contains the mechanically actuated lock-up device which brakes payout of the line positioning the subsurface buoy 100 meters below the surface (Figure 2-10). The bottom finding ball is secured in the end face of the anchor shell with explosive bolts as shown in Figure 2-11.

Shortly after splashdown, current generated from a seawater-activated battery fires the four explosive bolts which secure the anchor assembly to the subsurface buoy permitting the anchor to start its descent to the bottom.

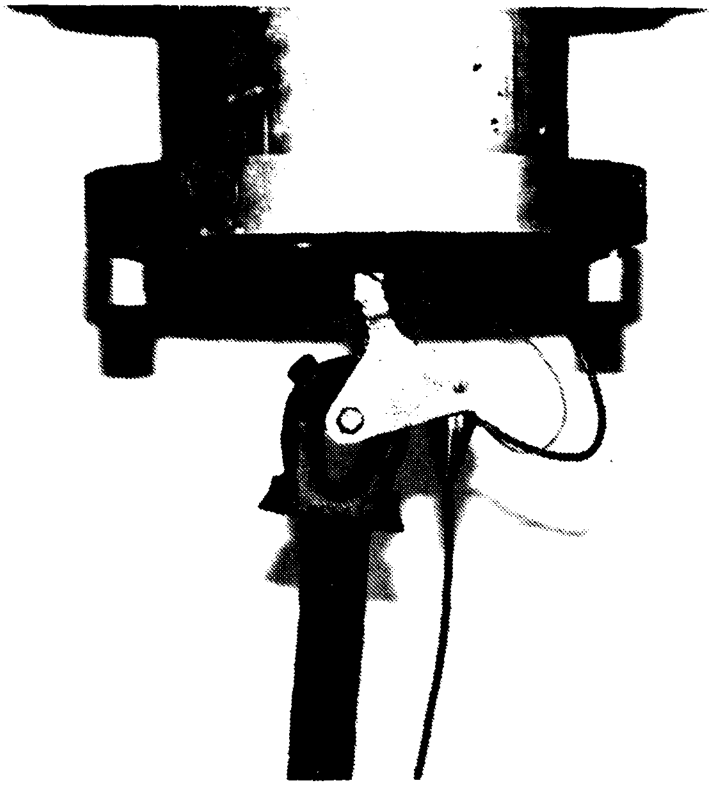

Figure 2-5. Surface Float Fittings

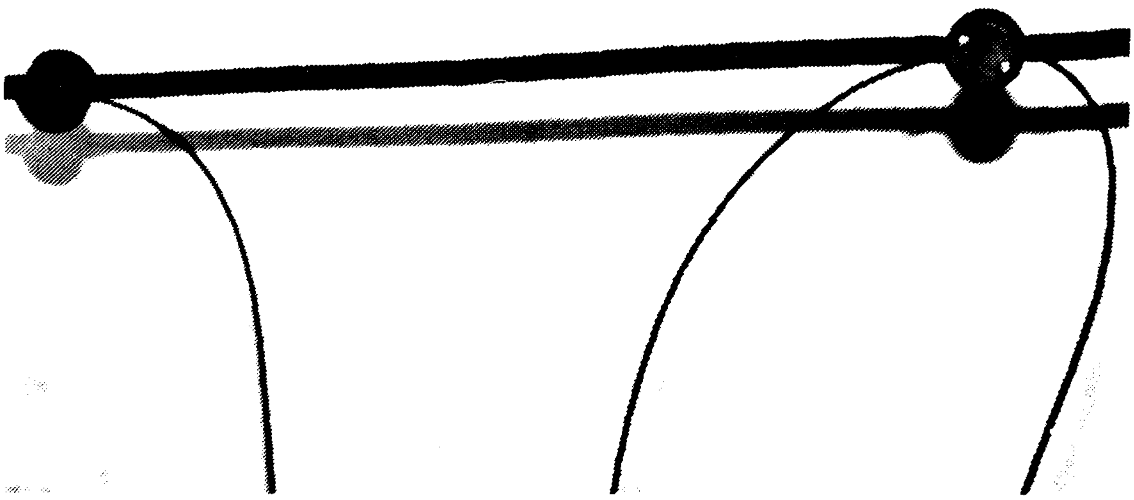

Figure 2-6. E/M Natsyn Clamp

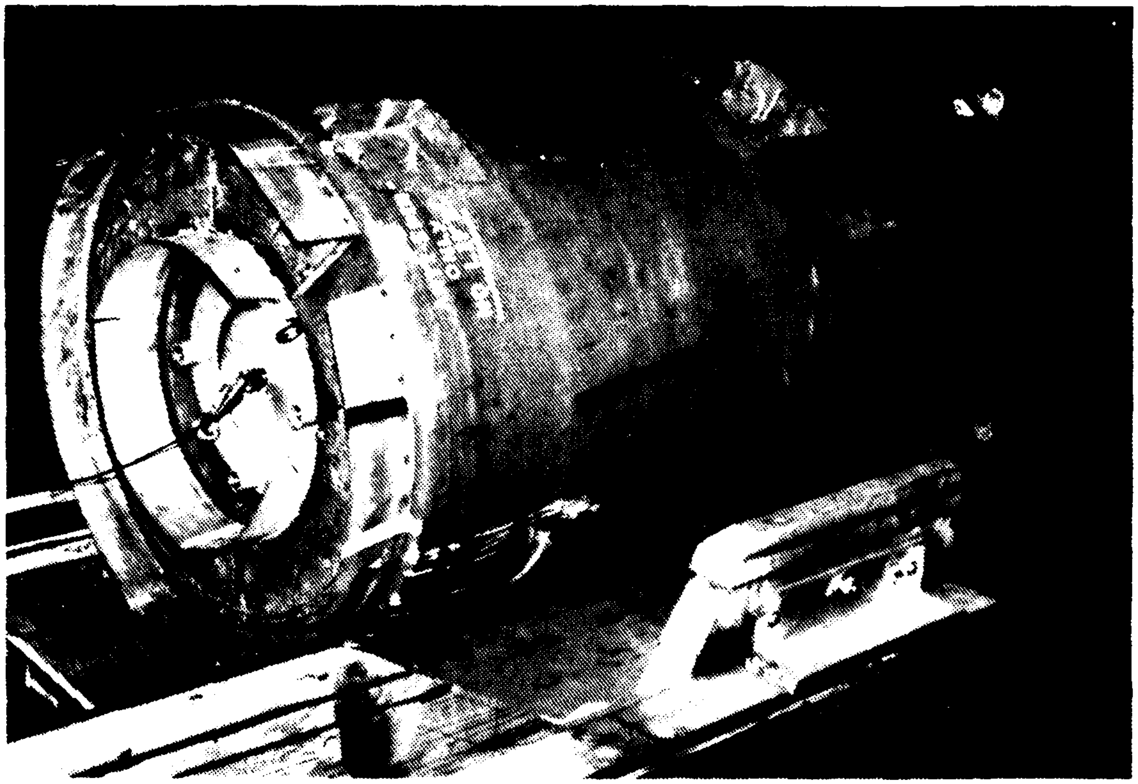

Figure 2-7. Subsurface Buoy

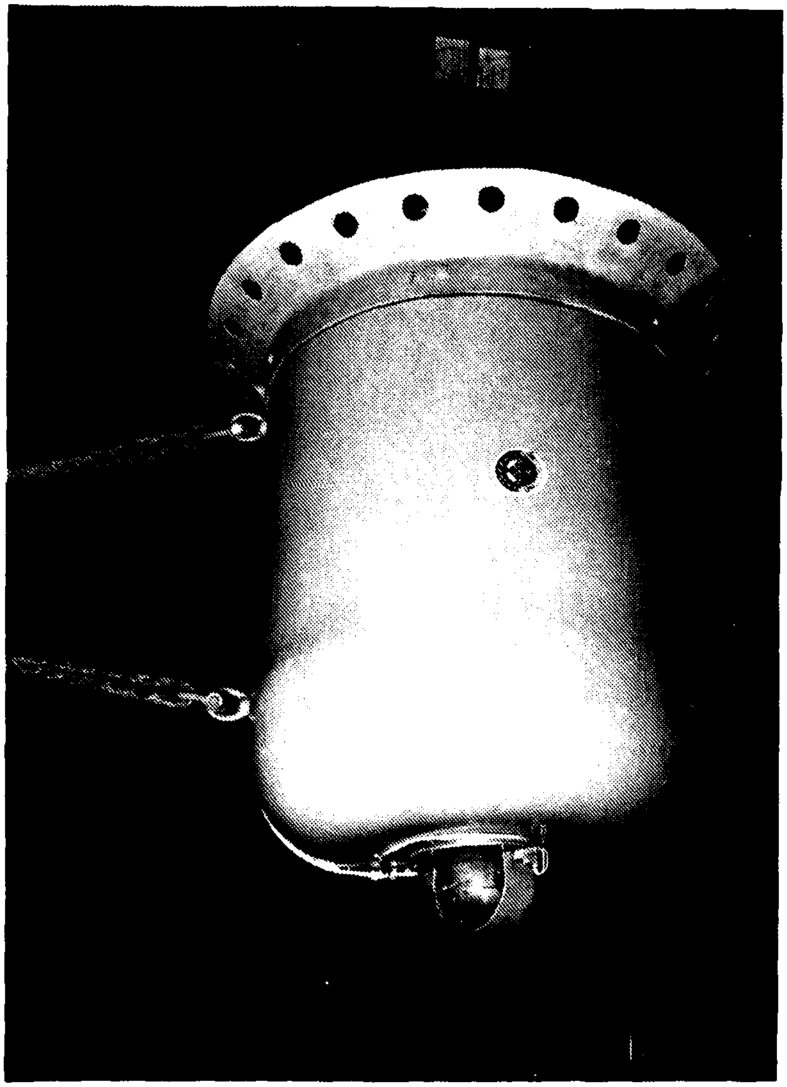

Figure 2-8. Anchor Assembly

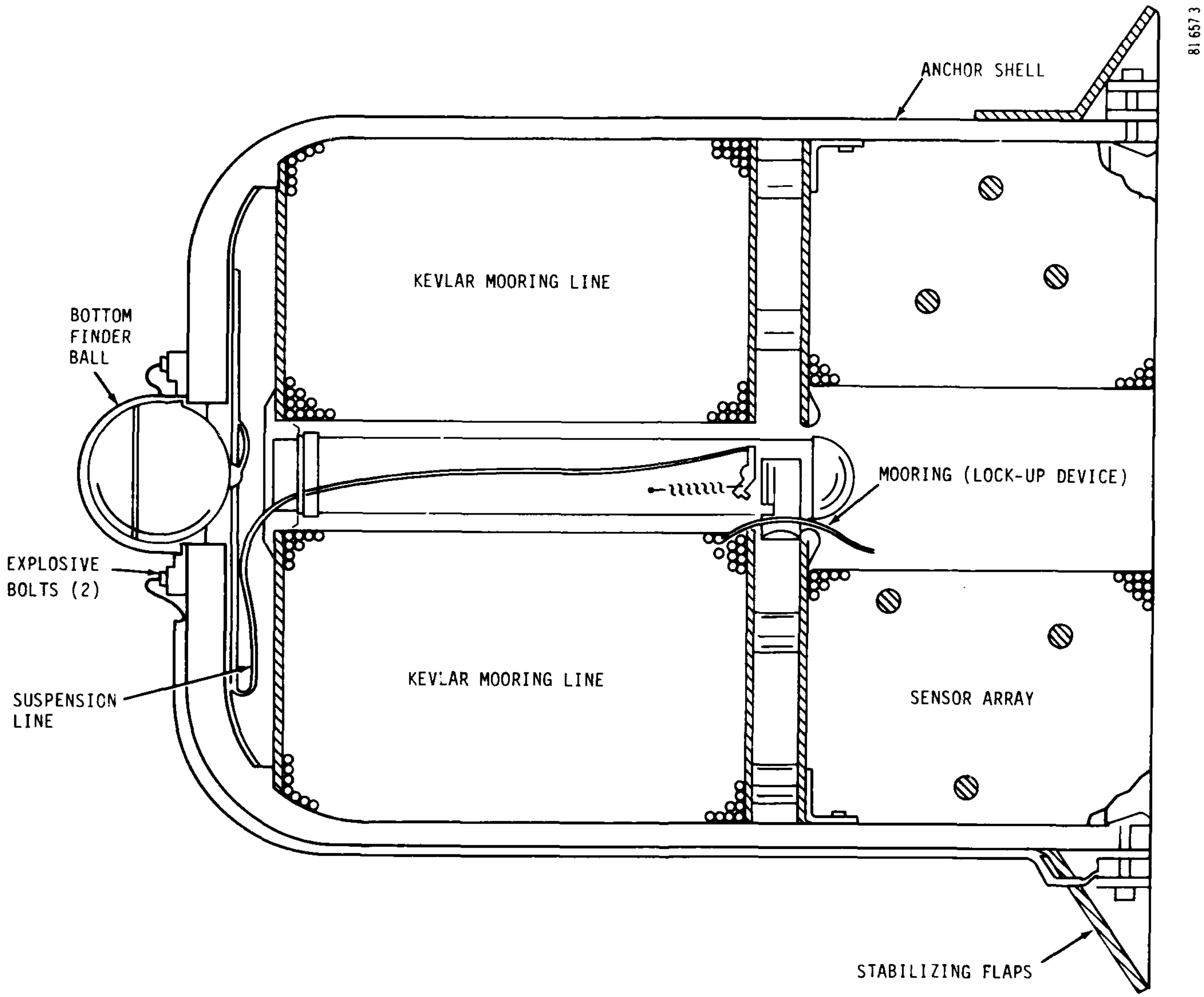

Figure 2-9. Anchor Assembly (Section View)

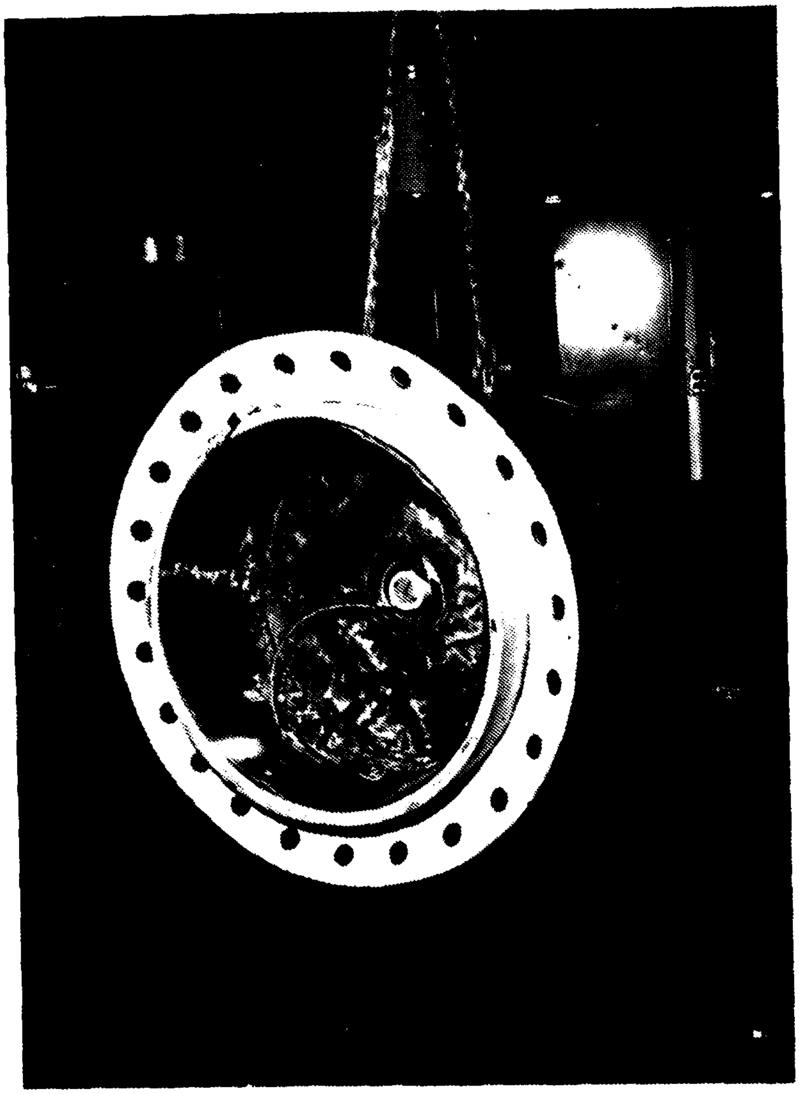

Figure 2-10. Mooring Line and Lock-Up Device Post
(Sensor Array Removed)

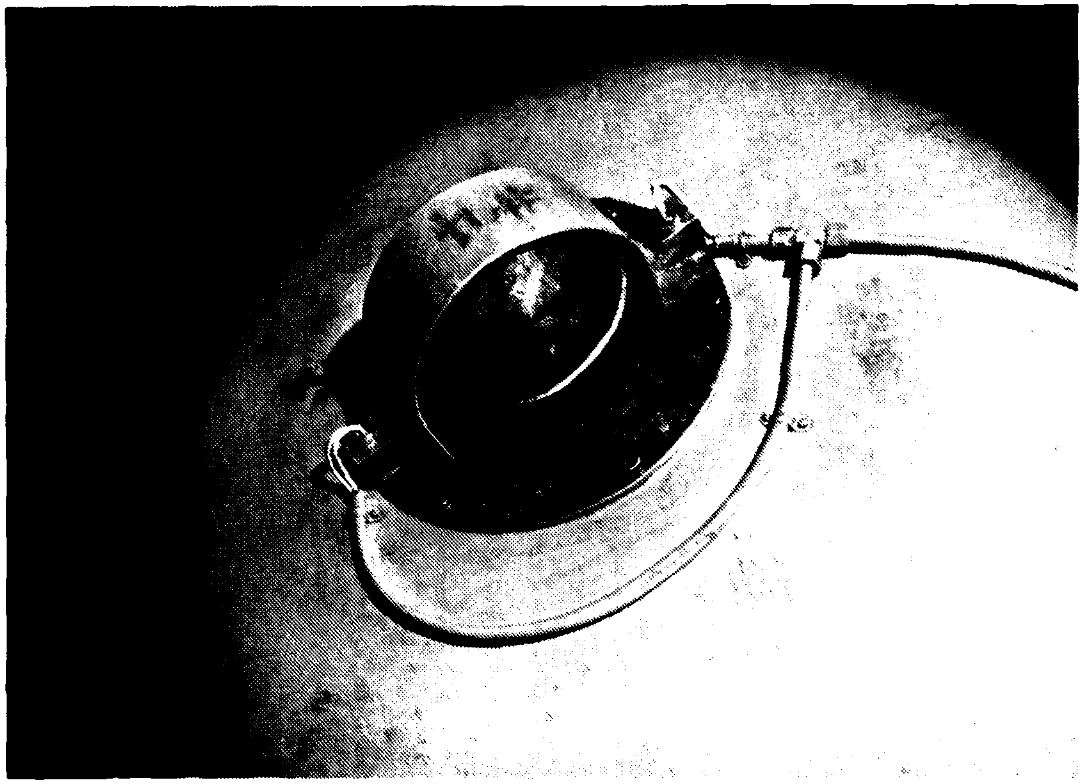

Figure 2-11. Bottom Finder Ball Secured to Anchor Shell

Simultaneously, two explosive bolts securing the bottom finder ball to the nose of the anchor are fired permitting the ball and 120 meters of Kevlar line to descend ahead of the anchor. As the anchor descends, the 1500m sensor array is payed out top end first. When the lower end of the array deploys, a lanyard pulls a pin from the lock-up device which arms it. The Kevlar mooring line then pays out. When the anchor is 120 meters off bottom, the bottom finder ball touches bottom, removing tension in the bottom finder line. This trips the lock-up device, preventing further payout of the Kevlar mooring line. The subsurface float is submerged a nominal 100 meters as the anchor descends to the bottom, allowing 20m for mooring line stretch and other factors.

The electromechanical cable and sensors consisting of 1500 meters of cable and 10 sensors are coiled into the anchor using a "one over/one under" coiling technique to assure that the cable pays out with no turns that could cause kinking. The coils are secured with a special, high-temperature wax in a manner similar to the tether line bonding.

The 4500 meters of Kevlar mooring line are specially wound in a bale that fits into the lower section of the anchor. During the winding process, a turn is induced into the line for each turn on the bale to provide a line with no turns in it when pulled out from the center of the bale. The line is wound using depolymerized rubber (DPR) as a binder which permits a controlled and orderly payout. The Kevlar line is 0.5 cm (0.20 in.) diameter with two contrahelically wound stranded layers which provide torque-balance, covered with a braided polyester jacket, and has a rated breaking strength of 14,600N (3280 lb).

During 1980, the bottom finder operation was analyzed to determine the tension in the line after deployment of the 120 meters of line and before bottom impact. If this tension falls below a critical value (3 pounds), the mooring latch will release before the ball reaches bottom, dragging the subsurface buoy under prematurely. The bottom finder ball weight was increased from 11 Kg to 14 Kg (25 to 30 lb) with a special Kevlar line (3/64 in.) to increase the tension value during descent to 53N (12 lb) - four times the critical threshold value.

Two anchor drops were made from the R/V OCEANUS 33 km west of Barbados, BWI, in 2000 meters water depth to evaluate the mooring line lock-up when the bottom finder ball impacts the bottom. The bottom finder and cable were allowed to deploy completely before releasing the anchor in both drops in order to monitor its operation. The ball and line payed out satisfactorily. On the first drop, the latch released when the anchor was only 400 meters below the surface. The probable cause of premature lock-up was the angle of the bottom finder to the anchor at the time of launch, caused by a strong surface current which allowed the ball and line to stream out away from the ship. When the anchor was dropped, the line formed a bight above the ball, exaggerating the angle of the line at the anchor. This reduced the tension in the line and permitted the latch to trip. In the second drop the anchor was not released until the bottom finder line was vertical. Everything worked satisfactorily and the subsurface buoy was pulled down to a 95 meter depth. Figure 2-12 shows the anchor being readied for launch.

Another ADOM anchor was deployed on February 20, 1981, from the R/V CALANUS in the Tongue of the Ocean, Bahama Islands, BWI. Figure 2-13 shows two anchors prior to getting under way. The objective of this test was to confirm the proper operation of recent modifications. These modifications were: (1) depolymerized rubber (DPR) used as a binder for Kevlar mooring line instead of wax, (2) a new continuous fiberglass flap to replace the original four stabilization fins, and (3) a plastic sheath around the spindle of the mooring latch. The sheath prevents bits of DPR from jamming the latch mechanism inside the spindle. For the purposes of this test, the 1500 meters of EM sensor cable were replaced with 500 meters of Kevlar coiled like the sensor cable and waxed in place.

The drop was made at 25° 22'N and 77° 54.6'W in 500 meters water depth. The anchor was positioned over the stern 0.3m above the water. The bottom finder was released by firing two explosive bolts that hold the ball retainer band. Immediately thereafter, the anchor was released and fell away, paying out the 500 meter length of Kevlar. The bottom finder was calculated to be fully deployed when the anchor reached 226 meters. A lanyard couples the top end of the main Kevlar mooring line to an arming pin on the latch

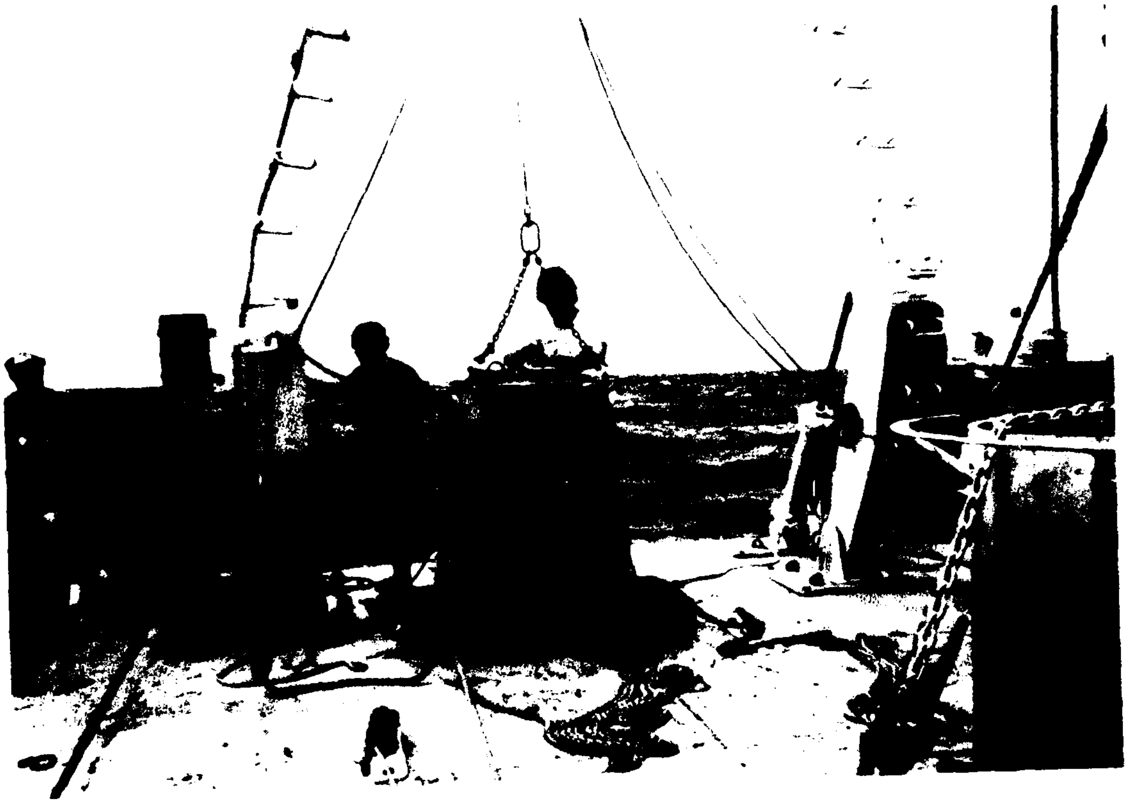

Figure 2-12. Anchor on Fantail of R/V OCEANUS

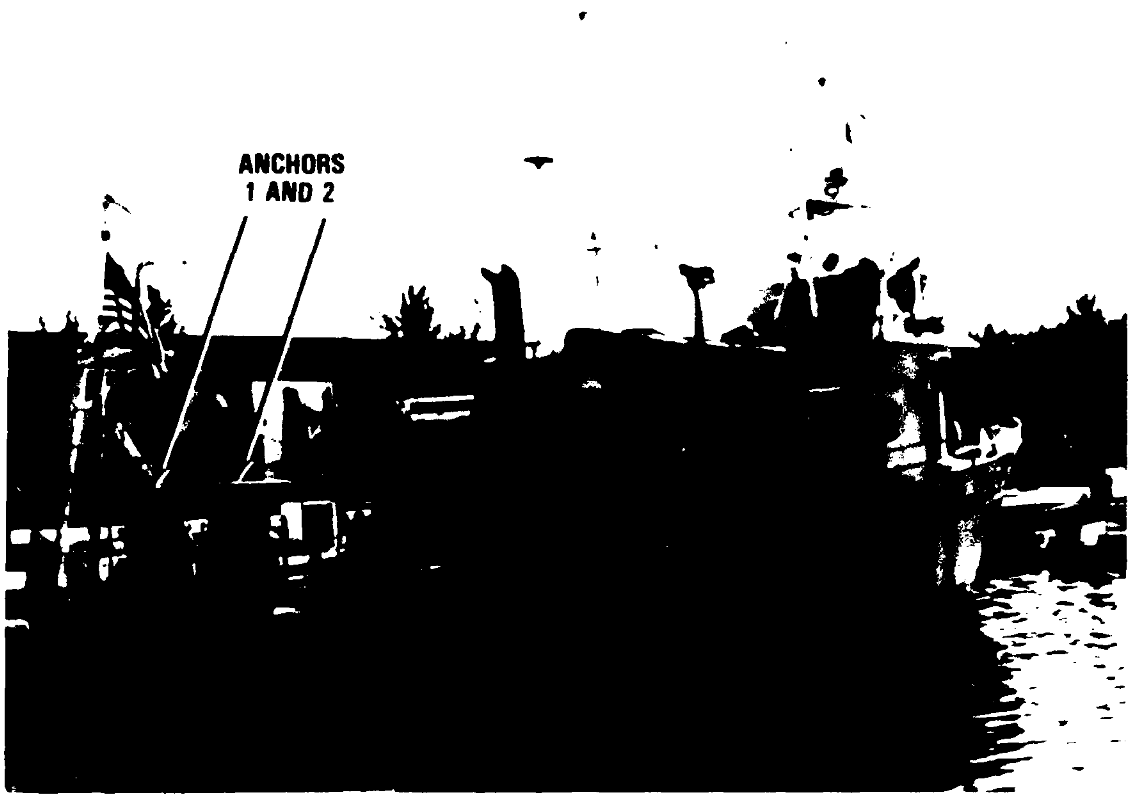

Figure 2-13. Two Anchors Aboard R/V CALANUS

that prevents lock-up until the sensor cable is fully deployed. When the 500 meter length of Kevlar simulating the sensor array was deployed, the interlock pin was withdrawn. As predicted, lock-up was initiated 5 minutes and 22 seconds after launch. The anchor pulled the subsurface buoy approximately 100-meters deep. The measured average terminal velocity of the anchor during fall was 4.26m/sec (14 ft/sec).

A total of six anchor drops have been made over the last 18 months of which four have been successful. Design refinements have been made and launch procedures changed to alleviate the causes of the unsuccessful drops. Based upon the results of these tests, the anchor assembly appears to be a reliable automatic mooring device, ready for integration with the ADOM system.

2.7 ELECTRONIC AND SENSOR SUBSYSTEM

The electronic and sensor system components are shown in Figure 2-14. The ADOM processor along with a data memory and power pack form the central electronic assembly. This assembly is contained in a 20.3 cm (8 in.) outside diameter aluminum-cylinder pressure housing in the ADOM subsurface buoy. The segmented sensor cable is terminated by a cable release mechanism attached to the mooring line. The cable's design allows for insertion of individually calibrated sensors. Above the central processor a cable extends to a surface float and telemetry unit.

An addition to the electronic system that has been made this year is a portable video terminal which can be connected to the final buoy assembly to monitor system operation and to allow updating the real-time clock.

2.7.1 PROCESSOR. The Intersil IM 6100 (CMOS) microprocessor was selected for ADOM. The complete microcomputer is shown schematically in Figure 2-15. The assembly consists of boards which plug into a computer backplane. The boards and their functions are:

AμP Microprocessor, connection to programming;
ARC Real-time clock, interval clock;

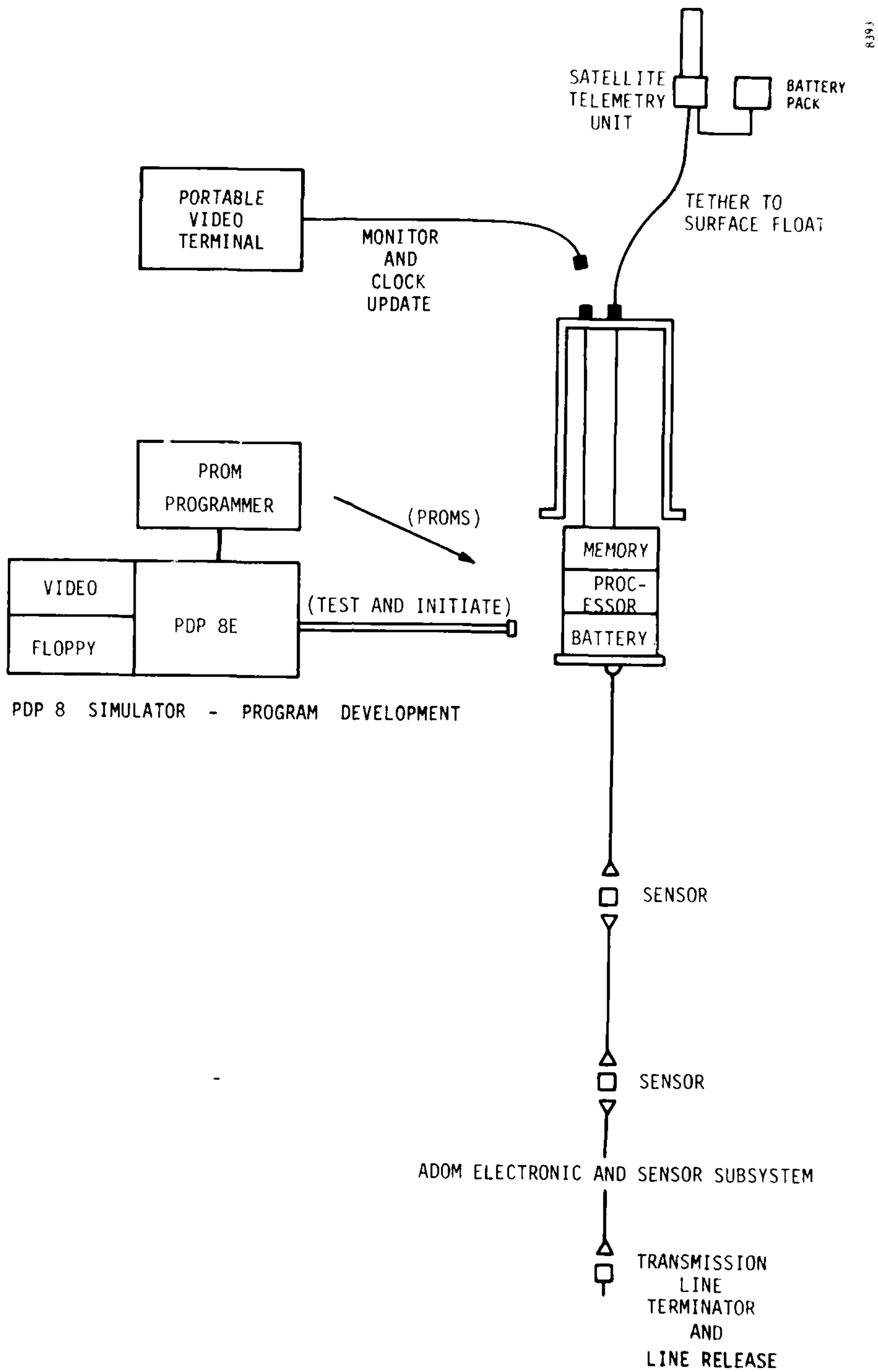

Figure 2-14. The ADOM Electronic and Sensor System

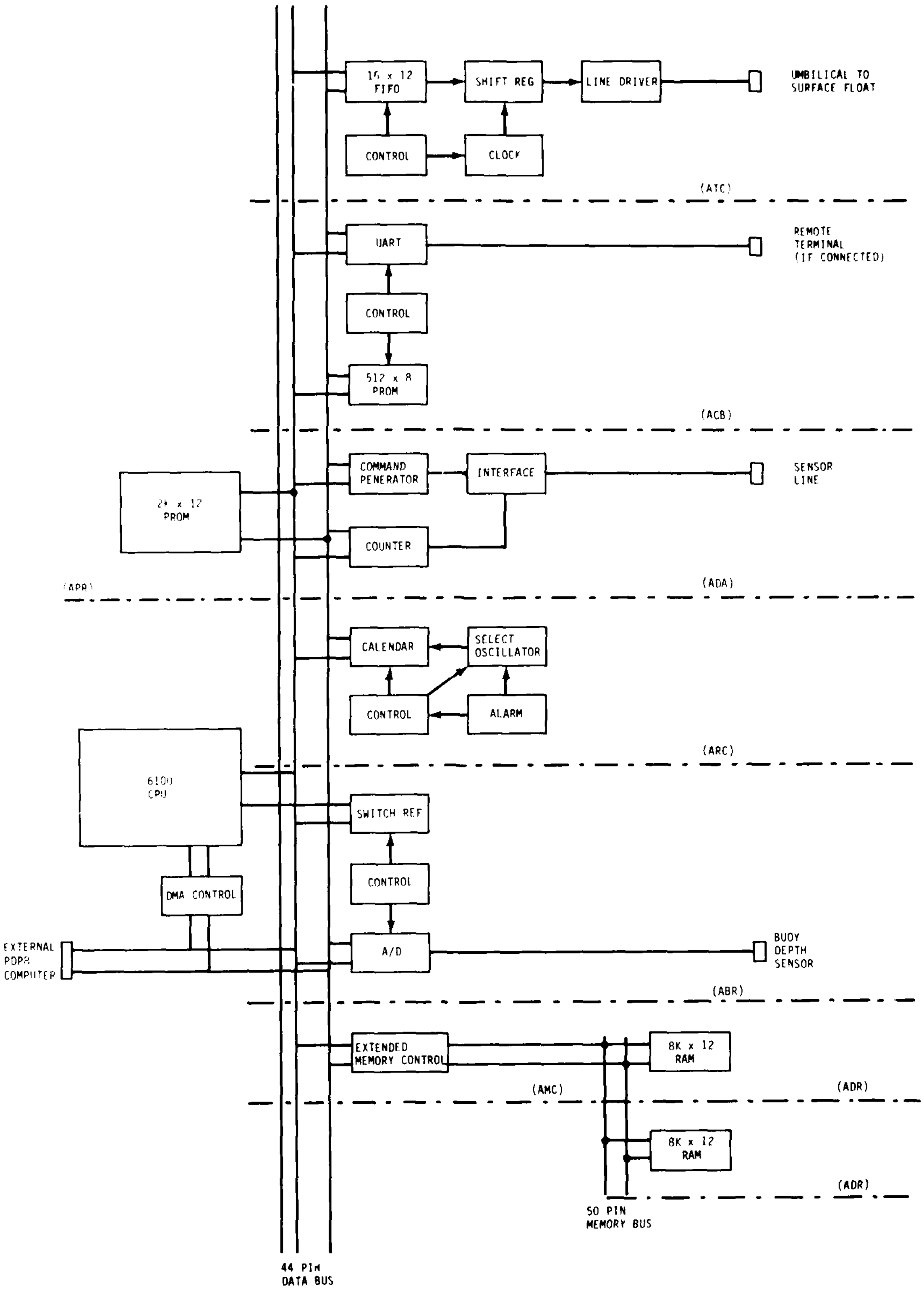

Figure 2-15. ADOM Processor Layout

ADA Data acquisition, sensor operation;

APR PROM, permanent program storage;

ATC Data telemetry control;

AMC Extended memory control;

ACB Interface to external terminal.

Each board uses the same pin connection to the backplane, and therefore, can be placed in any position.

The complete processor is constructed of CMOS components. Originally intended for Metal Oxide Semiconductor (MOS) PROMS, permanent program storage is now in 6653 CMOS Erasable Programmable Read Only Memory (EPROM). Since the 6100 is memory oriented, a working RAM memory is necessary. The computer has the full 32K addressing of the PDP 8 minicomputer, but the total data acquisition can be achieved with 1K of PROM and 1K of RAM for the program.

Software and hardware were developed simultaneously. To facilitate this, a PDP 8 with typical peripheral support was coupled to the microcomputer. Thus, a program can be written (in any language) on the PDP 8. A RAM memory module replaces the equivalent EPROM module and the PDP 8 program is written directly into ADOM. Direct readout of any part of the ADOM memory allows monitoring of the program operation. Special test programs with conventional break points are easily written, and hardware testing is rapid and very complete. Direct printout of the ADOM program and data are quickly effected. Once a program is evaluated and tested, it can be written directly into EMPROMS from the PDP 8, and the EPROM aboard replaced in ADOM. As an example of the speed of the process, a 1K word program was written, debugged, and burned into PROMS in less than 4 hours.

The processor of ADOM has been changed this year in two basic ways. A real-time clock, based on the OKI chip, has been added to the system. This clock is also used as the basic reference oscillator for the system. It has been found possible to obtain a clock accuracy of 1 in 10^6 with simple temperature compensation of the oscillator on this chip. This has resulted in

significant power saving. Since the device is a complete calendar, the software is simplified, especially with regard to transmission of the data through the LES-9 satellite.

It should be noted, however, that the clock accuracy can be achieved only over the temperature range experienced by the buoy during its operation. It is possible, of course, that higher temperatures can occur during storage or flight aboard the aircraft. During this period of time an accumulated error in the calendar can occur. For that reason, a video terminal can be connected to the computer. This allows a direct readout of the computer clock to provide monitoring of the data gathering and telemetry functions. By updating the clock prior to launch, the total accumulated accuracy of 30 seconds per year can be achieved without recourse to higher-powered temperature-compensating circuits.

A second change that has been made to the processor is a new interface module which allows communication with the terminal discussed above. It should be noted that the processor and the arrays can be assembled in any fashion and that their deployment in different locations might require different transmission points within the satellite window. It is felt that having different operating programs for each buoy is undesirable; however, the number of external parameters that can change is now considerable. To that end a CMOS PROM, which we call the "Customizing PROM", has been added to the ACB board. This PROM is programmed for a particular launch situation and buoy configuration and can be changed readily. The main program, which is universal in nature, merely accesses this PROM to obtain the information.

Data acquisition from the addressable sensors is achieved by the technique shown in Figure 2-16. Four sequential tones are generated by the processor. They are superimposed over a DC voltage (used for sensor power) on the cable. The first tone is used to lock a reference oscillator in each sensor to that in the processor. The next three tones (one of eight) are compared with internally generated signals. Hence, there are 8^3 or 512 unique addresses. Increasing the number of tones to 8, a maximum with the existing sensor hardware, allows 8^8 or over 16 million unique addresses.

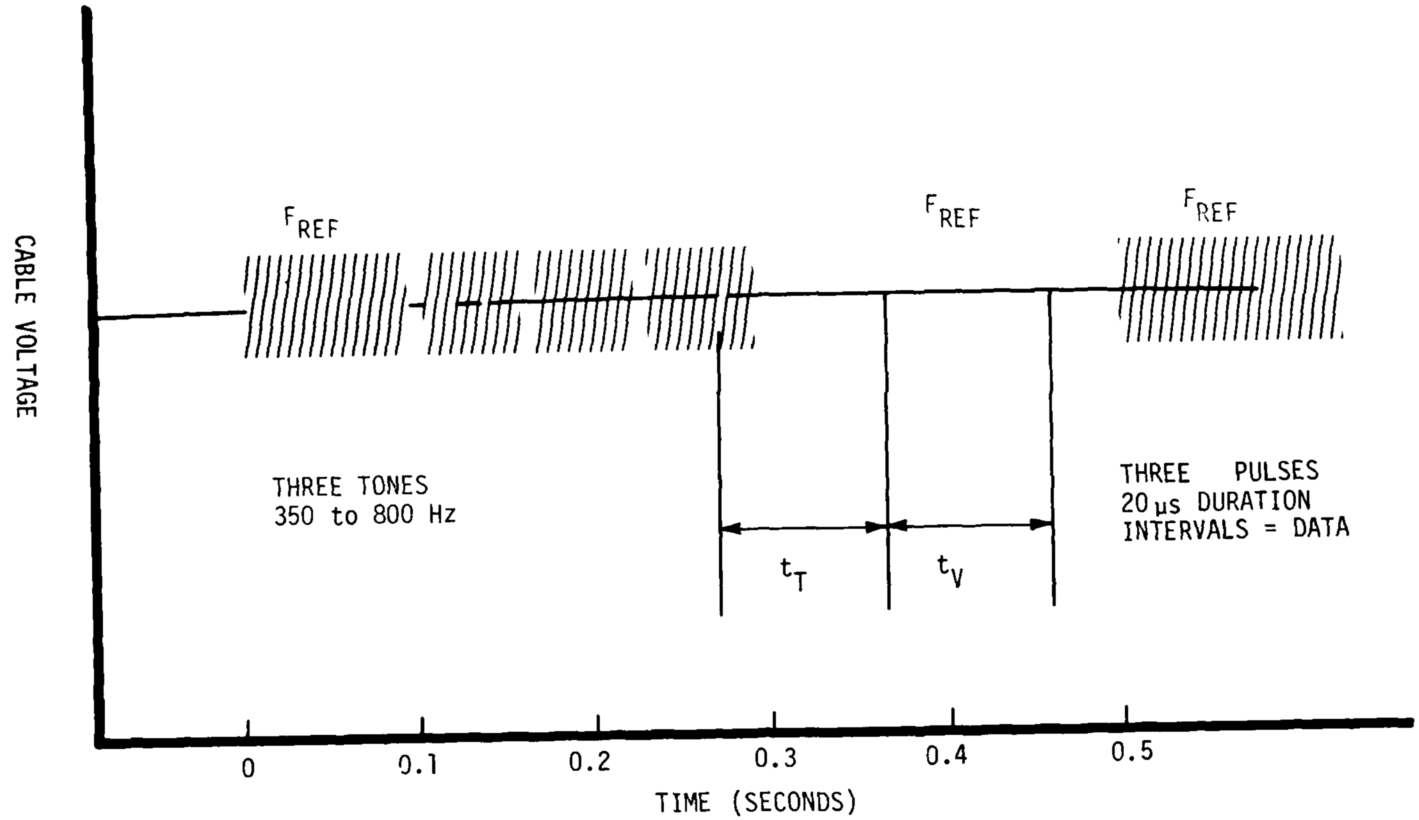

Figure 2-16. Sensor Cable Signals

The addressed sensor responds with three pulses, each of 20 microseconds (μs) duration and with separation times that are a function of temperature and voltage. The first of these allows determinaton of temperature to $\pm 0.1°C$ accuracy. It should be noted that a large unused spectrum exists on the sensor cable and this allows ready addition of other wideband signals simultaneously with the array.

The sensors operate over a voltage range of 3.4 to 8.0 volts with a consumption at 5.0 volts of 500 microamperes (μA). Signal attenuation in the cable limits the total to 180 sensors in a continuous 1500m array.

Considerable effort has been made in reducing the power consumption of the system. A variable speed microprocessor clock, from 7.8 kHz to 1 MHz, is featured, and the microprocessor adjusts its own clock frequency. During intervals between data acquisition and processing cycles, over 90 percent of the total system is in a quiescent state with an internal clock repowering the system after the preset interval. Data acquisition cycles can be fixed, controlled manually, or made dependent on the data. The total processor operates from 3.4 to 10.0V with an average power consumption of about 30 mW (at 5V) for a 12-minute data acquisition cycle.

2.7.2 SOFTWARE. As discussed earlier the ADOM buoys will communicate to the shore station through the LES 9 satellite. This satellite, operated by the United States Air Force, has limited access time available for the ADOM buoys. By agreement with the satellite operators, a 15-minute period from 1400 to 1415 hours (UT) on Tuesdays and Thursdays of each week was accepted as the initial window. With the modification to the processor of the OKI calendar chip it was found possible to reconstruct the software to operate in an entirely different manner.

In previous programs, the data gathering aspect of the program occurred on an even interval but with no specific start time for the first data point. The buoy was to be launched with its incremental clock at 0, a note made at the time of launch, and the buoy would gather data every 12 minutes. Any transmission of the data involved software calculations of the absolute time.

The OKI chip carries the calendar in hardware rather than in software and includes the day of the week in the data. Therefore, the program shown in Figure 2-17 is now used. This program uses data gathering at even intervals following the hour. For example, with a 12-minute data gathering interval the computer would calculate the data gathering points as 0, 12, 24, 36, and 48 minutes past each hour. Other data intervals are programmed into the Custom PROM. Telemetry options are selected through the switch register as once per hour, once per day, once per week, or twice per week with the period following the hour also selected through the switch register. Thus, any buoy can be selected to transmit at a specific period with the periods incorporated into the PROM assembly.

The program now runs once per minute. When seconds equal 0 the program is initiated, reads the switch register, reads the time from the clock and then, based on the time, determines whether to get data, to transmit, or to fire the release. If none of these are opportune, the system sets the alarm for the number of seconds necessary to reach the next minute and halts. If any operation occurs, the correct interval is calculated so the system restarts at the next minute. Thus all data are gathered on the minute. In the event that the external monitor is attached the computer will display the time or, if the input mode is selected, will allow input to the computer. A normal running time each minute is approximately 30 milliseconds. A data gathering period lasts approximately 10 seconds. The transmission period will depend on the amount of data to be transmitted and the baud rate that is selected.

The telemetry of the three buoys anticipated to be in operation during 1981 can be performed sequentially in a 15-minute interval with approximately 1 minute between buoys. This is consistent with our clock accuracy.

Normally access to the buoys is not needed. However, for safety, the buoy release is programmed into the Customer PROM. In the event that the PROM needs to be changed, access to the buoy is necessary. It should also be noted that the operation of the buoy recognizes the volatility of data in RAM, and in the event that this data is damaged, the buoy would continue to operate reestablishing RAM information on a new basis.

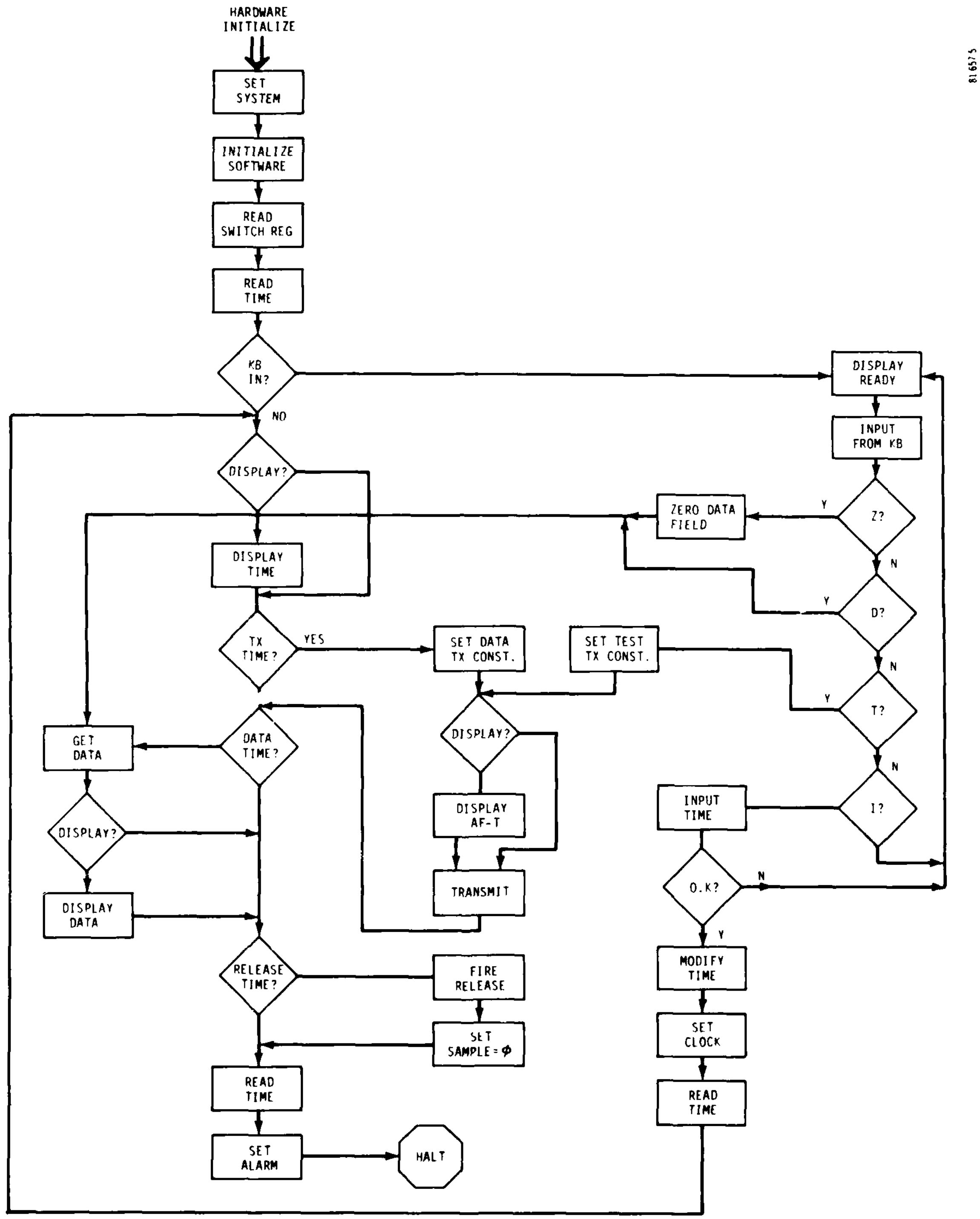

Figure 2-17. Basic ADOM Software

2.7.3 DATA MEMORY. Solid state memory stores sensor data for transmission via satellite link to shore. The size of this depends directly on the operating mode of the system. Access to the satellite is expected to be once or twice a week; data storage for 8 days is provided. Since approximately 10^5 bits of data per day would be expected (if the temperature array contains 50 sensors) then 8×10^5 bits are needed for the 8-day requirement.

The choice of components for the design of the memory was dependent on the packing density and the cost. After review of existing components, the HITACHI 4315P CMOS RAM was selected. This package contains 4K of memory as a 4K x 1 array, and 12 are needed to provide 4K words (12 bits). It was found possible to pack twice this amount on a single board. The board then contains 8K x 12 bits or approximately 10^5 bits, corresponding to one day of data accumulation. The rack is sufficiently large to contain 12 boards or 12 days of data. This was found to be adequate for all immediate applications.

Competition in the marketplace has caused a drastic reduction in the price of these chips. This is typical of electronic chips, and was a major reason why the CMOS RAM was selected as a component for the system.

The cost per bit is now approximately 0.12 cents and this is expected to reduce further in the future. It should be noted that the bubble memory devices have always been actively evaluated as possible components for this system. However, even though some cost reductions of these devices have been achieved, it is still not cost competitive with the CMOS RAM. A new board design using the competetive Harris chip has been made and would allow both devices to be incorporated into the system at any time.

It should be pointed out that the software and hardware are directly expandable to provide much large memories. The memory is directly addressable by the processor; it uses the same addressing and operating instruction for the 32K of memory as does the standard PDP 8E. An additional 3 bits

(called the data area) selects areas of data each equivalent to the 32K of data. Only a single additional instruction is needed to select the data area. The engineering and technology for larger memories has been developed. With the present scheme, a maximum of 256K x 12 bit words is directly addressable. This corresponds to 3 x 10^6 bits of data. An additional single instruction would allow an additional factor of 8 to be included.

An important change has been made to the processor. The processor now uses a different physical bus structure than that earlier employed. The new bus uses flexible cable for the conductor with card edge connectors which are pressed into place. The conductor reliability, using 3M Scotch-Flex components, has been excellent, and the cost of components is identical to the earlier arrangement which used 44 pin connectors soldered into a motherboard; however, the manufacturing time has been reduced considerably, and this reduces the cost and the skills needed.

Some 4000 hours of processor operation and approximately 2000 hours of memory operation have been achieved so far. The first field test of the processor array was carried out aboard a 28-foot boat. Completely satisfactory operation of the processor was achieved.

2.7.4 SENSOR ARRAY. The sensor decoder uses digital techniques. Each frequency received is compared with one generated in the decoder itself. The local oscillator is set by sampling a reference frequency. From one to eight pulsed tones are possible with only simple wire jumper changes needed to select the number and the actual address. The frequency bursts can be on the order of 50 ms in duration, but must have a 5 ms gap between tones. An important factor is that the decoder works over a cable voltage range of 4.1 to 7.5V, and this eliminates the need for voltage regulation with its attendant increased currents.

The temperature sensor is quite simple. A 4548 CMOS pulse generator uses a thermistor for the timing circuit. The resulting pulse is differentiated to provide timing pulses at the start and stop of the 4528 pulse. Accuracies on the order of 0.1°C over the range 0-30°C are achieved, and

this becomes 0.01°C with suitable correction for the supply voltage variation. To determine the voltage, each sensor also transmits a pulse, the duration of which is a function of the supply voltage.

Considerable effort was expended in minimizing the sensor package dimensions since any increase in these would cause the overall sensor package to increase. The actual electronics assembly measures 48 mm x 26 mm x 22 mm, not including the connector pins. Conventional Dual In-Line Pins (DIP) packaging is used for the nine integrated circuits which comprise the sensor. The dimensions could be reduced by employing hybrid construction of the bare chips themselves but was not deemed necessary at this time.

The sensor housing and the cable terminations are constructed of hard anodized 6061- T6 aluminum. The cable terminations are held in place with threaded sleeves and the whole assembly locked in place, after assembly, with a pin that also provides the ground connection. A polyurethane boot at each end streamlines the assembly and smooths deployment.

As an initial test, 10 sensors were assembled into a 1500-meter array and individually pressure tested to 3000 psi in a test rig. All sensors worked satisfactorily. The array was deployed over the side of a vessel. Approximately two-thirds of the array were deployed for a period of 4 hours. No problems with the sensors under the combined pressure and tension were observed. Tensile tests of the sensor showed that it is as strong as the cable.

An explosive release was designed and tested for the lower end of the sensor array. A small explosive bolt is used in the assembly. This bolt is fired by applying a voltage of 14.5 volts to the sensor array. It is possible to evaluate or fire the release from the processor, or an external voltage will cause release. The release has a tensile strength of 3000 pounds.

Two sensor arrays have been constructed to date. The first of these was deployed during a Drift Test, but was damaged through failure of another component. It has been fully repaired. The modular construction of the

array simplifies such reconstruction. A third array will be constructed during this coming year so that three complete systems are available.

2.7.5 BATTERY PACK. Tests on Lithium D cells at 20°C and -40°C continued. Tests were made at 500 mA, 8 mA and 0.75 mA cell current, and at duty cycles consistent with the above for nominal 1-year operation for telemetry, processor, and memory operation, respectively. All batteries have been fully depleted. The Mallory batteries outperformed Power Conversion, Inc. (PCI) cells under all conditions. At the high current level, approximately 14 percent reduction of available energy occurs when the operating temperature is reduced from +20°C to -40°C (see Table 2-1).

Using these tests and the data observed during calibration of the hardware, 24 Lithium D cells have been specified to power the processor and another 24 Lithium D cells power the telemetry. This will be sufficient to power the ADOM system for well over one year.

TABLE 2-1. LITHIUM BATTERY TESTS

		MALLORY J/Gm	PCI J/Gm
Low Current (0.8 mA)	- 40°C	1220	1150
	+ 20°C	1060	1060
Med Current (8 mA)	- 40°C	1150	980
	+ 20°C	1170	1030
High Current (500 mA)	- 40°C	680	460
	+ 20°C	760	580

2.7.6 TELEMETRY. As originally conceived, telemetry to an aircraft over the buoy was an anticipated mode of data recovery. With increasing confidence in the survivability of the surface mooring and with increasing operating costs of the aircraft, a decision was made to use an RF data link via the U.S. Air Force LES-9 satellite. Discussions with the satellite operators

indicated that operation during a limited period would enable the satellite to be switched to a medium bandwidth operation. Tuesday and Thursday of each week from 1400 to 1415 hours (UT) were the initial proposed access periods, with more intense activity planned during early ADOM launches. Calculations indicated that with a 20-watt transmitter and a volute antenna (3 dB) the signal to noise at the satellite would be somewhat better than 10 dB for a bandwidth of 14 kHz.

The transmitter is combined with the antenna into a single sealed unit. It is encased inside the surface buoy during launch and is erected by a spring on release of the parachute.

The transmitter begins operation on receipt of the modulation. As an added feature in the event that the transmitter is below the ocean surface, an internal measurement of the reflective power from the antenna turns off the transmitter and indicates to the processor through the modulation line that transmission is not possible.

The design of the transmitter was completed and a prototype device manufactured during calendar year 1980. Measurements indicate a power output that peaks at about 24 watts for a 30-volt supply and with a linear variation of output power with voltage. This allows operation at reduced power without changing the transmitter design. Frequency stability was achieved using a temperature compensation circuit applied to the basic oscillator, and this was found to be well within the required range of ±200 Hz. Figure 2-18 shows the outline of the transmitter and Figure 2-19 shows the prototype. Figure 2-20 shows the performance in terms of the supply voltage. Measurements at intermediate frequencies used during the multiplying stages indicate all other outputs are at least 50 dB below the primary output. A frequency of 303.150 MHz was selected so as to stay within USAF authorized frequencies.

Concurrent with the above development a shore station was assembled to receive telemetry from the satellite and to convert the data into useful information. Figure 2-21 shows the principal components of the shore station. A helix antenna is adequate for these purposes and was placed on a steerable

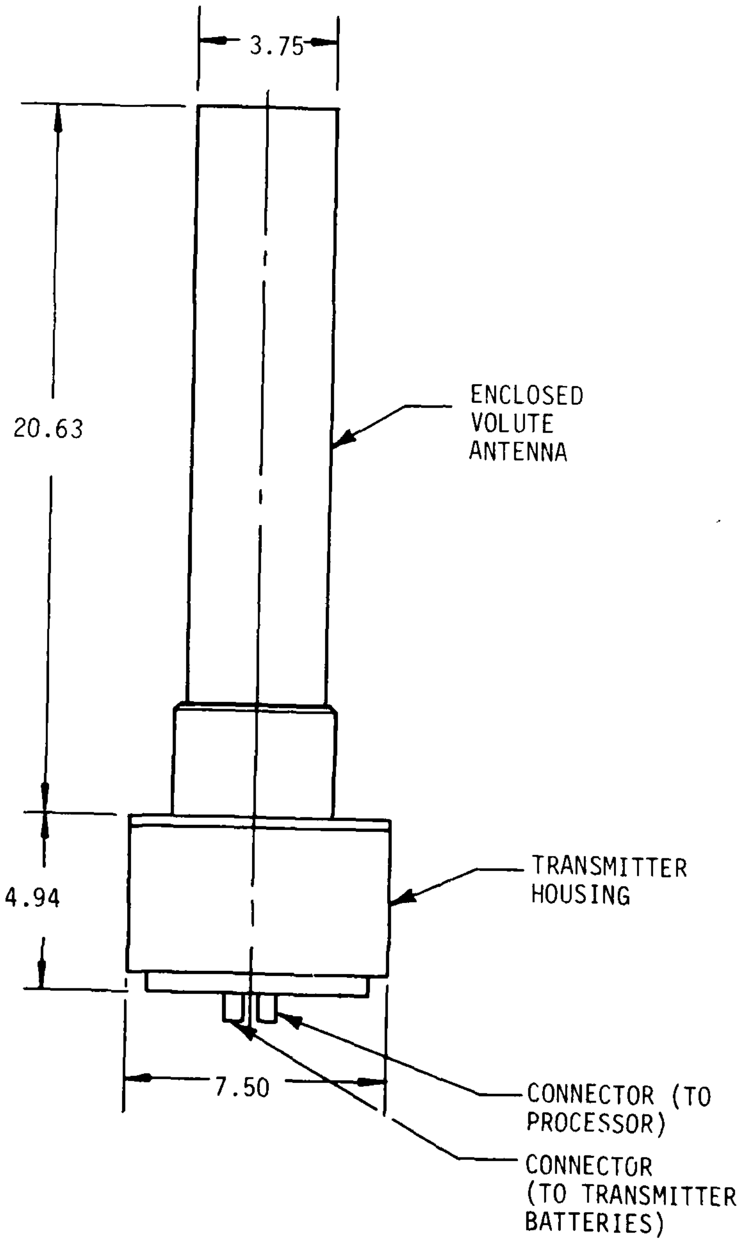

Figure 2-18. Satellite Telemetry Assembly

Figure 2-19. Transmitter

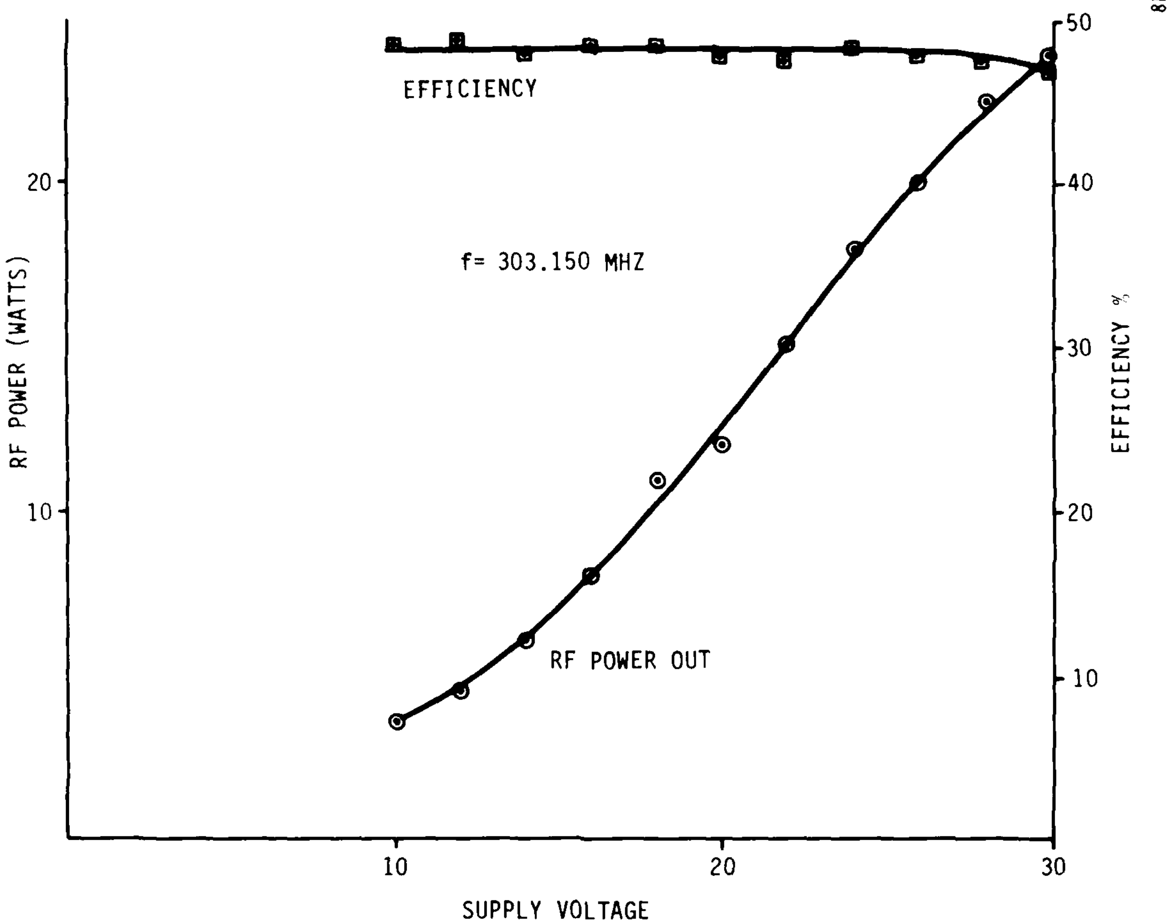

Figure 2-20. Transmitter Power

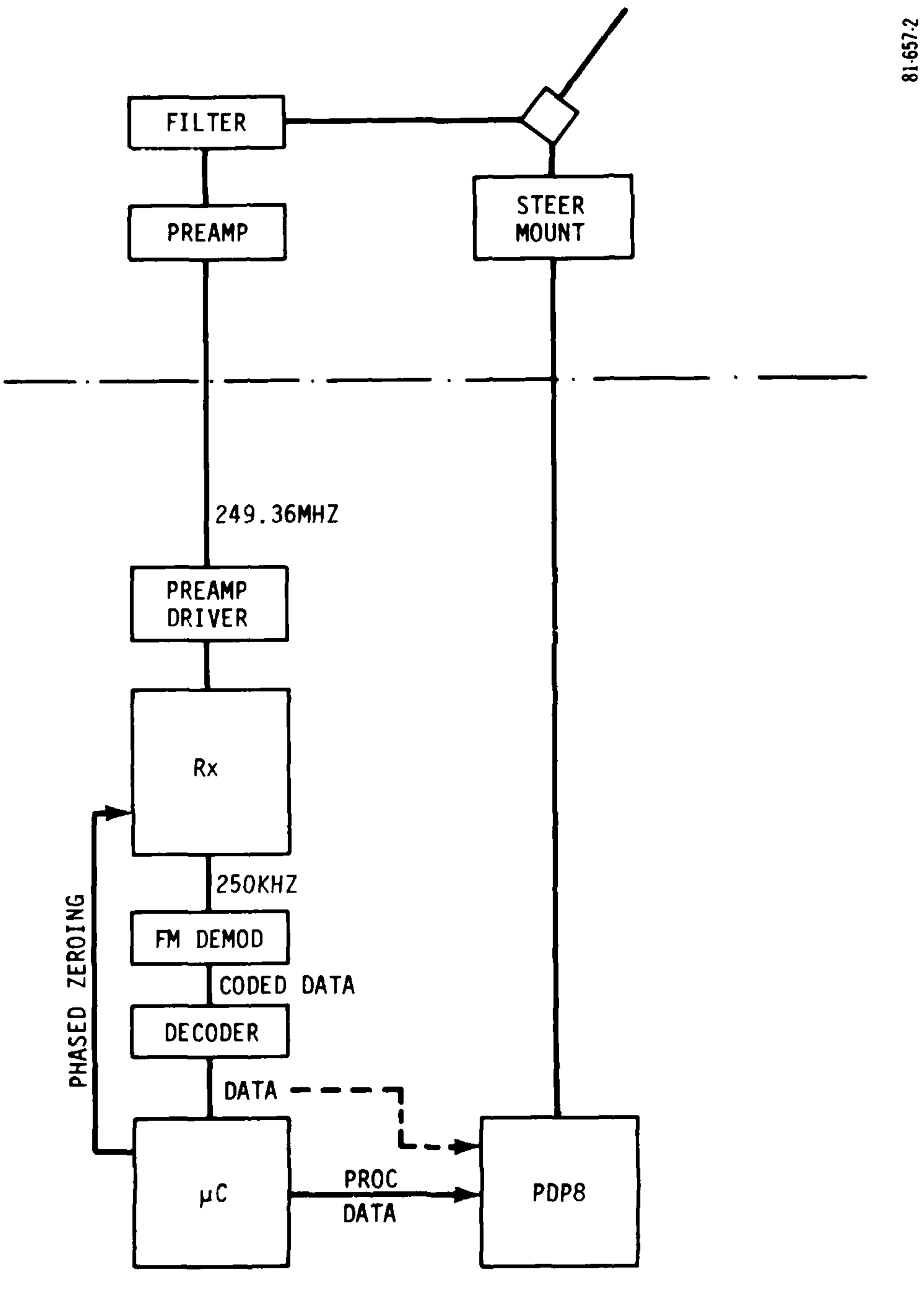

Figure 2-21. Shore Station

mount so as to follow and track the satellite. (It should be observed that LES-9 is geosynchronous but not geostationary and moves relative to the earth in a slender figure "8" such that the longitude remains nearly constant but the latitude varies from 25° north to 25° south.) A sharp bandpass filter was necessary to isolate signals from local commercial stations and a low-noise preamplfier allowed for a connection to a receiver in the lab. A decoder capable of decoding signals with low bit error rate (BER) with S/N greater than 6 dB was designed and the data input to a computer. The receiver is a service monitor, slightly modified, and allows the monitoring of signal strength and noise levels.

A computer program was written to calculate the position of the satellite, its elevation and azimuth from the shore station by Key Biscayne, Florida; and to compute the uplink and downlink signal levels. A sample printout is shown in Table 2-2. The computer also is used to examine and decode the input data as well as calculate bit error rates.

Early in calendar year 1981 some transmissions were made through LES-9 with the transmitter located on the roof of the building adjacent to the receiver antenna. No interference between the two was observed but the signal back from the satellite exhibited poor S/N. Initial indications were that the best value was approximately 3.5 dB; 7 dB lower than expected. The experiment was repeated with the satellite at both low and high elevations.

As a result of the rather disappointing measurements, the transmitter was disassembled and completely retuned with a slight increase of approximately 1 dB in the output power. The experiments were repeated with the transmitter mounted in a surface buoy moored in Biscayne Bay (Figure 2-22). This experiment verified that the roof mounting with an artificial ground plane was a reasonable simulation of ocean conditions. Experiments at 31° and 45° elevations were made giving a best signal noise of 5.7 dB. The experiments were continued by coupling the transmitter directly to the helix antenna on the roof. MIT Lincoln Labs measured the signal strength received at the satellite. As an additional check, data from a FLTSATCOM satellite with known signal strengths were received. These signals had the signal strength expected. It should be observed that the downlink power from LES-9

TABLE 2-2. COMPUTED SATELLITE INFORMATION

DAY (JULIAN)	57	SATELLITE LONGITUDE	97.8 W
TIME (ZULU)	18 37 0	SATELLITE LATITUDE	8.2 S
ANTENNA ELEVATION	46.8	ELEVATION NUMBER	3.2
ANTENNA HEADING	209.1	HEADING NUMBER	3.5

SYSTEM PERFORMANCE	UPLINK	DOWNLINK	
POWER OUT	43.8	44.3	DBM
ANTENNA GAIN	2.8	9.7	DB
EIRP	46.6	54.0	DBM
PATH LOSS	-173.5	-171.9	DB
POWER AT ANT INPUT	-126.9	-117.8	DBM
ANTENNA SYSTEM GAIN	9.7	30.0	DB
POWER AT RECEIVER	-117.1	- 87.8	DBM
NOISE AT RECEIVER	-128.0	-103.1	DB
SIGNAL/NOISE	10.9	15.3	

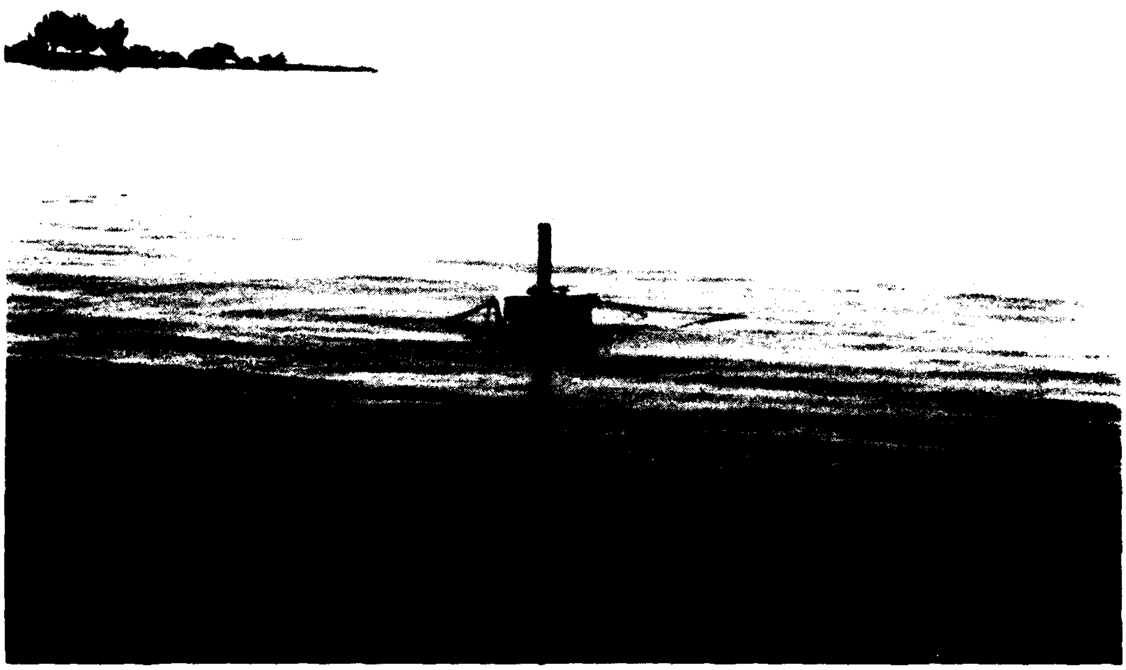

Figure 2-22. Telemetry Tests from Surface Buoy

was also as expected. Hence the poor performance was attributed to a high output noise at the satellite. Measurements by Lincoln Labs indicated that the received signal strength at the satellite appears to be 26 dB below that expected. Accordingly, with the present hardware the best S/N appears to be 5.6 dB at low satellite elevations and 5.7 dB at its upper elevation. A summary of some of the tests is shown in Table 2-3.

As a result of these experiments, a new decoder is being designed that should enable decoding of signals of -2 dB S/N and with bit error rates about 10 ppm. If this is achieved, then the link can be used with no further hardware changes.

2.8 DECELERATOR ASSEMBLY

The Navy PCU-8/A parachute is used as a decelerator for the Open Ocean ADOM. The PCU-8/A system consists of a pilot parachute attached to a deployment bag containing a two-stage main parachute. The pilot parachute is a 1m (3 ft) diameter ribless guide surface canopy and the main parachute is a two-stage 10.4m (34 ft) diameter conical ringslot parachute. This decelerator system, when used on a 1100 kg (2400 lb) OO-ADOM buoy, will have a terminal descent velocity of 20 m/s (65 ft/s).

Figure 2-23 shows the ADOM parachute attachment and jettison assembly. Each riser line of the PCU/8/A main parachute is attached to one of the four cross arms using a high-strength bolt. This cross is then attached to the ring by two 19 mm (0.75 in.) explosive bolts. The ring is threaded onto the center tubular structure of the surface float. A lightweight protective shield contains the riser lines and protects the parachute during transport and launch. The bolt firing circuitry is contained in a box mounted between the cross arms. Upon water impact, saltwater batteries power the firing circuit. The bolts separate, releasing the parachute, cross, and electronics box from the ADOM buoy.

Figure 2-24 shows the ADOM tiedown technique, as well as the rigging required for air deployment. The buoy is shown in a parachute-first/anchor-last launch position. The ADOM sits on a reinforced wooden pallet which is compatible with the C-130 cargo roller system. The ADOM is

TABLE 2-3. SOME PRELIMINARY TELEMETRY RESULTS

		Transmitter			Shore Station		Signal At Satellite**	
Date	Satellite	LOC	Elev (deg)	Po (dBm)	Signal (dBm)	S/N (dB)	Measured (dB)	(Calculated) (dB)
1/ 5/81	LES-9	Roof	35	42.2	-88	3.5		
1/ 7/81	LES-9	Roof	34	42.2	-88	-		
1/ 9/81	LES-9	Roof	33	43.0	-88	4.1	-120.3	(-118)
1/ 9/81	LES-9	Roof	42	43.0	-88	4.9		
1/13/81	FLTSATCON	-	-	-	-82	-		
1/16/81	LES-9	Bay	31	43.0	-88	4.6		
1/16/81	LES-9	Bay	45	43.0	-88	5.7		
2/13/81	LES-9	Roof*	29	42.6	-	-		
2/13/81	LES-9	Roof	41	43.8	-88	5.5	-111.7	(-108)

* Connected to HELIX (13 dB antenna gain).

** Per Lincoln Laboratory.

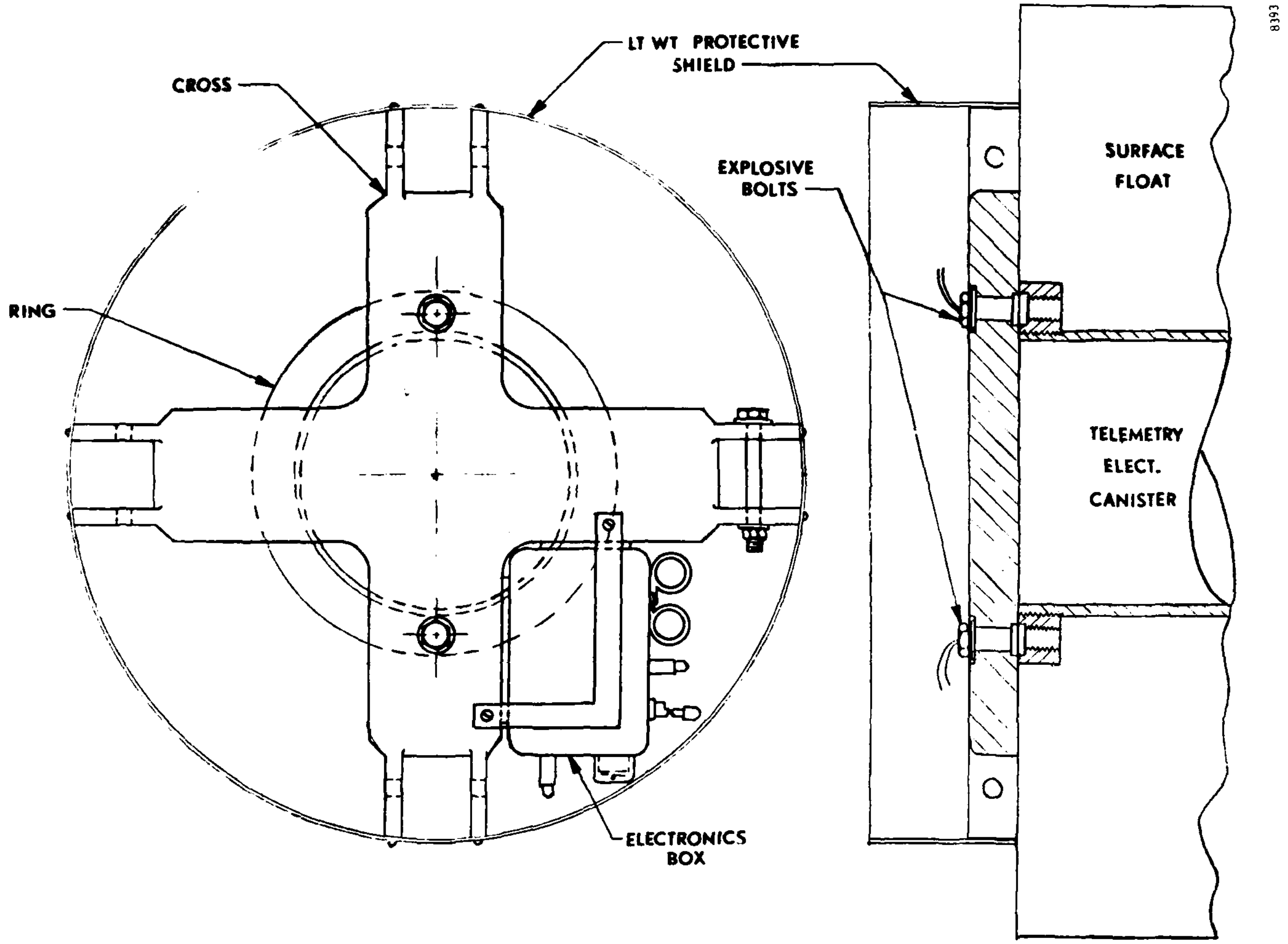

Figure 2-23. ADOM Parachute Attachment Assembly

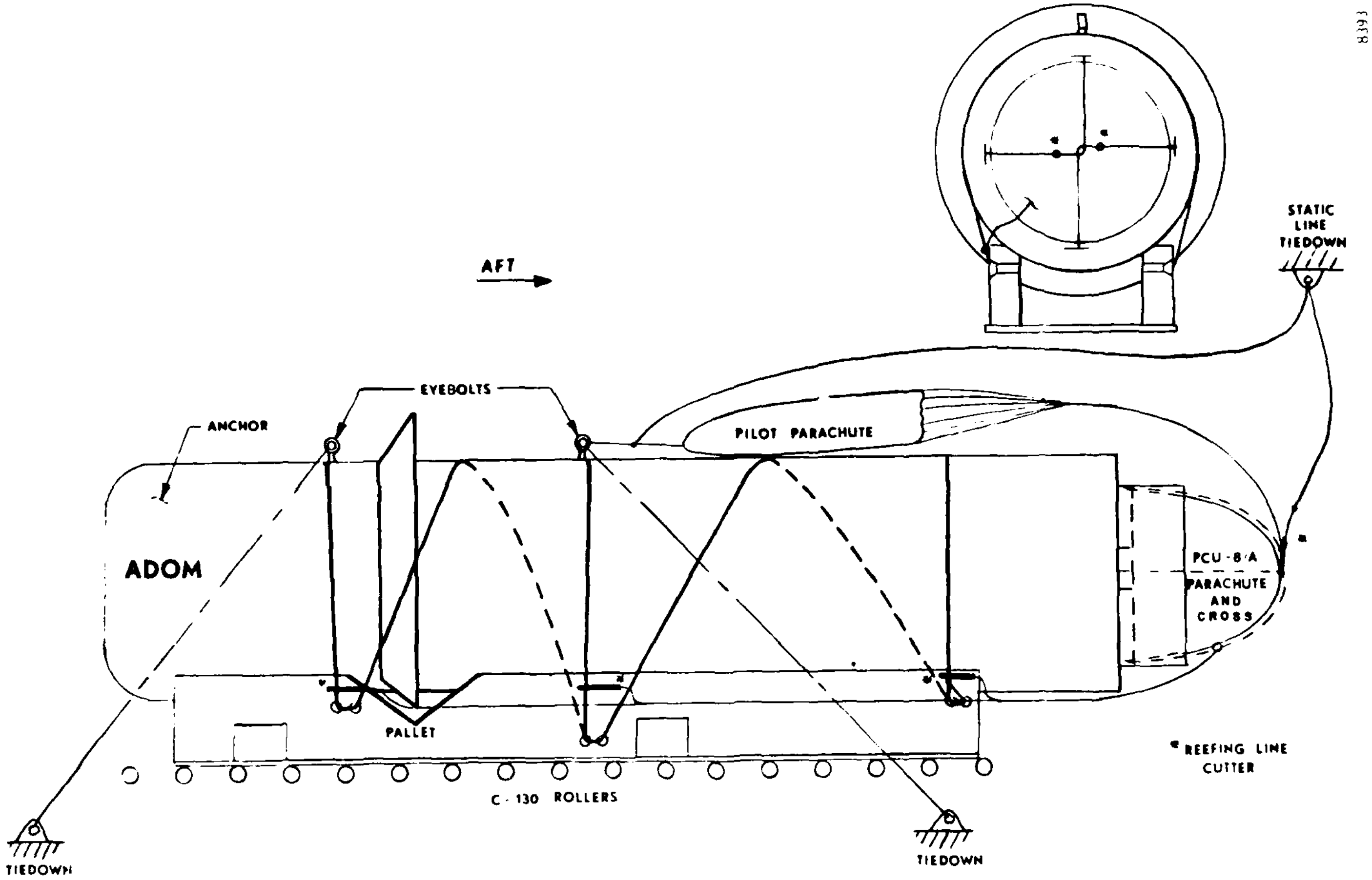

Figure 2-24. ADOM Rigged and Secured Aboard C-130 Aircraft

restrained during transport by heavy chains run from eyebolts on the ADOM to the C-130 floor tiedown rings. The eyebolts are spaced 38 cm (15 in.) on either side of the center of gravity, similar to those for a store to be suspended from a bomb rack. The parachute and attachment cross is shown in position on the ADOM. The parachute is held in this position during transport and the initial seconds of air descent by two crossed lines attached to the ends of the parachute cross arms. Pyrotechnic cutters shear each restraint line to deploy the parachute after the buoy clears the aircraft. A continuous line zig-zagged over the ADOM buoy attaches the buoy to the pallet. Three explosive line cutters, initiated by the parachute deployment, sever this line, releasing the pallet before water impact. The pallet release, parachute release, and parachute jettison all feature redundancy in their design for high reliability.

The pilot parachute is laid in a bag on top of the unit and tied to the aft eyebolt with a light line. A heavy static line, attached to the aircraft, retains the pilot parachute deployment bag in the aircraft. As the ADOM unit rolls out the aircraft ramp, the pilot parachute is extracted from the bag and aligns with the airstream.

Figure 2-25 shows several stages of the ADOM deployment from the C-130 aircraft. In Step 1, the ADOM unit is inside the C-130, tied down for transport, the Aircraft static lines attached. Shortly before launch, the heavy restraints are removed and the buoy is restrained by a single quick-release strap. At launch, the strap is released and the ADOM rolls out of the aircraft and off the ramp as the plane climbs. As it leaves the aircraft (Step 2), the pilot parachute is released and the two explosive line cutters are armed by the static lines attached to the aircraft. A pyrotechnic delay in the cutters prevents their firing until 1.5 seconds after launch. The buoy descends under the pilot chute (Step 3) for this period. When the cutters sever the parachute containment lines, the main parachute deployment bag is released (Step 4). The pilot parachute extracts the main canopy from the deployment bag while simultaneously arming three cutters on the pallet attachment line. At first, the mouth of the main parachute is

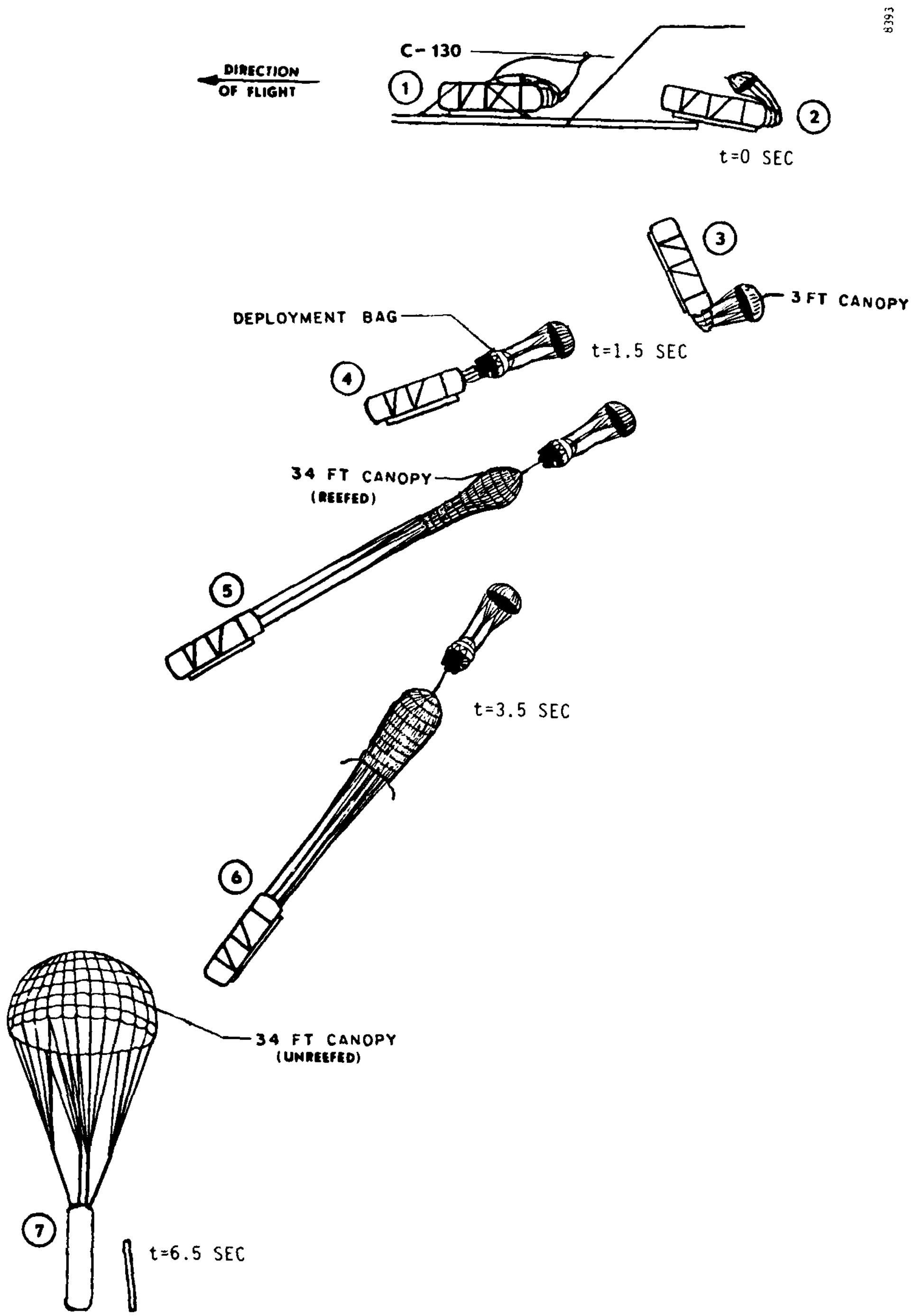

Figure 2-25. ADOM Deployment Sequence

constricted to a smaller diameter by a reefing line (Step 5). After 2 seconds in the reefed condition, two explosive reefing line cutters allow the main canopy to open fully (Steps 6 and 7). Approximately 3 seconds later, the pallet is released and falls away from the buoy. Upon water impact, explosive bolts fire releasing the parachute from the unit. The entire deployment sequence was demonstrated successfully in 1979. During 1980, two pallets were fabricated incorporating modifications determined from the 1979 tests, and the decelerators were refurbished.

2.9 DRIFT TEST

This test was conducted to verify separation of the anchor, subsurface buoy, and surface float, as well as deployment of the sensor array and tether cables. A simulated anchor housed the sensor array and provided sufficient weight to submerge the main buoy. It was fabricated from part of the pipe used for the mass models tested in 1979. Twenty-five meters of 13 mm diameter nylon line connected the anchor to the release under the sensor array. The nylon line minimized the shock loading on the array cable when it became taut after the anchor was dropped. Extra buoys were tethered by a slack line to the subsurface float to minimize the risk of losing equipment. A time release was attached to the bottom of the array for jettisoning the simulated anchor.

Staging was done aboard the R/V HARRIS in Port Everglades, Florida. The test was conducted in the Tongue of the Ocean, at 25° 10'N, and 77° 52'W, along the 1000 fathom curve, on 16 September 1980. The buoy was suspended over the stern of the ship by a bridle rigged to the top of the surface buoy (Figures 2-26a and 2-26b). The nylon lifting line attached to the bridle was slashed to deploy the buoy.

Once in the water, the anchor separated from the surface/subsurface buoy combination as planned (10 seconds afterlaunch). One and one-half minutes after launch, the surface/subsurface buoy combination became upright indicating that the sensor array had become taut. Calculations indicated this should have occurred 7-1/2 minutes after launch. A rubber raft

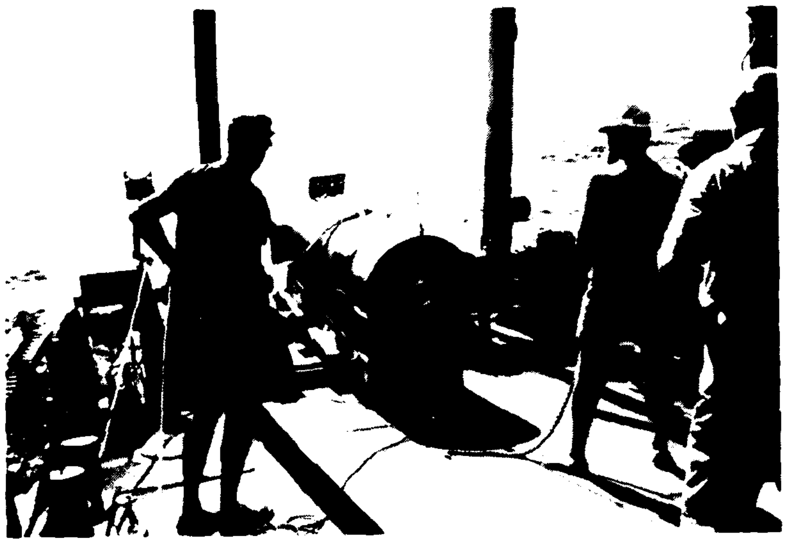

Figure 2-26a. ADOM on Deck of R/V HARRIS Ready for Lifting

Figure 2-26b. ADOM Being Lifted

was launched to allow close observation of the surface/subsurface separation scheduled for 30 minutes after launch. The raft returned to the ship for fuel after 45 minutes. The raft returned to the buoy approximately 30 minutes later but separation had taken place. Although separation did not take place as scheduled, 30 minutes after launch, the explosive bolts did fire in proper sequence and the tether deployed cleanly. The Natsyn rubber was stretched, sharing the load with the E/M cable. The surface float was awash when swells passed. No pitching or rolling of the surface float was noted. The buoy system was allowed to drift approximately 2 hours before retrieval commenced.

The recovery sheave at the A-frame on the fantail was suspended from a compliant line to minimize the dynamic loading of the E/M and sensor cables due to fantail motion. The surface float was retrieved with little difficulty (Figure 2-27a). Then the E/M tether was brought aboard until the subsurface float was just astern of the ship. The tension in the tether showed that the anchor had not separated from the subsurface float. The subsurface buoy was lifted aboard (Figure 2-27b) and retrieval of the array cable commenced. Approximately 525m along the array cable, there was a tangle of array cable and the 13 mm nylon line which connected the end of the array cable to the anchor through the time-actuated explosive release. The release had functioned properly, but the fouled array cable and nylon line prevented separation of the anchor.

It is believed that the tangle between the array cable and nylon line was caused by the flow of water through the open ended pipe used to simulate the anchor. The flow carried the nylon into the array cable housing through a hole in its bottom. Since the nylon line was an add-on for the Drift Test, failure of the array cable to deploy fully did not affect the anchor design or erode confidence in that design. The fouled cable and array were retrieved along with the simulated anchor.

After retr'eval, the computer, housed in a water-tight can in the subsurface float, was removed and taken to the laboratory for review of the data. No data were obtained due to a failure of the lithium battery. The

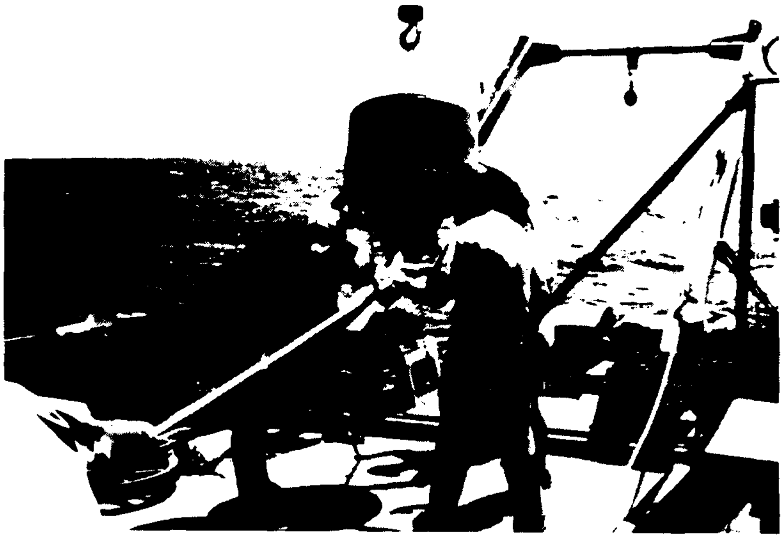

Figure 2-27a. Recovery of the Surface Float

Figure 2-27b. Recovery of the Subsurface Buoy

battery's impedance had changed, causing a voltage drop from 9 volts to 3 volts. This was below the 4-volt threshold voltage required for the computer to function. A faulty cell was identified and returned to the supplier for analysis. They found that the failure was caused by a broken internal weld. The manufacturer indicated that the probability of recurrence was very small because a design change has been made.

As designed, the computer checkout system cannot detect battery failure - only sensor failure. It is believed that the battery failed some time after the computer had been installed in the instrument can. Other investigations revealed that the delayed separation of the surface buoys was caused by a "potting" leak in the separation timing circuit.

The Drift Test validated the ADOM components' separation, and tether and array payout. The anchor separated from the surface/subsurface buoy combination on schedule. The surface/subsurface buoys separated approximately 30 minutes late due to a potting leak in their timing circuit. Late separation would not adversely affect an operational deployment.

Tether payout appears to work well. Approximately 525m of sensor array cable paid out flawlessly before becoming tangled with the nylon line. Since the nylon line was added for the test, the failure of the array to deploy fully does not affect the anchor design or erode confidence in that design.

The timed release and compliant sheave retrieval equipment employed in this test worked well. However, the following areas for improvement were noted:

a. Modify the mechanical interface between the surface/subsurface buoy to ease assembly by the addition of pilot surfaces to align the buoys.

b. Add an electrical connector and appropriate circuitry to the subsurface buoy so that complete checkout of the system can be accomplished just prior to deployment. This could detect battery and other component failures and allow minor adjustments without opening the electronics housing.

SECTION III

FINDINGS - ARCTIC ADOM

3.1 GENERAL.

Deploying the Open Ocean ADOM in the Arctic is precluded by the ice pack, but the ice provides a convenient support for the sensor array. The Arctic ADOM (A-ADOM) is dropped to the ice by parachute. Upon landing, a thermal drill melts a hole through the ice. The sensor array cable follows the drill through the ice into the ocean beneath (Figure 3-1). A control computer and telemetry transmitter remain on the ice.

Accomplishments in the Arctic ADOM program during 1980 include:

a. Validation of the thermal drill concept was completed at the U.S. Army Cold Regions Research and Engineering Laboratory.

b. The Concept Validation Model thermal drill was built.

c. Prototype programs for the control computer were written.

d. Development of the electronic circuits to couple the control computer with the sensor array and telemetry system was begun.

e. Construction was started on a prototype structure for the ice lander frame.

f. A method to cushion the impact of the lander on the ice was selected from several concepts that had been analyzed.

g. Preliminary design and testing of components for the impact cushion were begun.

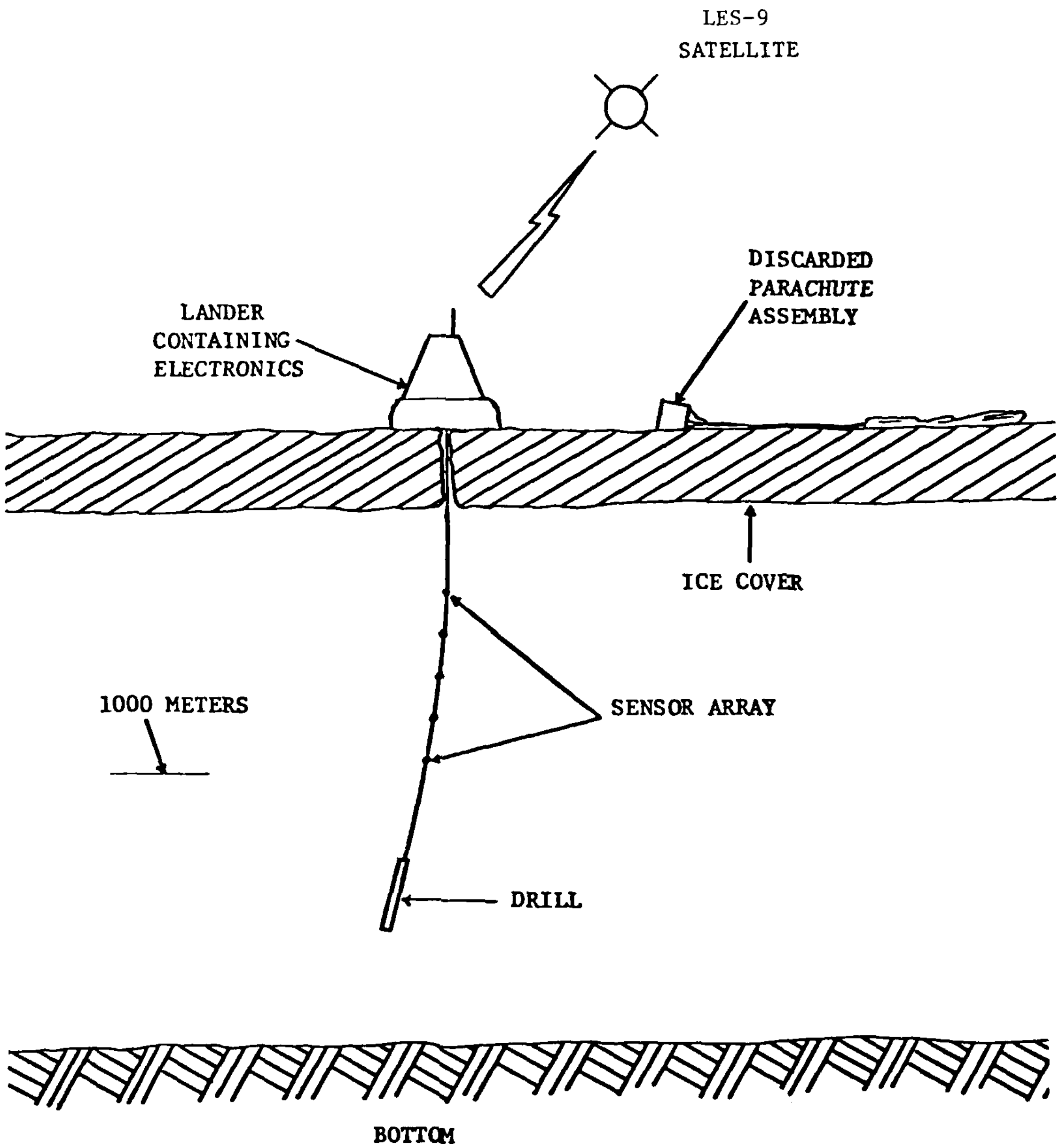

Figure 3-1. Arctic ADOM Configuration

3.2 RECIRCULATING WATER JET DRILL

The Advance Development Model (ADM) ice drill fabricated during 1980 is illustrated in Figure 3-2, showing the internal parts of the drill. Figure 3-3 is a photograph of the drill as manufactured. Ice drilling is started with a resistance heated parabolic point. Later the melt water is recirculated into the drill and pumped out as a warmed jet stream. The jet stream transfers heat from the drill to the ice much faster than natural conduction and convection.

Before jet drilling can begin, an adequate supply of water must be provided. A parabolic hot point melts the drill into the ice until the pump is primed with melt water. Should the melt water be lost, as could happen by drilling into a large void, the pump is primed again through the action of the hot point. The hot point also serves as a backup drilling system.

The recirculating melt water is heated by high wattage cartridge heaters in the heating chamber (six parallel banks) and in the hot point (three parallel banks). These heaters allow variation of power input and add redundancy to the system. Power for the drill comes from batteries in the surface lander. A 1 horsepower, 220 volt AC standard deep-well submersible pump drives the jet stream.

The drill is controlled by a microcomputer encased in its top. Water-level sensors and temperature sensors in the hot point and on the cartridge heaters provide control input. The microcomputer uses these signals to control the starting sequence of the pump and prevent overheating under the varying conditions of sea ice and pressure ridges.

Preliminary specifications for the ADM are shown in Table 3-1. Table 3-2 defines the conductors for the drill power cable. The conductors will be sheathed within a single jacket.

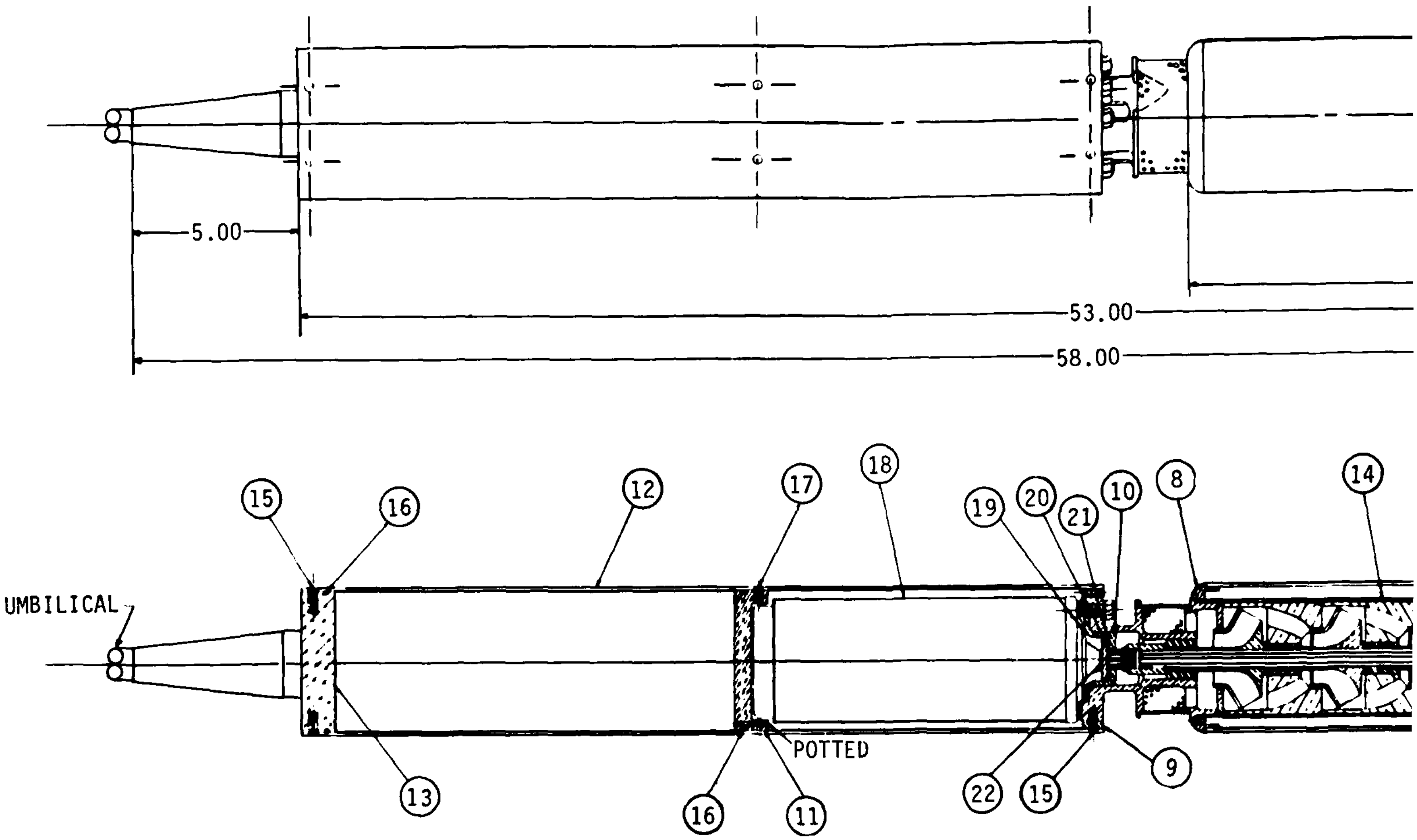

NOTES:
1. ALL WIRING OMITTED FOR CLARITY-SEE DRAWING NO.
2. ALL POTTING EMERSON & CUMMINGS STYCAST 2651
3. ALL FASTENERS STAINLESS STEEL
4. ITEMS 2-4 MADE OF PHENOLIC MATERIAL

ITEM	DESCRIPTION
29	E5A45 WATLOW FIREROD
28	PARKER NO. 018 O-RING
27	PARKER NO. 230 O-RING
26	PARKER NO. 238 O-RING
25	¼-28 x 1 ALLEN FLAT HEAD CAP SCREW
24	G2A146 WATLOW FIREROD
23	¼-24 x 7/8 ALLEN SET
22	1.360D x .622ID x .122 STAINLESS THRUST
21	1.240D x .630ID x .100 NYLON THRUST WAS
20	1.350D x .630ID x .013 TEFLON BEARING R
19	.20 x .20 x .030 NEOPRENE PADS
18	1 HP. SUBMERSIBLE MOTOR
17	¼-28 x ½ ALLEN SET

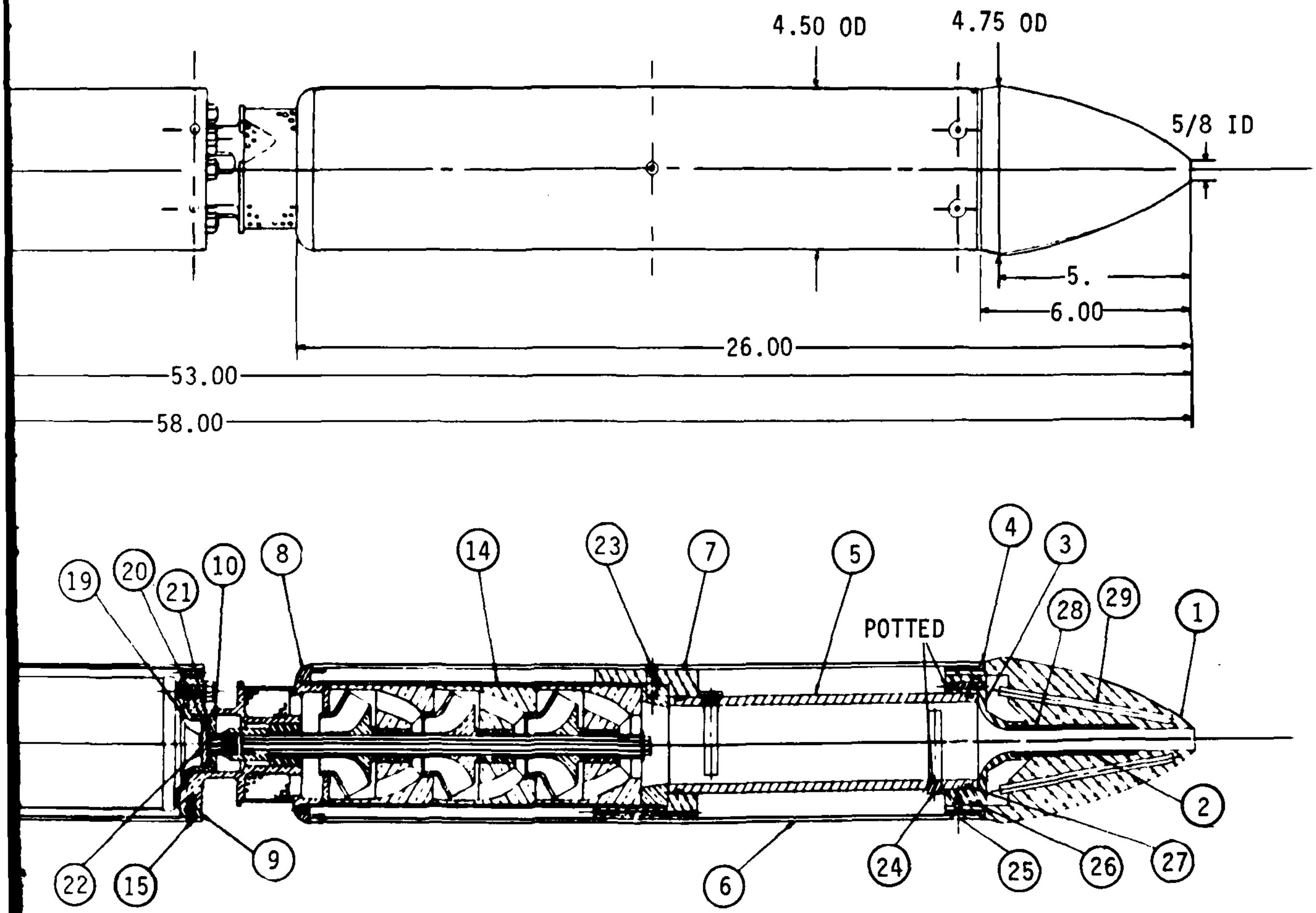

			16	PARKER NO. 242 O-RING		2
			15	¼-28 x 75 ALLEN SET		12
			14	3-STAGE PUMP	100038	1
29	E5A45 WATLOW FIREPOD	9	13	COMPUTER SECTION TOP		1
28	PAR· · NO. 018 O-RING	1	12	UPPER SHEATH		1
27	PARKER NO. 230 O-RING	1	11	COMPUTER SECTION BASE		1
26	PARKER NO. 238 O-RING	1	10	THRUST BEARING CUP	100034	1
25	¼-28 x 1 ALLEN FLAT HEAD CAP SCREW	6	9	UPPER SHEATH RING		1
24	G2A146 WATLOW FIREROD	14	8	LOWER SHEATH CAP		1
23	¼-24 x 7/8 ALLEN SET	4	7	HEATER-PUMP COUPLING		1
22	1.360D x .622ID x .122 STAINLESS THRUST WASHER	1	6	LOWER SHEATH		1
21	1.240D x .630ID x .100 NYLON THRUST WASHER	1	5	HEATER BARREL		1
20	1.350D x .630ID x .013 TEFLON BEARING RING	1	4	LOWER SHEATH RING		1
19	.20 x .20 x .030 NEOPRENE PADS	3	3	FLOW RING		1
18	1 HP. SUBMERSIBLE MOTOR	1	2	NOZZLE INSULATOR		1
17	¼-28 x ¼ ALLEN SET	6	1	PARABOLIC HOTPOINT		1
ITEM	DESCRIPTION	REQ'D	ITEM	DESCRIPTION	DRAWING NO.	REQ'D

81-897

Figure 3-2. Advanced Development Model (ADM) Drill Assembly

3-5/3-6 Blank

PRECEDING PAGE BLANK-NOT FILMED

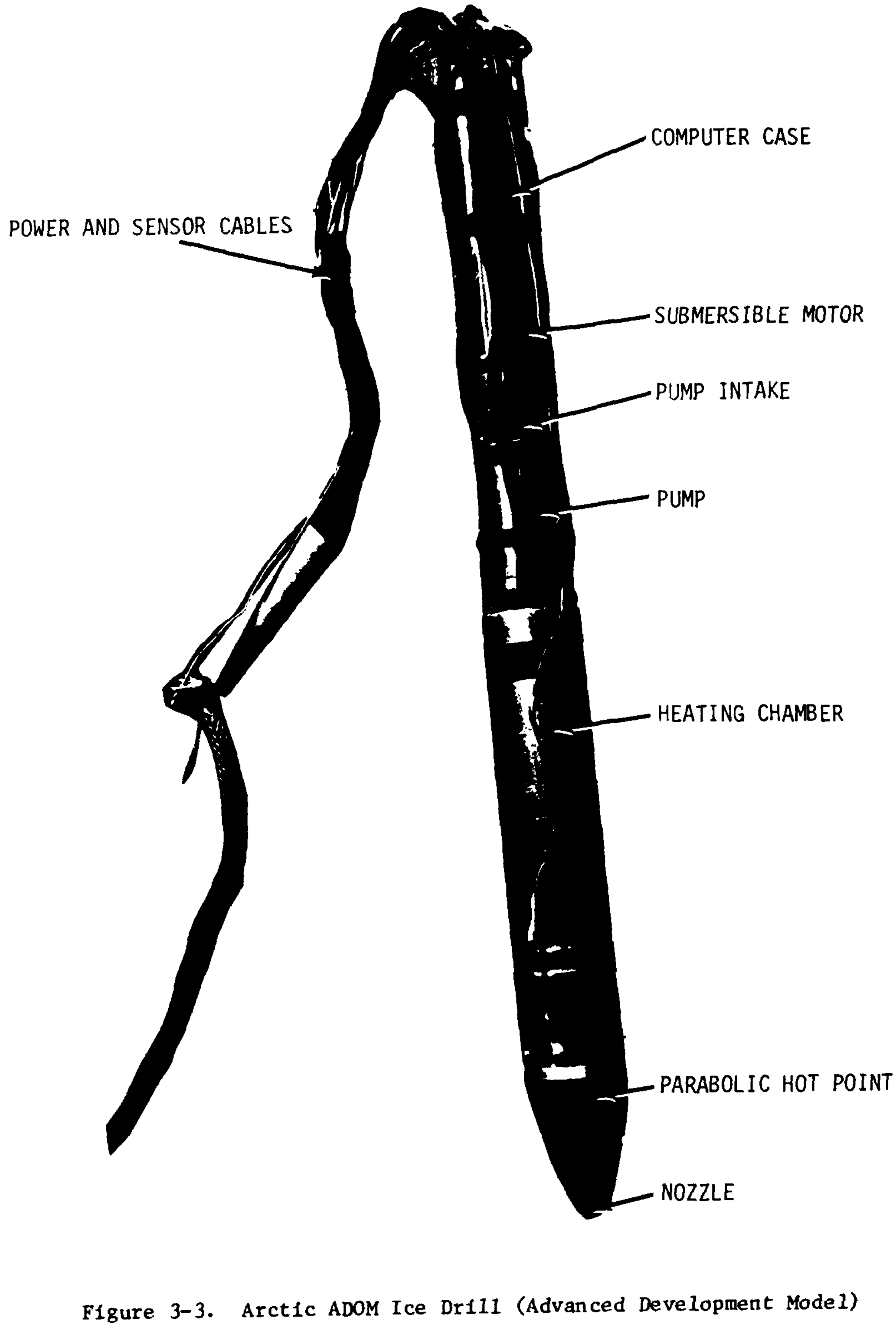

Figure 3-3. Arctic ADOM Ice Drill (Advanced Development Model)

TABLE 3-1. PRELIMINARY DRILL SPECIFICATIONS

Pump	3 Stage
Motor	1.1 kW @ 220 VAC
Hot Point	3.5 - 4 kW @ 350 VDC
Heating Chamber	12 - 36 kW @ 350 VDC
Nozzle Diameter	15.9 mm
Pumping Rate	150 liters per minute
Length	1.5 m
Weight in Air	45 kg
Weight in Water	28 kg
Control	Microcomputer

TABLE 3-2. POWER CABLE

Description	Number of Conductors	Size & Type of Conductor
Communication	2	COAX RG59u or equivalent
Computer Power	2	Twisted pair - 16 GA or standard 16 GA
Motor Power	2	1.5 HP @ 230 VAC 16 GA (may be 18) stranded
Heated Power	2	12 KW @ 350 VDC 10 GA stranded
Case Ground	1	16 GA stranded battery negative terminal to case
TOTAL	9	

A Concept Validation Model (CVM) probe was constructed from commercial PVC plumbing fixtures. Minor machine work was required for the nozzles and the internal check valve. Nozzles were assembled with standard pipe threads so that they could be changed easily. An external 30 kW immersion heater simulated the drill's internal heating chamber.

Testing of the CVM drill at the U.S Army Cold Regions Research and Engineering Laboratory was completed in 1980. Drilling was performed in a cylindrical ice sample, 1.8 meters in diameter and 2.5 meters in height, that was contained in a refrigerated tank. Flow rate was monitored by a Bendix-Q series impeller mounted inside a 10 cm PVC pipe. Thermistors measured water temperature, and thermocouples measured the ice temperature. Figure 3-4 shows a typical drilling profile. An hour and 50 minutes are required for the hot point to immerse the pump intake port in typical Arctic ice at a temperature of -35°C. After another 15 minutes, sufficient melt water has accumulated to prime the pump. The drilling rate increases dramatically when the jet pump starts.

Results of the experiment are listed below:

a. Hole diameters of approximately 15 cm were achieved as predicted;

b. Terminal steady state drilling rate is proportional [illegible] ›wer;

c. Thermal efficiencies are high, averaging appro[illegible]ately [illegible] percent;

d. Approximately 2.4 kilowatt hours of electrical energy are required to bore a 15 cm diameter hole through 1 meter of this typical ice. This represents 37 kWh for an ice thickness of 15m or 26 kWh for an ice thickness of 10.6m; and,

e. Computer model predictions are within 10 percent of the physical test results.

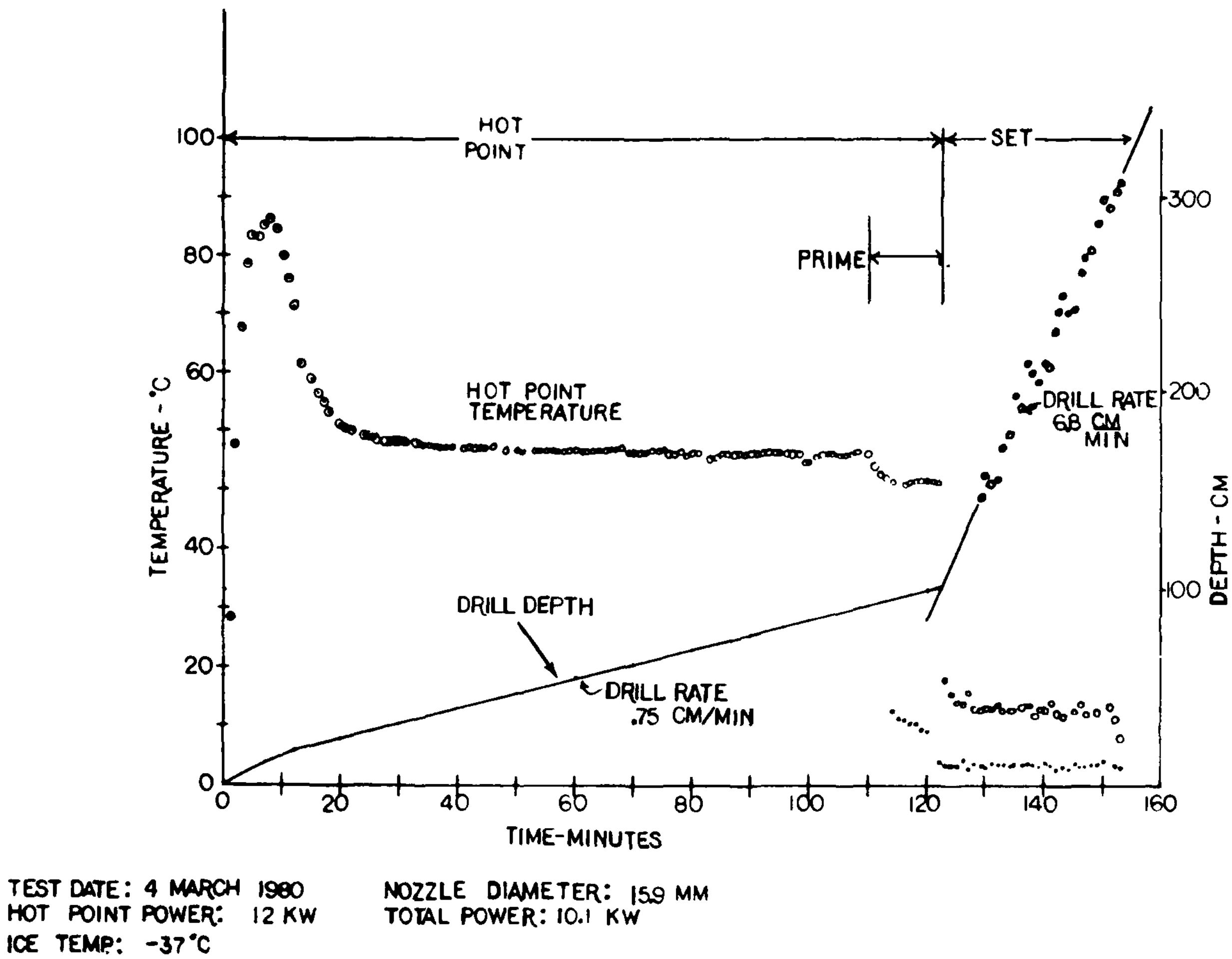

Figure 3-4. Typical Drilling Profile

3.3 CONTROL SYSTEM

The components of the Arctic ADOM control system are shown in Figure 3-5. The processor, memory, power switches, and supporting circuitry are sealed in a cannister at the top of the drill body. Control sensors are located at several key points in the drill body. The descending thermal drill drags sensor and power cables from the lander body, where the batteries are stored. When the probe breaks through the ice, it pulls a connector free in the lander, turning the drill off. A communicator port to the computer is provided on the lander for external checkout of the control system.

3.3.1 MICROCOMPUTER. During 1980, prototype programs were written for the control computer in the ice drill. Microcomputer control adapts the drill to abnormal conditions and provides optimum drilling efficiency. Since large amounts of power are used in the drilling operation, it is very important that this energy be used efficiently. It is equally important that the heaters be shut down to avoid burnout when the drill encounters a void in the ice layer where no melt water is present.

The microcomputer monitors the operation of the drill components. Failed parts are isolated while drilling continues with the remaining portions of the system. Two separate mechanisms are included to shut off a heater whose temperature rises unacceptably. If the microcomputer fails, the system makes a final drilling attempt with the hot-point heater.

3.3.1.1 System Concepts. The microcomputer will be required to perform several different tasks. Since some of these tasks must be performed concurrently (drill task and data acquisition task), multitask operating software has been designed into the system.

The software for this system is separated into two layers. A coarse control task monitors melt-water level and heater temperature. It also turns on heaters in sequence to minimize current surges. A second, fine control task monitors the temperature of the melt water and maintains maximum efficiency by switching on only as much heat as is needed to maintain proper

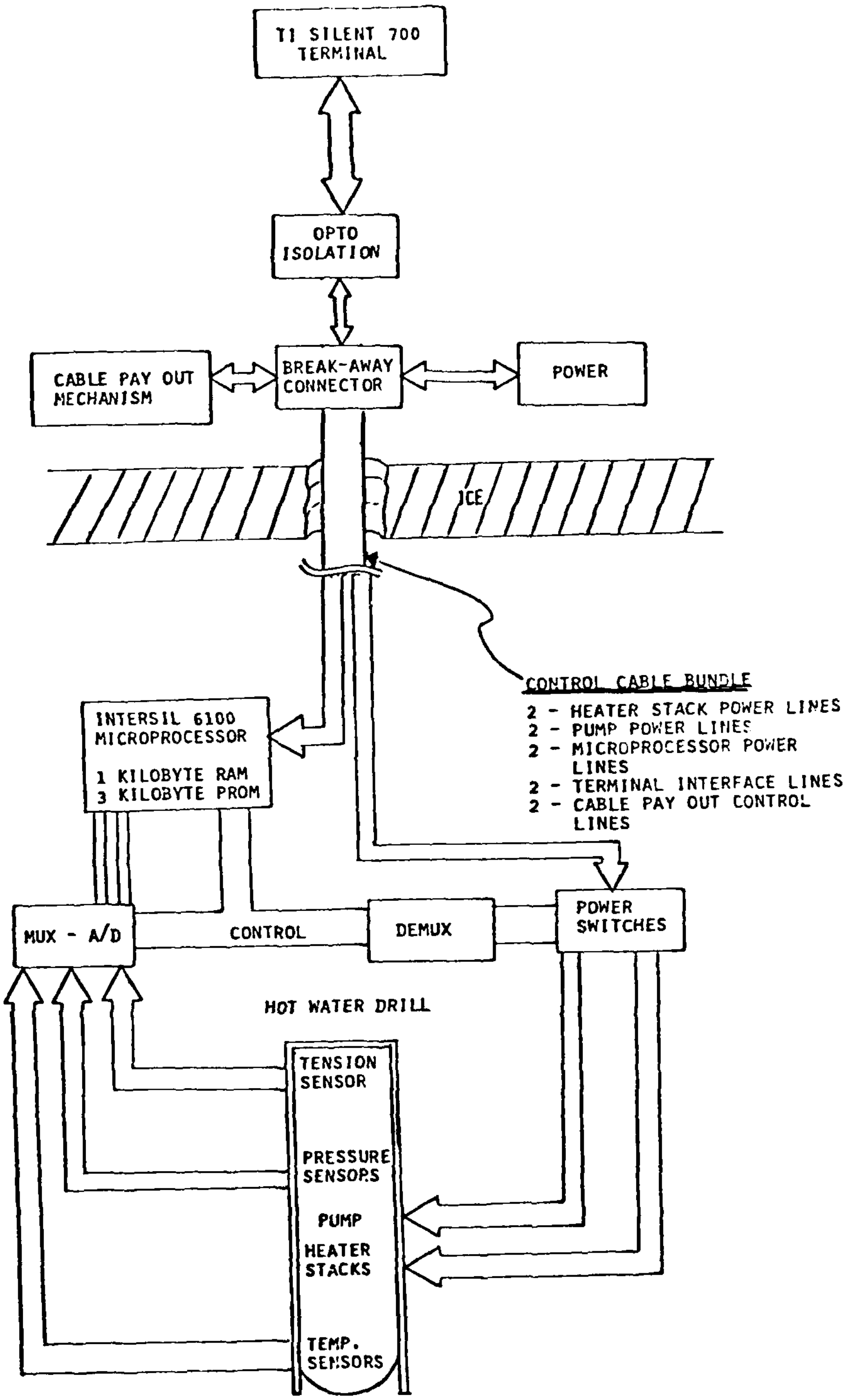

Figure 3-5. Arctic ADOM Control System

drilling action. The drill uses large amounts of power to melt through the ice and uses the cold melt water to cool itself. The drill must turn off quickly if the water flow is interrupted to avoid overheating the cartridge heaters. The control logic analyzes the drill status sensor data to detect malfunctioning sensors. Failed devices are isolated while drilling continues.

There is also the possibility of microcomputer failure. An independent hardware timer is periodically reset by the software during normal operation to detect this malfunction. If the program fails to reset the timer before its time expires, it will restart the microcomputer and operate normally. If the microprocessor requires restarting more than a few times, it will be restarted with a simpler coarse-control program. If this also fails, hardware will switch over to the hot-point heaters in a final attempt to melt through the ice.

3.3.1.2 Software Modules. The drilling operation begins by applying power to the heaters in the aluminum hot point. The drill melts into the ice until the pump intake is immersed, then the pump and cartridge heaters are turned on. The melt water is heated by the cartridges and pumped out the tip of the drill to melt more ice from beneath the drill. The water temperature normally rises only a few degrees in this process. Pumping usually continues until the drill has penetrated the ice. If the drill enters a void in the ice, the melt water drains away and the controller stops the pump and heaters to prevent overheating. Then it restarts the drill by switching power back to the hot point.

The drill software consists of five modules that sample temperature sensors, control the pump and heaters, and monitor the system's performance. The modules are sensor acquisition, rough control, fine control, sensor filtering, and failure detection. A layered approach is used that first manages the heaters in a very simple on/off fashion. A subsequent fine control module adjusts individual heaters to supply just sufficient heat for proper performance of the drill. This structure allows the system to operate efficiently and yet permits some control in the event of serious malfunctions. Processing

is never halted while waiting for a temporary malfunction to be corrected. Thus, the modules are linked together in a cyclic loop which repeats the control sequence a number of times each second. During each cycle, the independent timer is reset. If the software fails to reset this timer, the control system will be restarted. The modules are summarized as follows:

a. Drill Data Acquisition Module. A 16-channel, 8-bit, analog-to-digital converter is provided in hardware to measure 14 resistance temperature sensors. Three of these operate in self-heating mode to detect the presence of melt water in the pump intake manifold. Another three sense the temperature of the hot point. The remaining eight are associated with four banks of cartridge heaters with two sensors and four heaters in each bank.

During each cycle of the drill control algorithm, these sensors are sampled and the data stored in memory. Sensors rejected by the Failure Detection Module are masked; otherwise, the reading from each sensor is compared to a standard value. If the reading exceeds its standard, a temperature flag is set for that sensor. If not, the flag is cleared. The Rough Control Module (RCM) uses these flag settings to evaluate the drill status.

b. Rough Control Module. If the drill is just starting or has entered a void in the ice, the pump intake temperature flags will be set. The RCM responds by turning on the three hot-point heaters (one at a time to reduce the power surge). When melt water cools the intake temperature, the RCM starts the pump and turns on the four banks of cartridge heaters. If the temperature flag of a bank is set, the bank is turned off until the flag is cleared. All the banks turn off if the intake temperature flag is set (loss of coolant).

The Rough Control and Data Acquisition Modules together are sufficient to maintain coarse control of the thermal drill. These modules are used alone after the hardware monitor has restarted the microprocessor more than a preset number of times without returning to normal program control.

This software is implemented in such a way that the microprocessor does not have to wait for any time delays to expire to exit to subsequent modules. If other control mechanisms fail, it can operate in conjunction with the data acquisition module to provide complete rough control. This configuration is established when the software fails to reset the independent timer and the system has to be restarted more than a preset number of times.

c. Fine Control Module. The fine control task conserves battery power by warming the melt water to the lowest temperature needed to drill efficiently. It switches each bank of cartridge heaters off when its temperature exceeds an upper bound and restarts it when the temperature falls below a lower bound. The heater switches are controlled by setting bits in a heater status register. This is combined with the rough control register to decide which heater register banks are actually turned on. Fine control is disabled during coarse control.

d. Filter Module. The Filter Module keeps a running average of the temperature difference between paired sensors in a pair in order to detect the failure of a sensor. This module provides the history needed for the Failure Detection Module.

e. Failure Detection Module. This module monitors the sensor histories to detect failed cartridge heater temperature sensors. If the two temperature sensors in a cartridge heater bank consistently give different readings to the Filter Module, then the Failure Detection Module examines their output more closely by observing the values while the heaters are cooling (turned off) and heating (turned on). The algorithm identifies if a sensor has failed, and whether it has failed at a high value or a low value. Failed sensors are masked from the coarse and fine control algorithms. The Failure Detection Module continues to monitor failed sensors and may clear the mask when a sensor starts functioning again. When both sensors in a cartridge heater bank fail, fine control of that bank is linked to an adjacent bank.

3.3.2 MICROCOMPUTER HARDWARE DEVELOPMENT. Automation of the ADOM thermal drilling process requires a complex strategy. A simulation computer was developed to define and perform initial testing of the candidate control strategies.

The simulation computer uses a series of potentiometers to simulate the analog signals from the temperature sensors in the ADOM thermal drill. The computer analyzes the simulated data and generates a control response. The control response is displayed visually as lights on a control panel marked to indicate which heater banks should be turned on, whether the pump should be running, etc. The control signal is also available at an output port that can be connected to the actual thermal drill control lines. Further, the actual drill temperature sensors can be connected to the computer in place of the potentiometers. Thus, the ADOM drilling control simulator is actually an ADOM thermal drill control computer.

Hardware development of the ADOM drill control simulator was completed in 1980. Figure 3-6 is a photograph of the front panel of the unit. Figure 3-7 shows the inner wiring. Development of the simulator hardware has led to a design for the final ADOM computer hardware. The software realizes that the ADOM control strategy has been run on the simulator and is in the process of being evaluated. What remains to be done is to complete the packaging to the final ADOM computer and perform system evaluation tests.

The Arctic ADOM controller hardware consists of electronics external to the microcomputer system which allows the system to perform the necessary data acquisition, heater control, and sensor monitoring functions of the drilling system.

The data acquisition portion of the system consists of a 16-channel, 8-bit, analog-to-digital (A/D) converter which receives analog signals from the drill assembly. For testing and simulation purposes, a set of 16 potentiometers has been used to replace the sensor inputs from the drill assembly. A multichannel switching system is provided on the monitor box so that each analog channel may be observed and recorded.

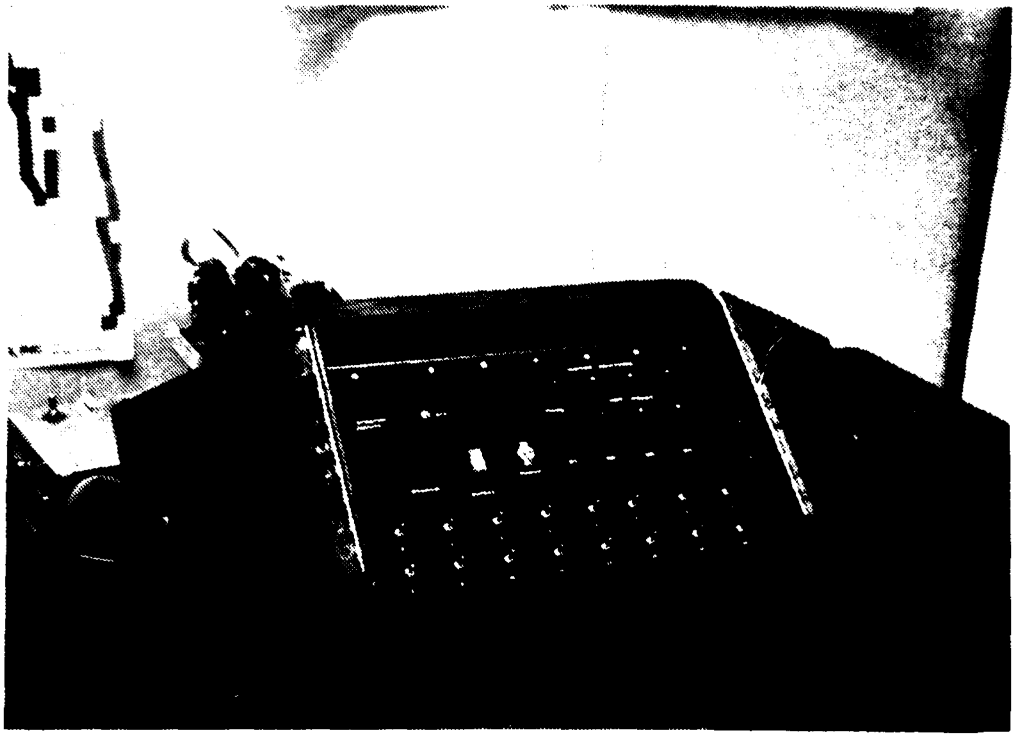

Figure 3-6. Simulation Computer

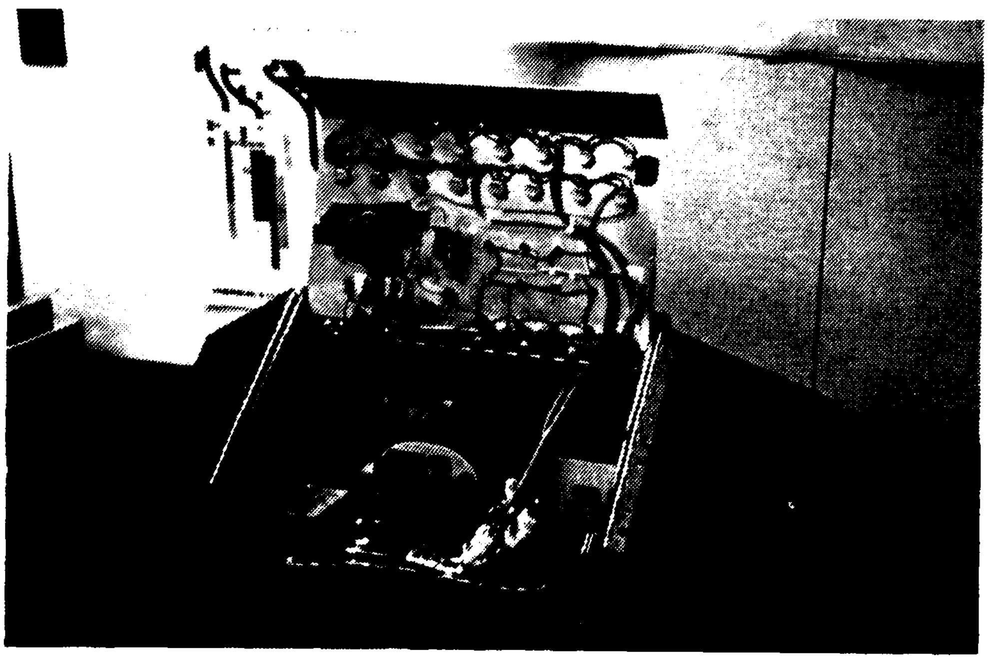

Figure 3-7. Drill Data Simulators
in Computer Simulator

Also included in the system is a standard interface for an RS232 communication link. This interface eliminates the need for a special interface card in the drill controlling computer.

For simulation purposes, all control decisions (e.g., turn-on of pump, hot-point, water heaters) are displayed by status lights controlled by the CPU. The simulator has four extra status lights to display diagnostic information. When the power switches for the drill assembly's pump and heaters are built, the simulator will be modified so that the CPU controls the drill with the status lights used for monitors.

A software counter is provided in the controller to direct hardware commands. The "watch dog" counter is periodically "reset" by the software during proper operation. If the watch dog counts to zero, the computer is restarted. Mutliple restarts, indicating a serious computer failure, will turn the pump and heaters off and turn the hot point on indefinitely.

3.4 LANDING SUBSYSTEM

About 10 percent of the Arctic ice pack is covered by pressure ridges. Devices proposed for landing on pressure ridges are not considered likely to succeed. Simpler landing devices are suitable for the remaining 90 percent of the Arctic. Even in ridged areas like the Offshore Province, successful landings can be made over three-fourths of the time by matching the launching strategy with surface terrain.

The Arctic ADOM lander is sketched in Figure 3-8. Illustrated in this figure are the major components: parachute assembly, impact absorbing torus, flotation material, as well as the recirculating jet drill, power cable, batteries, sensor string, and electronics housing. The torus is capable of absorbing impact from any direction with deceleration rates less than 100g's. All electronics are sealed in watertight pressure housings for protection during open-water landings. The lander floats upright. This is achieved by placing the batteries and cable assemblies on the bottom, electronic packages near the top, and by filling voids with foam. This geometry also helps keep ADOM upright when landing on ice.

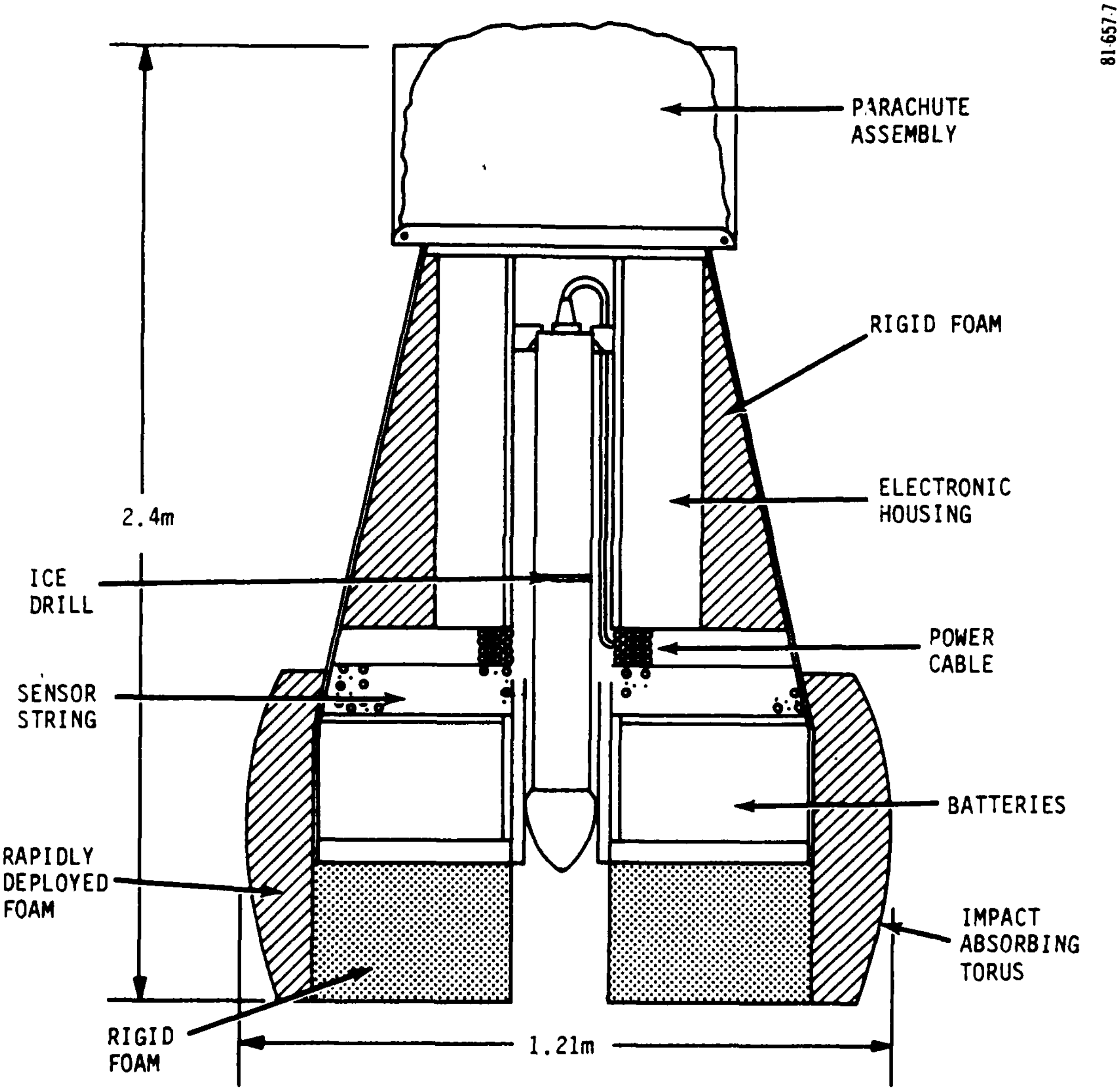

Figure 3-8. Arctic ADOM Lander

The Arctic ADOM uses the same telemetry antenna design as the open-ocean model. A second antenna is required for navigation. The parachute assembly holds each antenna in a tube over a compressed spring. When the parachute is jettisoned after touch-down, the spring pops the antenna up from its tube. This parachute assembly is similar to the Open Ocean ADOM Design.

Table 3-3 summarizes the preliminary Arctic lander specifications.

TABLE 3-3. PRELIMINARY ARCTIC LANDER SPECIFICATIONS

Diameter	1.21 m
Height	2.4 m
Weight	453-680 kg
Maximum Impact Velocity	12-17 m/s
Maximum Deceleration	100 g

Like the Open Ocean ADOM system, Arctic ADOM is designed for delivery from C-130 transport aircraft. Figure 3-9 shows a full scale mock-up of the lander structure.

3.4.1 IMPACT ATTENUATION. The impact of the Arctic ADOM on the ice must be cushioned to prevent damage. Effective attenuation of impact forces requires stopping the ADOM descent without recoil. This has been done by squirting oil or other fluids through a small hole, or by crushing a material with an open structure.

Hydraulic shock absorbers are suitable when the ram axis can be aligned with the impact direction. The ADOM impact, however, is complicated by non-vertical loads due to wind and terrain. For such omni-directional impacts, crushable pads are more suitable. The disadvantages are that the cushion must extend in all directions of potential impact and a bulky cushion wastes storage space.

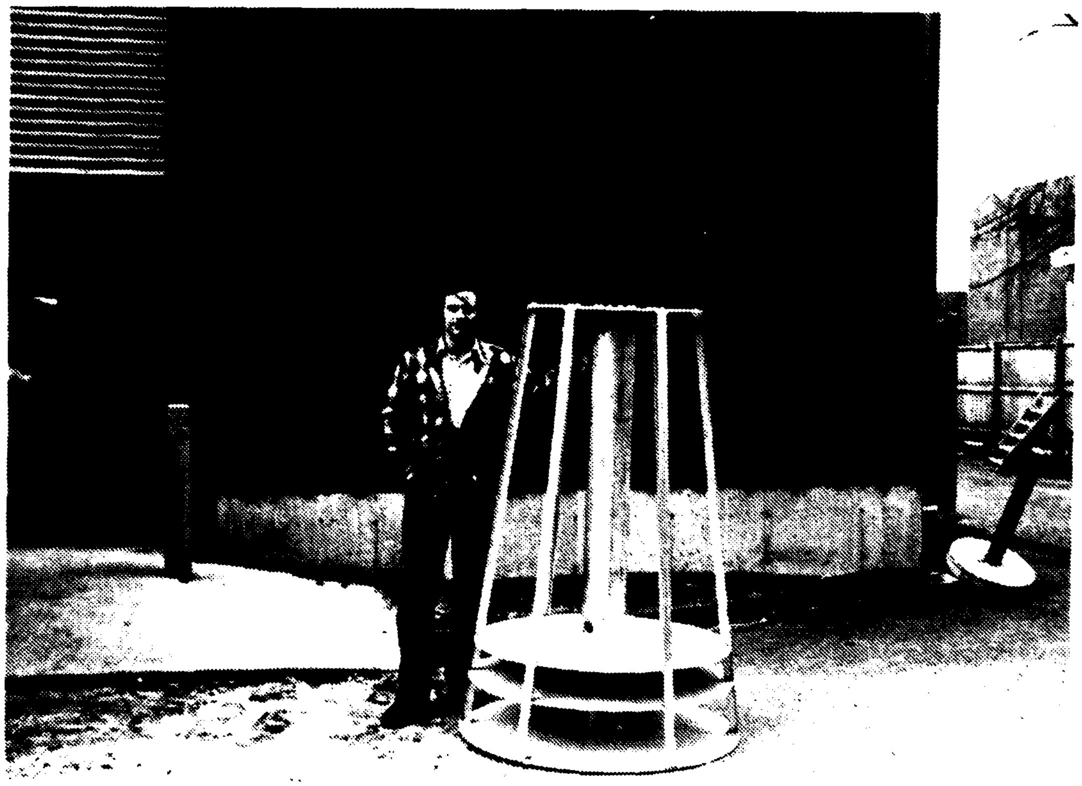

Figure 3-9. Full Scale Mock-Up of Lander Structure

This problem can be avoided in the A-ADOM design by using a variable volume cushion. During the descent by parachute, the cushion is inflated with a plastic foam that cures before impact. This increase in base diameter adds to the tipping stability after impact (defined by the ratio of ADOM maximum diameter to the height of the center of gravity).

Based on the preceding arguments, the inflatable cushion concept will be used for small aircraft Arctic ADOM units, since its storage, transportation, deployment, and landing operations would be more efficient than a pre-formed pad. The Air Force Flight Dynamics Laboratory, Wright Patterson AFB, Ohio, conducted an extensive study of impact attenuation. These quantitative evaluations will greatly simplify system selection of a system for A-ADOM.

The small aircraft impact system is activated as soon as the lander is descending steadily under the main parachute, as shown in Figure 3-10. The two liquid foaming chemicals are forced through a mixing nozzle by compressed gas, producing a foam that fills a fabric bag folded around the ADOM. Fill time starts when mixing begins and ends when the reagents are expended. Rise time extends from the beginning of mixing until the foam has expanded to 95 percent of its final volume. The plastic foam sets quickly and is capable of absorbing impact energy.

The concept was discussed with chemists, chemical manufacturers, and engineers who have designed similar impact absorbers. Although any plastic can be produced as a foam, polyurethane foam has the following advantages:

- It can be generated easily on command;
- Does not require large pressure vessels;
- Is generated by an easily controlled reaction;
- Comes in a wide range of resiliencies and can be cured rapidly and reliably, based on recent advances in technology.

3.4.2 DRILL SUPPORT. A clamp holds the drill until the Arctic ADOM has landed. Since the drill weighs about 80 pounds, dynamic loading of 8000 pounds is produced by a 100g impact at touchdown.

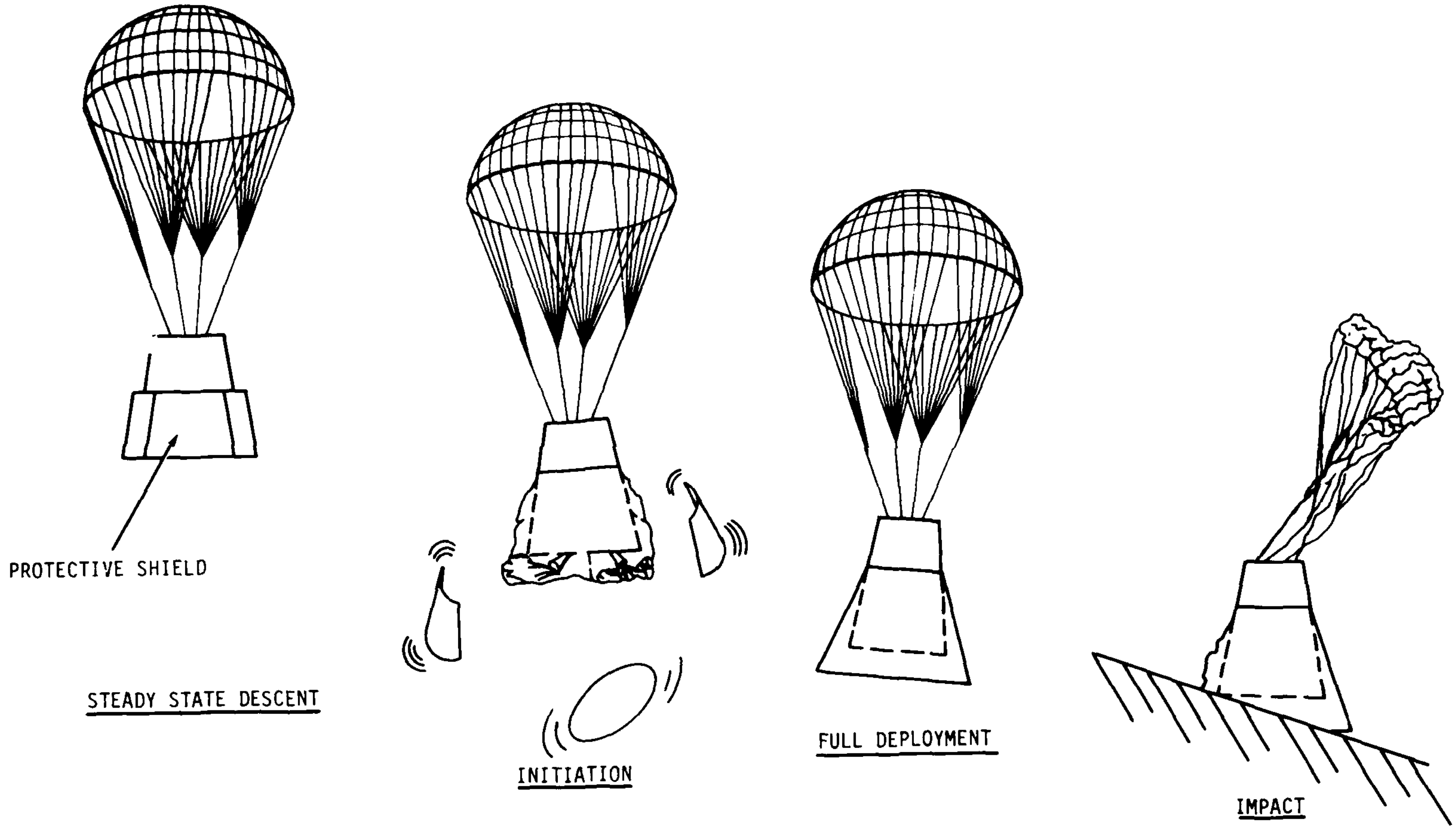

Figure 3-10. Plastic Foam Deployment Sequence

Two clamps were studied. One concept used a mechanical linkage. It was rejected because it was too complicated and bulky. Retracting the linkage after the impact made the device even more awkward. The clamp must retract, not only to release the drill, but also to permit unrestricted payout of the power and sensor cables.

The second concept is drawn as Figure 3-11. The downward thrust of the drill is restrained by three rods (Part 3) that project into the central tube where the drill is stowed. The rods, uniformly spaced around the tube, support the drill along the sloped sides of the hot point (Part 1), a massive metal part. They retract radially by sliding in guides (Part 8), under the combined wedging action of the probe surface and springs built into the guide members.

Prior to impact, the support rods are prevented from retracting by latches, not visible in Figure 3-11. The latches themselves are prevented from disengaging prematurely by a locking collar (below Part 9) that holds them down. A safety rod (Part 15) holds the locking collar down on the latches as long as the parachute is bolted to the top of the ADOM structure. During impact, the inertia of the latches as well as the locking collar acts to hold the latches engaged.

When the parachute is jettisoned, redundant spring actuators (Part 19) pull cables (Part 10) that lift the collar and the latches in turn. The guidesprings retract the drill clamp rods.

Rollers (Parts 12 and 16) support the drill during oblique impacts and guide it while it melts into the ice.

Key design factors in this concept are the safety of the latch prior to impact, strength of the support during impact, and reliability of the release after impact.

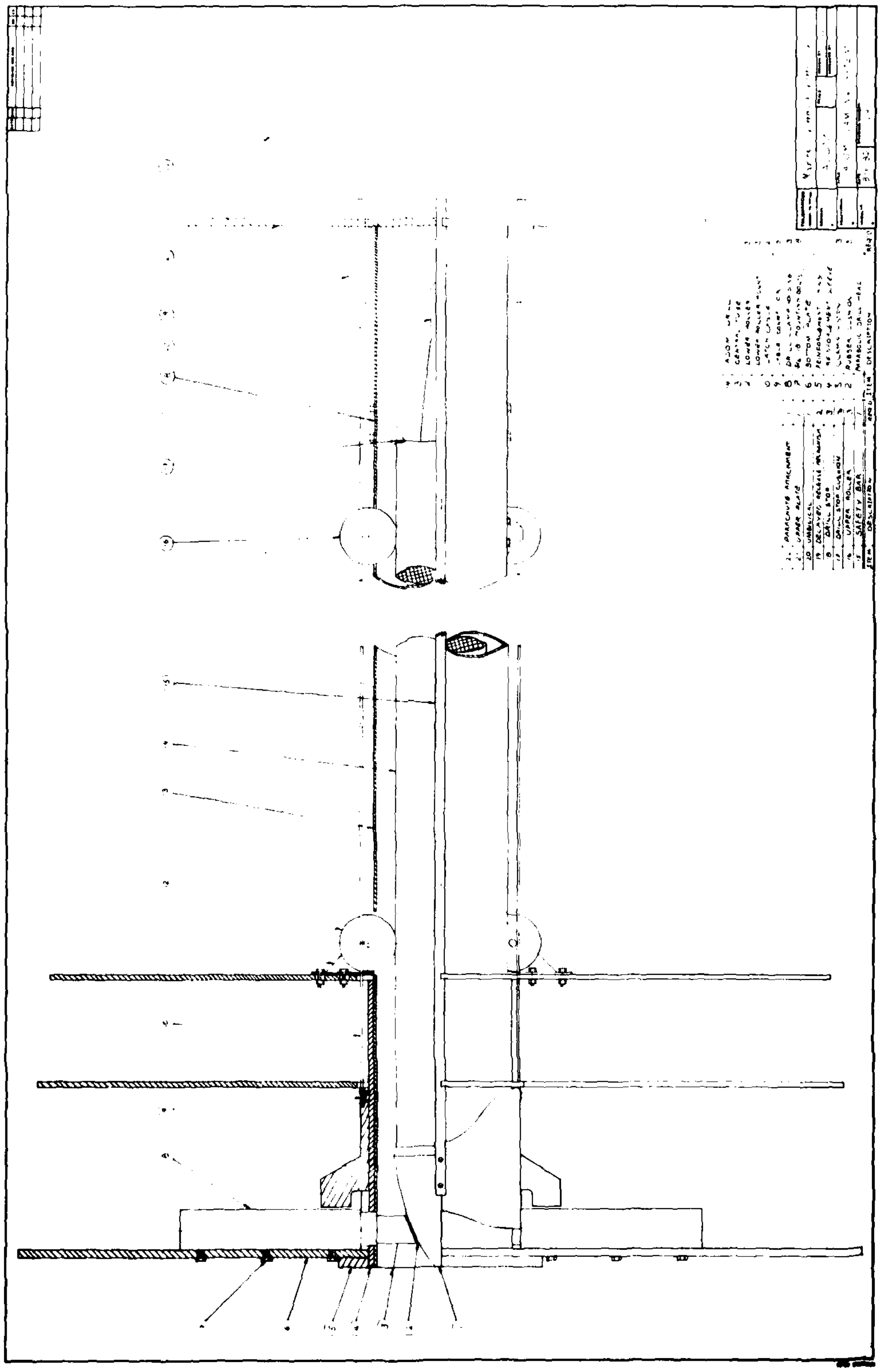

Figure 3-11. Arctic ADOM Thermal Drill Clamp

3.5 ENERGY SYSTEM

Lithium-based batteries are under study for powering Arctic ADOM. Of the several lithium-cell chemistries, the two most promising are lithium thionyl chloride ($SOCl_2$) and lithium sulfur dioxide (SO_2). The lithium/water cell is too complicated for ADOM applications at this time.

Sulfur dioxide cells are more widely used than thionyl chloride in lithium batteries, either for active power or reserve duty. A dominant property of these cells is their internal vapor pressure; the cells are hermetically sealed to conserve the reactants. Inadequate cooling combined with rapid discharge can overheat the cell producing vapor pressures up to 450 psi. Vents are required to relieve the excess pressure safely. This is a problem for the ADOM ice drill, which requires massive current from closely stacked cells.

Energy capacities for lithium sulfur dioxide cells range from 0.7 A-hr to 1600 A-hr. Capacity may be reduced as much as 50 percent by either extreme operating temperature or rapid discharge. In addition, cell capacity will be reduced by plate passivation if the current drain is not applied gradually.

As with the sulfur dioxide battery, lithium thionyl chloride batteries are used in both active or reserve duty. Available cell capacities range from 0.36 A-hr to 17,000 A-hr. Thionyl Chloride cells use materials less costly than are used in the sulfur dioxide cell. Current densities (5-10 mA/cm^2) are higher than are attained with sulfur dioxide cells. However, limited production of thionyl chloride cells results in higher cost.

After much investigation and interaction with almost all of the manufacturers of lithium based batteries it can be assumed that lithium batteries will be the power source for the Arctic ADOM system. However, it has been concluded that these batteries will not be available for 2-3 years at prices and in configurations suitable for use in current Arctic ADOM designs.

In order to continue with the feasibility study, a relaxation of the drilling depth has been defined (3m instead of 15m) which allows the Arctic ADOM to use ordinary batteries. The Arctic ADOM will be revised for lithium batteries when they become competitive.

AD-A101 090 EG AND G WASHINGTON ANALYTICAL SERVICES CENTER INC R--ETC F/G 8/10
AIR DEPLOYED OCEANOGRAPHIC MOORING (ADOM).(U)
APR 81 N00014-79-C-0227
UNCLASSIFIED EG/G-TR-0370-0003 NL

2 OF 2
AD
A101090

END
DATE
FILMED
7 81
DTIC

SECTION IV

FUTURE ACTIONS

4.1 GENERAL

This section describes the actions, further developments, and testing necessary in the continuation of the ADOM technology development. The OO-ADOM and the A-ADOM configurations are discussed below.

4.2 OPEN OCEAN ADOM

The planned actions during 1981 are as follows:

a. Ship-launch one complete ADOM buoy in June 1981, including the complete electronics and sensor array. Transmit data through the LES-9 satellite to the ADOM shore station in Key Biscayne, Florida. Recover buoy after 1 day and inspect it.

b. Air-launch two ADOM buoys in October 1981. Recover and inspect one buoy after 2 days. Recover and inspect the second buoy after 2 to 3 months. Throughout the deployed period, transmit data to Key Biscayne for processing and evaluation.

4.3 ARCTIC ADOM

The planned action for 1981 are as follows:

a. Complete the Advanced Deployment Model (ADM) control system software and computer development.

b. Complete ADM drill development, culminating in testing at Cold Regions Research and Engineering Laboratory.

c. Continue landing system design and component testing.

DISTRIBUTION LIST

Dr. James Browning
Browning Engineering
Laboratory
Hanover, NH 03755

Dr. E. R. Walker
Frozen Sea Research Group
Inst. of Ocean Sciences
9860 W. Saanich Road
Box 6000, Sidney, B.C. V8L 4B2

National Science Foundation
Polar Program
1800 G Street, N.W.
Washington, D.C. 20550

Mr. J. Dykins
Polar Research Group
Civil Engineering
Laboratory, NCBC
Port Hueneme, CA 93043

Dr. E. L. Lewis
Institute of Oceanography
Patricia Bay,
B.C., Canada

Dr. C. Collins
National Science Foundation
1800 G Street N.W.
Washington, D.C. 20550

Dr. Robert N. Cordy, Director
Ocean Engineering Dept.
Civil Eng. Laboratory, NCBC
Port Hueneme, CA 93043

Dr. Ken Hunkins
Lamont-Doherty Geological
Observatory of Columbia U.
Palisades, New York 10964

Mr. Edgar Reed
Naval Air Development Ctr.
Code 6013
Warminster, PA 18974

CDR V. Simmons USN
Defense Advanced Research
Projects Agency
1400 Wilson Blvd.
Rosslyn, VA 22209

Mr. William O. Rainnie
Chief, Engineering Division
NOAA Data Buoy Office
NSTL Station, MS 39529

Mr. Leo Markushewski
Naval Air Development Ctr.
Code 6013
Warminster, PA 18974

Dr. Myra Dunbar
Defense Research Establishment
Shirley Bay
Ottawa, Ontario, Canada

Mr. Luther Bevins
Office of Ocean Engineering
NOAA (OEX3)
6000 Executive Blvd.
Rockville, MD 20852

Naval Air Systems Command
Code 370
Surveillance Administration
Washington, D.C. 20361

Dr. L. F. Lewis
Env. Assessment Branch
Solar Technology Division
Dept. of Energy (Room 415)
600 E Street N.W.
Washington, D.C. 20545

Director,
Office of Marine Technology
National Ocean Survey
60001 Executive Blvd.
Rockville, MD 20852

Naval Electronics System
Command
PME-124/60
Washington, D.C. 20360

Mr. Leslie Bonde
EG&G Washington Analytical
Services Center, Inc.
2150 Fields Road
Rockville, MD 20850

Mr. Robert E. Wall
Oceanography Section
National Science Foundation
Room 611
1800 G Street, N.W.
Washington, D.C. 20550

Mr. R. Knudsen
Naval Electronics Systems
Command
PME -124/20
Washington, D.C. 20360

DISTRIBUTION LIST (Cont'd)

Naval Electronics Systems
Command
Code 03
Research and Technology
Directorate
Washington, D.C. 20360

Naval Ocean Research and
Development Activity
Naval Oceanographic Lab.
Code 300
NSTL Station, MS 39529

Mr. M. M. Kleinerman
Code WU401
Naval Surface Weapons Ctr.
White Oak Laboratory
Silver Spring, MD 20910

Naval Electronics Systems
Command
PME 124-30
RDSS Division Director
Washington, D.C. 20360

Mr. Charles E. Stuart
Naval Ocean Research and
Development Activity
Code 520
Ocean Exploratory Dev. Ofs.
NSTL Station, MS 39529

Mr. Peter C. King
Naval Underwater Systems Ctr.
Fort Trumbull
New London, CT 06320

Naval Electronics Systems
Command
Code 320
Undersea Surveillance Div.
Washington, D.C. 20360

Commanding Officer
Naval Ocean Research and
Development Activity
NSTL Station, MS 39529

Naval Underwater Systems Ctr.
Code 311
New London, CT 06320

CDR J. A. Stamm CEC, USN
Naval Facilities Eng. Command
Chesapeake Division (FPO-1)
Bldg. 200
Washington Navy Yard
Washington, D.C. 20374

Mr. Richard J. Boyle
Arctic Submarine Laboratory
Code 54, Bldg. 371
Naval Ocean Systems Center
San Diego, CA 92152

Dr. Eric Softley
Ocean Electronic Applic. Inc.
245 Ridgewood Road
Key Biscayne, FL 33149

CDR D. R. Wells, CEC, USN
Director, Ocean Facil. Prog.
Naval Facil. Eng. Comm. (PC-2)
200 Stovall Street
Alexandria, VA 22332

Dr. Waldo K. Lyon, Director
Arctic Submarine Laboratory
Code 54, Bldg. 371
Naval Ocean Systems Center
San Diego, CA 92152

Dr. E. A. Silva, Code 485
Office of Naval Research
Ocean Science & Techn. Div.
800 N. Quincy Street
Arlington, VA 22217

Naval Facilities Eng. Comm.
Code 03
Assist. Commander for R & D
200 Stovall Street
Alexandria, VA 22332

Naval Research Laboratory
Code 8160
Large Aperture Acoustics
Washington, D.C. 20375

Office of Naval Research
Ocean Science & Techn. Det.
Code 480
NSTL Station, MS 39529

Naval Material Command
Code 0345
Oceans and Atmosphere
Washington, D.C. 20360

Naval Research Laboratory
Code 8109
System Analysis Group
Washington, D.C. 20375

Dr. Leonard Johnson
Office of Naval Research
Code 461
Arlington, VA 22217

Mr. R. C. Swenson
Code 350
Naval Ocean Research and
Development Activity
NSTL Station, MS 39529

Naval Research Laboratory
Code 8120
Applied Ocean Acoustics
Washington, D.C. 20375

Mr. Ron McGregor
Office of Naval Research
Code 461
Arlington, VA 22217

DISTRIBUTION LIST (Cont'd)

Mr. Ben Cagle
Office of Naval Research
Branch Office
1030 E Green Street
Pasadena, CA 91106

Mr. Carl S. Christensen
TETRA TECH, Inc.
1911 Fort Meyer Drive
Arlington, VA 22209

Dr. Lloyd Breslau, Director
U.S. Coast Guard Research
and Development Lab.
Groton, CT 06340

Dr. Alan Sykes
Office of Naval Research
Code 421
Sensor Systems Prog.
800 N. Quincy Street
Arlington, VA 22217

Dr. Halmar Aamot
U.S. Army Cold Regions
Research & Eng. Lab.
Hanover, NH 03755

Mr. John B. Gregory
U.S. Geological Survey
Conservation Division
Mail Stop 620
12201 Sunrise Valley Dr.
Reston, VA 22092

Office of Naval Research
Undersea Techn. Prog. Mgr.
Code 220
800 N. Quincy Street
Arlington, VA 22217

Dr. Andrew Assur
U.S. Army Cold Regions
Research & Eng. Lab.
Hanover, NH 03755

Chief of Naval Operations
OP-0952D
U.S. Naval Observatory
Washington, D.C. 20360

CAPT Alex Anckonie
Office of the Assistant
Secretary of the Navy
(Research, Eng. and Sys)
Pentagon, 5E787
Washington, D. C. 20360

Dr. Ginny Frankenstein
U.S. Army Cold Regions
Research & Eng. Lab.
Hanover, NH 03755

Dr. W. S. Gaither, Chairman
Polar Panel - Marine Board
College of Marine Studies
University of Delaware
Newark, DE 19711

Office of the Chief of Naval
Operations
OPNAV Code 987
ASW & Environmental Plans
Washington, D.C. 20350

Dr. Dean Frietag, Director
U.S. Army Cold Regions
Research & Eng. Lab.
Hanover, NH 03755

Mr. Richard Blidberg
University of New Hampshire
Marine Program Office
Kingsbury Hall
Durham, NH 03824

Dr. George Hobson
Polar Continental Shelf Prog.
880 Wellington Street
Ottawa, Ontario, Canada

Mr. Austin Kovacs
U.S. Army Cold Regions
Research & Eng. Lab.
Hanover, NH 03755

Dr. Robert W. Corell
University of New Hampshire
Marine Program Office
Kingsbury Hall
Durham, NH 03824

Dr. R. M. Koerner
Polar Continental Shelf Prog.
880 Wellington Street
Ottawa, Ontario, Canada

Dr. David Paskausky
Chief, Oceanographic Branch
U.S. Coast Guard R & D Ctr.
Avery Point
Groton, CT 06340

Mr. Arthur S. Westneat, Jr.
University of New Hampshire
Marine Program Office
Kingsbury Hall
Durham, NH 03824

Mr. B.M. Buck, President
Polar Research Lab., Inc.
123 Santa Barbara Street
Santa Barbara, CA 93101

Dr. Paul Greisman
U.S. Coast Guard R & D Ctr.
Groton, CT 06340

Mr. G. Ross Peters
Faculty of Engineering and
Applied Science
University of Newfoundland
St. Johns, Newfoundland
A1C557

DISTRIBUTION LIST (Cont'd)

AIDJEX Data Bank
AIDJEX Program Office
University of Washington
4059 Roosevelt
Seattle, WA 98105

Dr. Allan Thorndike
AIDJEX Program Officer
University of Washington
4059 Roosevelt
Seattle, WA 98105

Dr. Gary Maykut
Dept. of Atmospheric Science
University of Washington
4059 Roosevelt
Seattle, WA 98105

Mr. Robert G. Walden
Woods Hole Oceanographic Institution
Woods Hole, MA 02543

END

DATE
FILMED

7-81

DTIC